Streptococcus mitis bacteriocins drive contact-dependent lysis of *S. pneumoniae* facilitating transformation in multispecies environments

João Borralho[1], João Lança,[1], Joana Bryton[1], Wilson Antunes[2], Raquel Sá-Leão[1]*

[1] Laboratory of Molecular Microbiology of Human Pathogens, Instituto de Tecnologia Química e Biológica António Xavier, Universidade Nova de Lisboa, Oeiras, Portugal

[2] Centro de Investigação da Academia Militar (CINAMIL), Unidade Militar Laboratorial de Defesa Biológica e Química (UMLDBQ), Av. Dr. Alfredo Bensaúde, 1849-012, Lisboa, Portugal.

* Corresponding author: rsaleao@itqb.unl.pt

Keywords: Horizontal gene transfer, competence, interspecies interactions, predation, biofilms

Abstract

Natural competence allows bacterial species like *Streptococcus pneumoniae* and *S. mitis* to acquire environmental DNA, driving horizontal gene transfer (HGT) and adaptation. In *S. pneumoniae*, a human pathogen, competence-induced predation is well characterized and involves the release of bacteriocins and a murein hydrolase to lyse noncompetent siblings and liberate DNA. In contrast, in the human commensal *S. mitis*, mechanisms mediating DNA acquisition remain poorly understood. Here, we identify a diverse set of competence-associated bacteriocins (*cab*) that are produced by *S. mitis* during the late phase of competence. We focus on one bacteriocin pair, CabAB, that triggers contact-dependent growth inhibition and lysis of *S. pneumoniae* through activation of the major pneumococcal autolysin LytA. We demonstrate that CabAB compromises *S. pneumoniae* membrane integrity, leading to formation of intracellular membrane aggregates and the release of cytoplasmatic content, thereby increasing available DNA, which enhances HGT from *S. pneumoniae* to *S. mitis* in biofilms. These findings uncover a mechanism of interspecies predation and gene acquisition, revealing a critical role for competence-associated bacteriocins in shaping evolutionary dynamics of streptococci.

Importance

Many streptococci are naturally competent, acquiring environmental DNA through transformation. This includes pathogens like *S. pneumoniae* and commensals like *S. mitis,* which can exchange genetic material through horizontal gene transfer (HGT). For example, *S. mitis* can acquire pneumococcal capsules, leading to its misidentification in polymicrobial samples such as those obtained from the upper respiratory tract. Understanding the drivers of HGT between these species is therefore critical. Here, we characterize a competence-induced bacteriocin cluster in *S. mitis*. These bacteriocins lyse pneumococci, promoting DNA release and enhancing gene transfer in dual-species biofilms. Our findings uncover a mechanism by which competence-associated predation promotes interspecies HGT, shaping the evolution and epidemiology of streptococcal populations.

42 **Introduction**

43 Natural competence for genetic transformation is a developmental program found in certain
44 bacterial species that enables the uptake of naked DNA from the environment. Once internalized, this
45 DNA can be incorporated into the genome through homologous recombination, making natural
46 transformation one of the main modes of horizontal gene transfer (HGT). This phenomenon was first
47 described in *Streptococcus pneumoniae* (or pneumococcus), a species capable of exchanging
48 pathogenic traits such as the capsule by taking up DNA from other pneumococci (1).

49 In *S. pneumoniae*, competence is a tightly regulated transient physiological state which is
50 governed by a cell-cell signaling system. The competence-stimulating peptide (CSP), encoded by
51 *comC*, is processed and exported via the ATP-binding cassette transporter ComAB. Extracellular
52 CSP is sensed by the membrane-bound histidine kinase ComD (2-4), which undergoes
53 autophosphorylation triggering subsequent phosphorylation of the response regulator ComE (5).
54 Phosphorylated ComE increases expression of the early competence cascade including *comAB* and
55 *comCDE*, creating a positive feedback loop. It also induces expression of the two copies of the
56 alternative sigma factor (*sigX1* and *sigX2*), marking the onset of the late phase of competence (6).

57 In the late phase of competence, expression of all genes required for DNA uptake, processing
58 and recombination – the transformasome – is induced (7). Here, pneumococci produce the
59 competence-induced bacteriocins A and B (CibAB), along with the immunity protein CibC, which
60 provides self-immunity to CibAB (8). Because competence may not be synchronized across the whole
61 population (9-11), CibAB release on solid media may lead to lysis of genetically identical (kin)
62 noncompetent cells that have not yet expressed *cibC*. Additionally, expression of the murein
63 hydrolase CbpD, against which competent cells are protected via ComM expression, is essential for
64 kin predation in liquid cultures. Notably, CbpD has also been implicated in lysis of non-kin, closely
65 related streptococci, thereby expanding the gene pool from which *S. pneumoniae* may acquire DNA
66 (12). CibAB and CbpD have also been associated to competitive interactions *in vivo*, where their
67 expression by colonizing pneumococci provides a competitive advantage over other *S. pneumoniae*
68 invaders (13).

69 A close relative of the pneumococcus, *S. mitis*, is also naturally transformable. *S. mitis* is a
70 common commensal of the human nasopharynx and oral cavity, where it typically establishes long-
71 term colonization without causing disease (14). Despite close phylogenetic relationship with *S.*
72 *pneumoniae*, and a strikingly similar competence regulatory network, *S. mitis* exhibits key differences
73 in terms of bacteriocin content. While *S. mitis* typically encodes *cbpD*, most strains lack *cibAB*,
74 suggesting that *S. mitis* may rely on an alternative mechanism for predation during competence (15-
75 17).

76 Although the frequency at which *S. mitis* acquires DNA from *S. pneumoniae* is not well
77 established, such events have been documented. These include, for example, the acquisition of
78 pneumococcal *pbp2x* mosaic blocks (18-20). Some *S. mitis* have also been found to express some
79 pneumococcal or pneumococcal-like capsules, which can cross-react with antisera against serotypes
80 1, 5, 17F, 18A, 19C, 21, 39 and 40 (21-24).

81 A competence-associated bacteriocin (*cab*) cluster, which is absent in *S. pneumoniae*, has
82 been identified in *S. mitis*. This cluster is located upstream of the competence transporter *comAB* and
83 can encode multiple *cab* bacteriocins distinct from CibAB (15, 16, 25-27). However, the role of *cab* in
84 *S. mitis* predation of kin and non-kin, and its contribution to DNA acquisition, remains unexplored.

85 Here, we characterize the arsenal of *cab* bacteriocins carried by *S. mitis* and provide evidence
86 that some specifically mediate lysis of *S. pneumoniae*. We also show that pneumococcal DNA can
87 be efficiently taken up and recombined by *S. mitis* and that Cab-mediated lysis accelerates gene
88 transfer from *S. pneumoniae* to *S. mitis*. Together, these findings shed light on previous observations
89 of pneumococcal DNA integration in *S. mitis* genomes.

90

91 ## Results

92 ### *S. mitis* encodes a diverse arsenal of competence-associated bacteriocins (*cab*)

93 We previously identified and characterized a limited number of *S. mitis* strains encoding multiple
94 competence-associated bacteriocins (*cab*), most of which lacked the pneumococcal bacteriocins
95 *cibAB* and associated immunity protein *cibC* (27). To investigate the broader distribution of *cab* and

96 *cibAB* in *S. mitis*, we surveyed publicly available genomes, leveraging the conserved genomic context
97 of *cab* clusters – located upstream of *comAB* and downstream of *plsX-acpP*. This region was identified
98 and extracted from 253 of 332 *S. mitis* genomes (Fig. 1A and Table S1). The remaining genomes had
99 contig breaks and were excluded from further analysis.

100 Among the 253 genomes analyzed, 26.9% harbored *cibABC*, a striking contrast with *S.*
101 *pneumoniae*, where these genes are universally present. An additional 13.0% of strains carried *cibC*
102 but not *cibAB* – often referred to as "cheater" phenotype (28), in which strains are immune to CibAB-
103 mediated killing but do not produce the bacteriocins themselves. In contrast, 47.4% of *S. mitis*
104 encoded between one to eleven unique *cab* genes that contain a double glycine leader sequence
105 ((M/L/V)XXXXGG), which is recognized by ComAB (29). We defined *cab* bacteriocins as all non-*cib*
106 bacteriocin genes that were found in this particular location. In total, 95 distinct Cab variants were
107 found, which grouped into 28 clusters based on sequence similarity (Fig. 1B and Fig. S1). Overall,
108 61.3% of *S. mitis* genomes carried at least one *cab* gene or the *cibABC* operon (Table S1).

109 Cab variants were present at low frequencies (<10%) in the *S. mitis* population, with 32 of 95
110 bacteriocin variants only being found in a single strain (Fig. 1B). Despite this extensive diversity,
111 rarefaction analysis suggested that Cab diversity is not yet saturated (Fig. 1C); sequencing more *S.*
112 *mitis* will likely reveal new Cab sequences.

113 These findings highlight *S. mitis* as a reservoir of highly diverse and largely unexplored
114 competence-associated bacteriocins.

115

116 **Cab bacteriocins are expressed in the late phase of competence**

117 *S. mitis* G22, previously described by us, encodes a *cab* operon consisting of two putative bacteriocins
118 and an associated immunity protein (hereafter referred as *cabAB* and *cabC*, respectively; *cabA*
119 belongs to cluster 7 and *cabB* belongs to cluster 21) (Fig. 2A and Fig. S1) (27). This strain was
120 selected to study *cab* regulation in *S. mitis* and its role in competitive behaviors. Both bacteriocins
121 and the immunity protein it encodes are rare (30) and thus unlikely to encounter pre-existing immunity
122 in other strains. Notably, its *cab* promoter contains five putative binding sites for the alternative sigma

123 factors (SigX boxes) (27), suggesting that *cabABC* may be expressed during the late phase of
124 competence.

125 To investigate the dynamics of *cab* expression, the native *cabABC* promoter was ectopically
126 inserted into the *S. mitis* G22 genome, upstream of a firefly luciferase reporter (*luc*). Expression of
127 *cabABC* was then inferred by expression of *luc* and compared to known early (*comCDE*) and late
128 (*sigX1* and *sigX2*) competence regulators. As expected, we observed that competence was not
129 induced under acidic pH (Fig. S2), unless exogenous cognate competence-stimulating peptide
130 (CSP_{G22}) was supplied (Fig. S3A). Upon CSP_{G22} treatment, *cabABC* expression followed a similar
131 temporal pattern to *comCDE*, *sigX1* and *sigX2*, peaking at approximately 70 min post-induction (Fig.
132 S3B). Thus, based on expression kinetics alone, early and late competence genes could not be
133 distinguished in this assay. This response was specific to CSP, as exogenous addition of cognate
134 bacteriocin-like peptide pheromones ($BlpC_1$ and $BlpC_4$), encoded elsewhere in the *S. mitis* G22
135 genome (30), failed to induce *cabABC* expression (Fig. S4).

136 Deletion of the early regulator *comE* abolished *cabABC* expression, a result expected for both
137 early- and late-regulated genes (Fig. 2B). Individual deletion of *sigX1* or *sigX2* partially reduced
138 expression of *cabABC*, while deletion of both resulted in complete loss of *cabABC* expression,
139 consistent with *cab* being expressed during the late phase.

140 Although multiple SigX boxes have been observed in *cab* promoters previously (16, 27), their
141 functional relevance has not been tested. To assess this, we compared expression driven by the full-
142 length *cabABC* promoter (containing all five SigX boxes) to a truncated version containing only the
143 most proximal SigX box. Deletion of four out of five SigX boxes reduced *cabABC* expression (Fig.
144 2C), indicating that tandem SigX binding sites enhance *cab* expression. In the *S. mitis* collection, all
145 *cab* loci harbored at least two SigX boxes, with one strain containing up to 38 boxes (Fig. 2D and
146 Table S1). These boxes were often spread throughout *cab* loci, and larger loci were associated with
147 higher number of SigX boxes, suggesting accumulation of boxes throughout these sequences.

148 Together, these results demonstrate that *cab* bacteriocins are specifically expressed during
149 the late phase of competence, and that the presence of multiple SigX binding sites likely amplifies
150 their expression.

151

152 **Expression of *S. mitis cabABC* is induced by pneumococcal CSP-1**

153 Mitis group streptococci naturally produce and recognize different CSP variants, known as pherotypes
154 (31). To investigate the specificity of *cab* expression, synthetic CSP variants from closely related
155 strains were tested for their ability to activate *cabABC*. CSP variants from three other *S. mitis*, one *S.*
156 *oralis*, and one *S. pneumoniae* strain failed to induce *cab* expression in *S. mitis* G22 (Fig. 3A). By
157 contrast, the most prevalent *S. pneumoniae* pheromone, CSP-1 (32), efficiently induced *cab* to the
158 same levels as native CSP_{G22}.

159 Comparison of the amino acid sequences of CSP_{G22} and the other CSP variants revealed a
160 single amino acid residue, Q14 (glutamine), that may explain the differences in induction. While both
161 CSP_{G22} and CSP-1 contain Q14, a polar residue, the non-inducing variants contain either a L14
162 (leucine) or a P14 (proline), both nonpolar. To investigate the importance of Q14 and polarity in
163 competence induction, CSP_{G22} variants with single amino acid substitutions at position 14 were tested.
164 Substituting Q14 with L significantly reduced *cab* expression, whereas replacing it with another polar
165 residue (N, asparagine) restored expression (Fig. 3B). This suggests that polarity of amino acid 14 is
166 important for CSP recognition by *S. mitis* G22. However, introducing Q14 into a non-inducing peptide
167 (CSP-2; L14Q) was not sufficient to convert it into a functional inducer, indicating that additional
168 residues beyond Q14 are required for efficient recognition by the membrane-bound histidine kinase
169 ComD of *S. mitis* G22.

170 To assess whether *S. pneumoniae* can also respond to CSP_{G22}, the *comCDE* promoter from
171 *S. pneumoniae* D39, a strain that produces and recognizes CSP-1, was transcriptionally fused to a
172 *luc* reporter and integrated in its chromosome. Competence in D39 was efficiently induced by both
173 CSP-1 and CSP_{G22}, confirming that *S. mitis* G22 and *S. pneumoniae* D39 can cross-communicate
174 through distinct CSP peptides (Fig. 3C). Similar to G22, *S. pneumoniae* D39 was also affected by
175 mutations at position 14: Q14L (polar to nonpolar) reduced induction. In contrast to *S. mitis* G22, the
176 substitution Q14N (polar with another polar amino acid), failed to restore it. Notably, the substitution
177 L14Q into CSP-2 (the second most frequent CSP in pneumococci) enabled competence induction.

178 These findings highligh the importance of Q14 in CSP recognition of pneumococci of the CSP-1
179 pherotype.
180 In the 253 *S. mitis* genomes analyzed, 2.8% encode CSP_{G22} (Table S1) indicating that more
181 *S. mitis* strains can induce competence in pneumococci of pherotype CSP-1.
182 These results reveal that cross-communications via CSP is possible between *S. mitis* and *S.*
183 *pneumoniae*, and that residue 14 plays a critical, but context-dependent, role in pheromone
184 recognition.
185
186 **CabAB mediates inhibition of *S. pneumoniae* in a contact-dependent manner**
187 Given that *S. mitis* G22 and *S. pneumoniae* D39 can cross-communicate through CSP, we
188 hypothesized both species would engage in competence-induced predation. Supporting this, *S. mitis*
189 G22 harbors the orphan immunity gene *cibC* (but not *cibAB*), suggesting it may be resistant to
190 pneumococcal CibAB attack (Table S1).
191 To investigate the specific role of the competence associated bacteriocins CabAB in *S.*
192 *pneumoniae* inhibition, we first deleted two bacteriocin clusters (*blp4* and *blp1*) with known anti-
193 pneumococcal activity (27), from the genome of *S. mitis* G22, as their activity could obscure CabAB-
194 mediated effects. All experiments in this section were, thus, performed using *S. mitis* G22 Δ*blp4*Δ*blp1*
195 and its derivatives as described below.
196 We grew dual-species biofilms of *S. mitis* G22 Δ*blp4*Δ*blp1* and *S. pneumoniae* D39 under
197 competence-permissive conditions. After 24 h, both species persisted in the biofilm (Fig. 4A and Fig.
198 S5). Deletion of *cab* from *S. mitis* led to increased pneumococcal loads, while constitutive expression
199 of *cab* via plasmid p(cab^+) (overexpressor mutant contains the native *cab* copy and carries an
200 additional constitutively expressed copy in plasmid p(cab^+)) reduced them, indicating that the
201 presence and expression levels of *cab* modulate competitive outcomes.
202 Bacteriocins are typically secreted to the extracellular environment (33). To test whether
203 CabAB exerts its activity as a secreted factor, we harvested cell-free supernatants (CFS) from *S. mitis*
204 strains and added them to pneumococcal cultures. CFS of *S. mitis* natively or overexpressing *cab* did

205 not inhibit *S. pneumoniae* growth (Fig. 4B), suggesting CabAB is not released into the medium. This
206 aligns with recent reports of bacteriocins, such as Listeriolysin S and contact-dependent inhibition by
207 glycine zipper proteins CdzCD (34, 35), that remain attached to the producer cell surface. In these
208 cases, inhibitory activity occurs via direct contact between producer and target cells.

209 To test whether CabAB could remain cell-associated, we heat-killed *S. mitis* strains (as
210 bacteriocins are typically resistant to high temperature treatments) and exposed them to *S.*
211 *pneumoniae*. Heat-killed *cab*$^+$ and p(*cab*$^+$) *S. mitis* extracts significantly inhibited pneumococcal
212 growth, while extracts from Δ*cab S. mitis* did not (Fig. 4B), supporting the idea that CabAB is retained
213 in producer cells.

214 We then tested whether direct contact between *S. mitis* and *S. pneumoniae* was required for
215 inhibition. Dual-species biofilms were grown either with or without a 0.4 µm transwell membrane
216 separating both species. When the strains were in direct contact with each other, *cab* expression was
217 associated with pneumococcal inhibition, whereas no inhibition was observed when both species
218 were separated (Fig. 4C). These effects were not due to differences in *S. mitis* growth, as bacterial
219 loads were consistent across conditions and genotypes (Fig. 4D).

220 We then sought to detect CabA and CabB on the surface of competent *S. mitis* cells. A mutant
221 lacking the native *cab* locus was used, into which we ectopically integrated cassettes containing
222 haemagglutinin-tagged (HA) CabA (*cabA-HA cabBC*) or CabB (*cabA cabB-HA cabC*), under native
223 regulation. Immunofluorescence microscopy of live *S. mitis* expressing *cabA-HA* using anti-HA
224 antibodies revealed discrete clusters of CabA on the cell surface (Fig. 4E). Of note, CabA was not
225 detectable in all cells. This may be due to several factors, such as CabA being occluded by the cell
226 wall or competence development being asynchronous, with different subpopulations of *S. mitis*
227 becoming competent at slightly different times. No signal was detected in strains lacking the HA
228 epitope, confirming specificity. Interestingly, no signal was observed in the *cabB-HA* strain,
229 suggesting that CabB may be less surface-exposed, that the N-terminal HA tag was not accessible
230 to antibody binding, or that tagging interfered with localization.

231 Together, these results demonstrate that *S. mitis* inhibits *S. pneumoniae* via CabAB in a
232 contact-dependent manner.

233

234 **CabAB is a two-peptide bacteriocin with LytA-dependent bactericidal activity**

235 CibAB has previously been shown to be a two-peptide bacteriocin, meaning its inhibitory activity
236 occurs only when both peptide components are present (8). To test if CabAB also functions as a two-
237 peptide bacteriocin, synthetic CabA and CabB were tested individually and in combination against *S.*
238 *pneumoniae* D39. No effect on pneumococcal growth was observed upon addition of DMSO (the
239 solvent used to resuspend the peptides), CabA alone, or CabB alone (Fig. 5A). In contrast, a single
240 treatment with equimolar amounts of CabA and CabB delayed *S. pneumoniae* growth for ~12 h,
241 indicating that both peptides are required for activity. This is consistent with the presence of multiple
242 GxxxG or GxxxG-like motifs in both bacteriocins (Fig. 5B), known to facilitate and stabilize two-
243 component bacteriocins (36-38). We also confirmed that CabAB can cross the membrane used in the
244 transwell assays, leading to a decrease in *S. pneumoniae* loads when added to opposite
245 compartments (Fig. S6).

246 We next investigated whether CabAB exerts bactericidal activity. Exponentially growing *S.*
247 *pneumoniae* D39 cultures were treated with CabAB or DMSO. CabAB-treated cultures showed
248 evident decrease in optical density, indicating lysis, while DMSO-treated controls did not (Fig. 5C).
249 Lysis induced by the related bacteriocin CibAB has been shown to depend on the action of the
250 pneumococcal autolysins LytA and LytC (8). Here, deletion of *lytC* from D39 had no effect on CabAB-
251 mediated lysis, whereas a Δ*lytA* mutant exhibited delayed growth but no decrease in optical density,
252 indicating that LytA plays a key role in CabAB-induced lysis. This does not exclude, however, the
253 possibility that limited lysis occurs concomitantly with growth.

254 Together, these findings show that *S. mitis* CabAB is a two-peptide bacteriocin with
255 bactericidal activity against *S. pneumoniae*, and that its lytic activity depends on the target cell LytA
256 autolysin.

257

258 **CabAB affects membrane homeostasis in *S. pneumoniae***

259 We sought to shed light on how CabAB affects pneumococcal physiology. To this end, *S. pneumoniae*
260 D39 cells were treated with CabAB or DMSO and imaged by scanning electron microscopy (SEM).

261 While DMSO-treated cultures displayed normal morphology, CabAB-treated cells appeared to be
262 encased in an extracellular matrix (Fig. 6A), suggesting leakage of intracellular material.

263 To test if membrane permeability was compromised, cells were stained with propidium iodide
264 (PI), a DNA-binding dye that only enters cells with compromised membranes. In DMSO-treated
265 cultures, only 3% were PI-positive, while CabAB-treated cultures contained 85% PI-positive cells (Fig.
266 6B). Doubling the concentration of CabAB further increased this proportion to 97%, indicating this
267 phenotype is concentration dependent. Deletion of *lytA* had no effect on these phenotypes,
268 demonstrating that membrane permeabilization occurs independently of autolysin-mediated lysis (Fig.
269 S7).

270 Time series measurements showed that PI signal intensity peaked at 30 min post CabAB
271 exposure, still being detected after 120 min (Fig. 6C). We also assessed pneumococcal membrane
272 depolarization using the fluorescent dye $DiBAC_4(3)$, which enters cells only when their membranes
273 are depolarized. Compared to DMSO, CabAB treatment led to a rapid and sustained increase in
274 $DiBAC_4(3)$ signal (Fig. 6D), indicating membrane depolarization.

275 Since some characterized two-peptide bacteriocins act by forming pores (39-42), we tested
276 whether CabAB treatment causes efflux of intracellular components from target cells. In wild-type *S.*
277 *pneumoniae* treated with CabAB, 80% of total ATP was detected in the supernatant (Fig. 6E), in
278 agreement with our previous observation of significant cell lysis (Fig. 5C). Interestingly, in CabAB-
279 treated Δ*lytA S. pneumoniae* cells, no decrease in optical density was observed over the course of
280 the experiment, yet 30% of ATP was still detected in the supernatant, suggesting that CabAB induces
281 leakage independently of cell lysis.

282 We next visualized CabAB-induced damages using transmission electron microscopy (TEM).
283 DMSO-treated cells appeared intact, whereas 17% of CabAB-treated cells contained large
284 intracellular aggregates (Fig. 6F). Based on our prior observations, we hypothesized these
285 aggregates would be membranous. Consistently, staining with the membrane dye FM4-64 revealed
286 intracellular foci in CabAB-treated cells, but not in control cells (Fig. 6G), confirming the formation of
287 membrane aggregates by CabAB.

288 Finally, lower-magnification fluorescent microscopy of CabAB-treated cultures stained with
289 DAPI and FM4-64 revealed frequent clumps of cells encased in nucleic acid and membrane material,
290 mirroring the SEM observations of surviving cells remaining embedded in an extracellular matrix (Fig.
291 S8)

292 Altogether, these findings show that *S. mitis* CabAB disrupts membrane homeostasis in *S.*
293 *pneumoniae* by permeabilizing and depolarizing membranes, leading to release of its intracellular
294 content.

295

296 **CabAB facilitates the acquisition of pneumococcal DNA by *S. mitis* in biofilms**

297 As previously shown, CabAB promotes release of DNA from *S. pneumoniae* cultures. Since *cab*
298 expression is synchronized with the competence period, we hypothesized that CabAB could enhance
299 DNA acquisition and HGT within biofilms. To test this, we grew dual-species biofilms under conditions
300 designed to study HGT (Fig. 7A), where: (i) DNA transfer is unidirectional, since the DNA donor strain
301 (*S. pneumoniae* D39) carries a deletion of the major competence pilus subunit gene, *comGC,*
302 rendering it nontransformable; (ii) the *S. pneumoniae* DNA donor harbors chloramphenicol (Chl^R) and
303 tetracycline (Tet^R) resistance cassettes integrated at opposite regions of the chromosome with high
304 sequence homology (89-98%) between DNA donor and recipient (Fig. S9); (iii) the DNA recipients (*S.*
305 *mitis* G22, wt and variants) are kanamycin resistant, allowing for discrimination between non-
306 transformed (Kan^R) and transformed *S. mitis* (Kan^R Chl^R, Kan^R Tet^R, and Kan^R Chl^R Tet^R); (iv) biofilms
307 are pre-grown under acidic pH for 24 h to promote biofilm establishment without inducing competence;
308 and (v) CSP_{G22} is added after 24 h to transiently induce competence. A noncompetent *S. mitis* Δ*comE*
309 mutant was used as a negative control, as it is unable to acquire Chl^R and/or Tet^R by transformation.
310 These experiments were conducted using the *S. mitis* G22 Δ*blp4* Δ*blp1* background.

311 To rule out the possibility that CabAB affects transformability rather than DNA availability, we
312 first replaced the donor strain with purified gDNA. Under these conditions, both cab^+ and Δ*cab S. mitis*
313 acquired resistance at similar frequencies (Fig. 7B), indicating that native *cab* expression does not

314 impact transformability. In contrast, overexpression of *cab* reduced transformation efficiency for one
315 antibiotic resistance, possibly due to the fitness burden associated with carrying p(*cab*$^+$).
316 In dual-species biofilms, *cab*$^+$ *S. mitis* efficiently acquired Chl^R and Tet^R from the DNA donor,
317 at a significantly higher frequency than the Δ*cab* mutant (Fig. 7C), indicating that CabAB contributes
318 to DNA acquisition. In contrast, overexpression of CabAB did not enhance transformation efficiency,
319 suggesting that a precise *cab* regulation might be necessary for optimal transformation. We extended
320 these findings to an additional *S. mitis* strain, C22, which harbors a distinct *cab* bacteriocin repertoire
321 (27). *S. mitis* C22 contains a *cab* cluster encoding two copies of the bacteriocin *cabD* (cluster 10), two
322 copies of the bacteriocin *cabE* (cluster 26), and two putative immunity proteins, *cabF* and *cabG* (Fig.
323 S10A). Wild-type C22 was able to acquire Chl^R and Tet^R from the *S. pneumoniae* DNA donor and
324 transformation frequencies were also reduced in the Δ*cab* mutant (Fig. S10B). Consistently, the
325 proportion of *S. pneumoniae* in dual-species biofilms with *S. mitis* C22 was lower when co-cultured
326 with C22 *cab*$^+$ than with Δ*cab* cells (Fig. S10C), showing that the cab locus of a different *S. mitis* strain
327 also mediates inhibition of *S. pneumoniae* and facilitates genetic exchange.
328 We then sought to investigate the specificity of CabAB-induced lysis. Synthetic CabAB was
329 tested against one representative strain of 26 bacterial species, including 18 streptococcal species,
330 four additional non-streptococcal Gram-positive and four Gram-negative species. All selected species
331 are human commensals or pathogens that can inhabit the oral and/or respiratory tract and could
332 theoretically encounter *S. mitis* and be exposed to Cab bacteriocins in natural environments. Addition
333 of 0.975 μM of CabAB to exponential cultures of these bacteria stalled the growth of some species
334 (Fig. 7D and Fig. S11 and S12). The most sensitive to CabAB were the representative strains of
335 Pyogenic Group streptococci (*S. pyogenes* and *S. agalactiae*). Gram-negative bacteria (*Haemophilus*
336 *influenzae*, *Klebsiella pneumoniae*, *Moraxella catarrhalis*, and *Neisseria lactamica*) were largely
337 unaffected. Despite growth inhibition in some species, lysis was only observed in two - *S. pneumoniae*
338 and *S. parasanguinis* - suggesting that CabAB-mediated lysis has limited specificity.
339 Finally, we investigated whether membrane aggregate formation was specifically associated
340 with species that undergo CabAB-mediated lysis. Aggregate formation was observed exclusively in

341 *S. pneumoniae* and not in *S. parasanguinis*, *S. pyogenes* and *S. agalactiae* (Fig. S13). Notably,
342 membrane aggregates were also absent in Δ*lytA S. pneumoniae* cells, indicating that aggregate
343 formation is specific to *S. pneumoniae* and that it requires LytA.

344 These results suggest that CabAB provides a competitive advantage by inhibiting the growth
345 of some bacteria, but that it also enhances DNA release in biofilms by selectively lysing a few closely
346 related species during competence, notably *S. pneumoniae*, thereby promoting gene exchange.

347

348 **Discussion**

349 During competence, streptococci scavenge extracellular DNA. In *S. pneumoniae*, where competence-
350 induced predation is best characterized, the coordinated action of CibAB, LytA, LytC, and the murein
351 hydrolase CbpD leads to lysis of noncompetent siblings (8). This process promotes DNA release and
352 facilitates HGT (12, 43, 44).

353 Although extensive genomic data suggests that *S. mitis*, a close relative of *S. pneumoniae*,
354 frequently acquires *S. pneumoniae* DNA (18, 19, 21-24, 45), the molecular mechanisms underlying
355 this exchange remained poorly understood. Understanding these mechanisms is relevant because
356 capsule acquisition by *S. mitis* can complicate DNA-based pneumococcal serotyping. In addition, *S.*
357 *mitis* has been associated with cases of infective endocarditis (23), highlighting the value of studying
358 how it acquires potentially pathogenic traits.

359 Here, we investigated the role of *S. mitis* competence-associated bacteriocins, CabAB, in
360 mediating interspecies interactions (Fig. 8). We show that CabAB is a two-peptide bacteriocin
361 produced during the late phase of competence, when cells are primed for DNA uptake and
362 recombination, capable of lysing *S. pneumoniae* in a LytA-dependent manner. Although LytA is
363 constitutively expressed throughout growth, its concentration increases during competence, owing to
364 a genomic architecture comprising three constitutive promoters and one competence-induced
365 promoter (7, 46-48). In this context, it is tempting to speculate that by inducing *S. pneumoniae*
366 competence via CSP crosstalk, and therefore increasing LytA concentration, some *S. mitis* could
367 further sensitize *S. pneumoniae* to Cab bacteriocins. Nonetheless, CabAB-induced lysis appears to

368 be independent of pherotype of target cells, as both *S. pneumoniae* D39 (CSP-1; used in most
369 experiments) and TIGR4 (CSP-2; included in the panel of 26 bacterial species) were lysed. These
370 pherotypes account for the vast majority (>95%) of pneumococcal strains (49-51).

371 Of the initial 332 *S. mitis* genomes analyzed, we were not able to retrieve the region upstream
372 of *comAB* from a substantial fraction of strains (23.8%), as their assemblies showed contig breaks
373 precisely at this locus. We propose this difficulty arises from the repetitive nature of the region, as
374 indicated by the presence of numerous SigX boxes. The number of boxes scaled linearly with the size
375 of *cab* loci, suggesting that SigX boxes have accumulated throughout these sequences. Repeats are
376 known to both promote and result from genomic rearrangements (52, 53). They are often remnants
377 of previous recombination events, with no known biological function (54). In this case, however,
378 accumulation of SigX boxes may provide a selective advantage by enhancing bacteriocin expression,
379 which could explain why they are enriched in this region. Consistent with this, the extensive genetic
380 rearrangements observed across multiple streptococcal species at this locus also suggests this is a
381 highly recombinogenic region (25, 26, 55). To the best of our knowledge, the *cab* locus appears to be
382 the only competence-induced locus in *S. mitis* whose promoters contain multiple SigX boxes; other
383 competence-induced genes typically harbor a single box (16).

384 Microscopic analysis revealed that CabAB-treated pneumococci often contain large
385 membrane-derived intracellular aggregates. Whether these structures are part of CabAB's
386 mechanism of action or represent a cellular stress response remains unclear. Intracellular vesicle
387 formation has been shown to be essential for the lytic activity of bacteriocin A37 (56). Consistently,
388 we have observed that deletion of LytA, required for CabAB-mediated lysis in *S. pneumoniae*, blocks
389 formation of intracellular aggregates.

390 We further demonstrate that CabAB-mediated inhibition of *S. pneumoniae* requires direct
391 contact between producer and target cells. Contact-dependent bacteriocin delivery has been
392 described in *Caulobacter crescentus* and *Listeria monocytogenes* (34, 35). In *L. monocytogenes*,
393 bacteriocins were only detected on the surface of producer cells following cell wall digestion. In
394 contrast, we detected CabAB on live *S. mitis* with intact cell walls, suggesting a distinct delivery
395 mechanism. Although CabAB activity strictly required both peptides, only CabA could be detected on

396 the surface of competent *S. mitis*. CabB was not detectable by immunofluorescence, which could
397 reflect limited surface exposure, inaccessibility of the HA tag, or altered localization caused by C-
398 terminal tagging. A similar pattern of differential detectability has been reported in the CdzC/D contact-
399 dependent bacteriocin system in *Caulobacter crescentus*: both CdzC and CdzD are cell-associated
400 and required for activity, but only CdzC is clearly visualized in surface aggregates, whereas CdzD is
401 not direcly observed on the surface (35). These observations suggest that, in two-peptide contact-
402 dependent killing systems, one peptide may be more readily surface-exposed. Contact-dependent
403 killing during competence is not unique to streptococci, despite differences in killing factors. *Vibrio*
404 *cholerae* produces a competence-induced type VI secretion system that kills nonimmune cells,
405 releasing DNA that becomes accessible for HGT (57). Contact dependence may be particularly
406 advantageous in biofilm contexts, a niche where extracellular DNA could be subject to rapid
407 degradation nucleases (58). Proximity within multispecies biofilms could enhance transformation
408 efficiency by increasing the local DNA concentration, given that DNA abundance and size influence
409 recombination success (59). Notably, biofilm conditions and cell-to-cell contact have been shown to
410 promote both the frequency and size of recombination events in pneumococci, respectively (60, 61).
411 Notably, the frequency of double transformants was higher under cocultivation conditions (*S. mitis*
412 and *S. pneumoniae*) than when genomic DNA was added to *S. mitis* biofilms. In coculture, DNA is
413 likely released continuously over the course of incubation, increasing its local concentration and
414 availability, which may favor sequencial uptake and recombination events. In contrast, purified gDNA
415 was added only once and could be subject to degradation by extracellular nucleases, thereby
416 reducing the probability of independent recombination events. Strikingly, among 26 tested species,
417 only *S. pneumoniae* and *S. parasanguinis* were lysed by CabAB, suggesting a narrow-spectrum
418 bactericidal activity. Whether this specificity is unique to CabAB or shared among other Cab
419 bacteriocins remains to be determined. Nonetheless, the ability to selectively target phylogenetically
420 related but distinct species suggests a potential trade-off between maximizing recombination
421 efficiency and accessing a broader gene pool. While high sequence identity between donor and
422 recipient promotes recombination (62), restricting lysis to closely related species could expand the
423 range of accessible alleles beyond conspecifics (*i.e.* beyond members of the same species). Thus,

424 the large diversity of *cab* sequences in *S. mitis*, in contrast to *S. pneumoniae*, which typically harbors
425 only *cibAB*, may represent one of several evolutionary forces contributing to the exceptional genetic
426 diversity observed in *S. mitis* (23, 63).

427 Importantly, CabAB also strongly inhibited the growth of other streptococcal pathogens,
428 including *S. pyogenes* and *S. agalactiae*, both of which are listed as priority pathogens by the World
429 Health Organization (30). This potent inhibitory activity suggests that the Cab arsenal carried by *S.*
430 *mitis* could be a promising source of antimicrobial agents against important clinical pathogens as
431 recently suggested by us (27).

432 In summary, our findings uncover a contact-dependent mechanism of bacteriocin delivery in
433 *S. mitis* that selectively targets closely related streptococci including *S. pneumoniae*. This process
434 promotes HGT and likely contributed to competitive fitness and evolutionary plasticity of streptococcal
435 populations.

436

437 ## Materials and Methods

438 ### Bacterial strains and culture conditions

439 Bacterial strains, oligonucleotides, plasmids and peptides used in the study are listed in Table S2.
440 Streptococci were routinely grown in C+Y_{YB} (64) (pH 7.4, unless otherwise specified) and plated on
441 tryptic soy agar with 5% defibrinated sheep blood (blood agar, BA). When appropriate, media was
442 supplemented with antibiotics at the following concentrations: 150 μg.mL^{-1} kanamycin, 200 μg.mL^{-1}
443 spectinomycin, 4 μg.mL^{-1} chloramphenicol, or 4 μg.mL^{-1} tetracycline.

444 *Staphylococcus aureus, Staphylococcus epidermidis* and *Moraxella catarrhalis* were grown in
445 tryptic soy broth (TSB); *Corynebacterium accolens* was grown in TSB with 0.5% Tween 80; *Klebsiella*
446 *pneumoniae* and *Escherichia coli* were grown in lysogeny broth; and *Neisseria lactamica*,
447 *Haemophilus influenzae* and *Dolosigranulum pigrum* were grown in C+Y_{YB} with 20 μg.mL^{-1} hemin and
448 20 μg.mL^{-1} NAD. For propagation of plasmids in *E. coli*, media was supplemented with 100 μg.mL^{-1}
449 kanamycin or 100 μg.mL^{-1} spectinomycin, as required.

450

451 **Identification of *cab* bacteriocins and *cibABC* in *S. mitis***

452 Publicly available *S. mitis* genomes (n = 322) were downloaded from PubMLST. An additional 10
453 genomes from reference or commonly used *S. mitis* strains were included, resulting in a total of 332
454 genomes (Table S1). To detect *cab* clusters, nucleotide sequences of *plsX-acpP* and *comAB* (from
455 *S. mitis* B6; GenBank Accession GCA_000027165.1), which flank the *cab* locus, were aligned against
456 all genomes using pairwise sequence alignment (Biopython v1.81; match = 2; mismatch = -1; gap
457 open = -5; gap extension = -0.5; minimum overall sequence identity ≥ 90%). Genomes in which *plsX-*
458 *acpP* and *comAB* were absent or located on separate contigs were excluded from further analysis.
459 This region was identified in 253 genomes.

460 To identify mature Cab bacteriocin sequences, extracted sequences were scanned for open
461 reading frames (ORFs) of 100-300 nucleotides, beginning with an ATG start codon and ending with
462 a TAA, TAG or TGA stop codon. Only ORFs whose translated sequences contained a
463 (M/L/V)XXXXGG double-glycine cleavage motif were retained. Mature Cab bacteriocins were
464 obtained by removing the N-terminal signal sequence upstream of the cleavage site. In this work, we
465 defined *cab* bacteriocins as all non-*cib* bacteriocin genes that were found in this particular location.
466 To explore diversity of Cab bacteriocins, sequences were converted into amino acid frequency
467 vectors. Pairwise dissimilarities between sequences were calculated using the Bray-Curtis metric
468 (ScyPy), followed by agglomerative hierarchical clustering (scikit-learn). To determine the optimal
469 number of clusters, silhouette scores (scikit-learn) were computed for cluster numbers ranging from
470 2 to 50. The number of clusters yielding the highest score was selected as optimal.

471 To assess the prevalence of *cibABC* in *S. mitis*, the nucleotide sequence of *cibABC* (from *S.*
472 *pneumoniae* D39, GenBank Accession NC_008533.2) was aligned against all *S. mitis* genomes using
473 NCBI BLASTn. Genomes with no detectable hit were considered *cibABC*-negative. For genomes with
474 partial matches (<100% query coverage), the locus was manually inspected to verify the presence or
475 absence of *cibA*, *cibB*, and *cibC* individually – a common occurrence in strains harboring *cibC* but not
476 *cibAB*.

477 To find SigX boxes, the consensus sequence (65) was searched within *cab* loci using Find
478 Individual Motif Occurrences (FIMO) v5.5.8 (66). Hits with *p*-value <0.001 were considered true SigX

479 boxes. The detection of Cab bacteriocins and putative SigX boxes was benchmarked against six *S.*
480 *mitis* strains with complete genomes and manually curated *cab* loci (27, 67).
481
482 **Phylogeny of *S. mitis***
483 Core genome single-nucleotide polymorphisms (SNPs) were called using Snippy v4.6.0
484 (https://github.com/tseemann/snippy) by aligning *S. mitis* genomes to the *S. mitis* B6 reference
485 genome. The resulting alignment was used to construct a maximum-likelihood phylogenetic tree with
486 FastTree v2.2 (68). The phylogeny was visualized and annotated using the Interactive Tree of Life
487 (iTOL) platform (69).
488
489 **Synthetic peptides**
490 Peptides were produced by solid-phase peptide synthesis with >95% purity (NZYTech) (Table S2)
491 (27, 49-51). CSP and $BlpC_1$ pheromones were resuspended in sterile ddH_2O; $BlpC_4$ was resuspended
492 in 10% acetic acid; and CabA and CabB were resuspended in DMSO. Peptides were serially diluted
493 in sterile ddH_2O and stored at -20ºC.
494
495 **Transformation**
496 For transformation of *S. mitis* and *S. pneumoniae*, cells were grown to an OD_{600} of 0.5, diluted 1:100
497 in pre-warmed $C+Y_{YB}$ and grown until an OD_{600} of 0.04-0.1. Cells were treated with 1 µM of cognate
498 CSP and transformed with 0.4 µg linear DNA, 1 µg plasmid DNA, or 10 µg chromosomal DNA.
499 Transformants were recovered for 4 h and plated in selective medium. Linear, plasmid and genomic
500 DNA were purified using the Zymoclean Gel DNA Recovery Kit (Zymo Research), ZymoPURE
501 Plasmid Miniprep Kit (Zymo Research) and EZ1 DSP Virus Kit (Qiagen), respectively.
502 For heat-shock transformation of *E. coli* DH10B or DH5α, $CaCl_2$-competent cells were mixed
503 with 10% (v/v) of ligation reactions and incubated on ice for 15 min. Cells were then heat-shocked at
504 42ºC for 40 s, immediately chilled on ice, and recovered with 900 µL of SOC (2% tryptone, 0.5% yeast
505 extract, 10 mM NaCl, 2.5 mM KCl, 10 mM $MgCl_2$, 10 mM $MgSO_4$ and 20 mM glucose; pH 7) for 1 h
506 before plating in selective medium.

507

508 **Construction of a fluorescence-luminescence transcriptional reporter**

509 A DNA cassette containing a *hlpA-mNeonGreen* fusion and plasmid pBIR, which integrates in the
510 genome of *S. mitis* G22 and *S. pneumoniae* D39, were synthesized (Twist Bioscience). The reporter
511 cassette and plasmid were amplified and blunt end ligated to generate plasmid pJB10. The firefly
512 luciferase *luc* (from pPEP-LGZ) and plasmid pJB10 were amplified and blunt-end ligated to create
513 plasmid pJB11 encoding a dual fluorescence-luminescence reporter. Transcriptional fusions were
514 created by digesting both pJB11 and promoter fragments with BsaI, followed by ligation. Variants of
515 pJB11 were linearized with BamHI and transformed into *S. mitis* G22 or *S. pneumoniae* D39.
516 Transformants were selected in BA with chloramphenicol.

517

518 **Expression of *cabABC* and other competence genes**

519 *S. mitis* and *S. pneumoniae* strains harboring transcriptional fusions of competence promoters were
520 grown in C+Y_{YB} at pH 6.6 (to prevent natural competence induction) until an OD_{600} of 0.5. To evaluate
521 natural competence dynamics, acidic precultures were diluted 1:100 in C+Y_{YB} (pH 6.6, 7.4 or 8.2)
522 containing 340 µg/mL D-luciferin (Abcam). To assess the effect of different pheromones on
523 competence induction, acidic precultures were diluted to OD_{600} = 0.1 in C+Y_{YB} (pH 6.6) with 340 µg/mL
524 D-luciferin. Then, CSP or BlpC variants (up to 1 µM), were added. Cultures were transferred to white
525 96-well plates with clear bottoms (Nunc). The OD_{595} and luminescence was recorded every 10 min
526 for 24 h in a BioTek Neo2 Multimode Reader with a gain of 185. Luminescence values were
527 normalized to the OD_{595}. D-luciferin was resuspended in sterile ddH_2O to 15 $mg.mL^{-1}$ and kept at -80
528 ºC in single-use aliquots.

529

530 **Construction of ComE, SigX1 and SigX2 deletion mutants**

531 The upstream and downstream flanking regions of *comE, sigX1, sigX2* were amplified from *S. mitis*
532 G22 gDNA. Kanamycin and spectinomycin resistance genes were amplified from pKan and pPEP-
533 LGZ (70), respectively. DNAs were ligated using Gibson Assembly (New England Biolabs) and

534 amplified with nested primers. Transformants were selected in BA with kanamycin (for *comE* and
535 *sigX1*) or spectinomycin (for *sigX2*).
536
537 **Biofilms and transwells**
538 *S. mitis* and *S. pneumoniae* were grown to exponential phase and mixed at a 1:1 ratio (10^5 CFU of
539 each strain) in $C+Y_{YB}$ with 1600 $U.mL^{-1}$ catalase. Two milliliters of the mixtures were added to tissue-
540 culture treated 12- or 24-well plates (Corning) and incubated 24 h at 34ºC with 5% CO_2. Non-adherent
541 cells were removed by aspiration, and biofilms were thoroughly resuspended in PBS. Initial biofilms
542 were performed in 24-well plates, while the remaining were performed in 12-well plates (since these
543 were the ones where we could fit a transwell insert).
544 For transwell biofilms, 1.5 mL of $C+Y_{YB}$ containing catalase and 10^5 CFU of *S. pneumoniae*
545 was added to wells of tissue-culture treated 12-well plates. Transwell inserts containing a 0.4 µm pore
546 polycarbonate membrane (Corning) were placed in the wells, and 0.5 mL of $C+Y_{YB}$ with catalase and
547 10^5 CFU of *S. mitis* were added to the upper insert. Biofilms were recovered from both compartments.
548 In dual-species biofilms, *S. pneumoniae* and *S. mitis* cells were enumerated by plating on BA
549 with chloramphenicol or kanamycin, respectively. In the transwell setup, where *S. pneumoniae* and
550 *S. mitis* were physically separated, biofilm suspensions from both compartments were also plated on
551 selective media to confirm that neither strain had crossed the membrane.
552
553 **Construction of an *S. mitis cab* overexpressor mutant**
554 The plasmid backbone was amplified from pDL278_P23-DsRed-Express2 (Addgene plasmid
555 #121505), and *cabABC* was amplified from *S. mitis* G22 gDNA. The two fragments were blunt-end
556 ligated, generating plasmid pJB09-*cabABC*, in which *cabABC* is placed under the control of the strong
557 constitutive P23 promoter. *S. mitis* transformants were selected in BA with spectinomycin.
558
559 **Inhibitory activity of cell-free supernatants and heat-killed cells**
560 *S. mitis* was grown to early stationary phase and centrifuged at 10,000 g for 30 min at 4ºC. Cell-free
561 supernatants (CFS) were obtained by filtration (0.22 µm). CFS were lyophilized by vacuum

562 evaporation using a SpeedVac concentrator (LabConco) and resuspended in ddH_2O to a
563 concentration of 10x before testing. $C+Y_{YB}$ medium was concentrated in parallel and used as a
564 negative control for inhibitory activity. Cell pellets were washed once in PBS and heat-killed for 15
565 min at 95 ºC. Complete lysis of pellet extracts was confirmed by plating in BA.

566 To test for inhibitory activity of CFS and heat-killed cells, *S. pneumoniae* D39 was grown to
567 an OD_{600} of 0.5, diluted 1:100 in fresh medium, and 180 µL of the dilution was added to clear 96-well
568 plates. Twenty microliters of treatments or water was added to each well and growth was monitored
569 by measuring the OD_{595} every 30 min for 24 h using a Tecan Infinite 200 Pro.

570

571 **Sensitivity of bacteria to CabAB**

572 Exponential-phase cultures of bacterial species (18 *Streptococcus* spp., four additional non-
573 streptococcal Gram-positive species, and four Gram-negative species) were diluted to OD_{600} 0.1 and
574 195 µL was added to wells of clear 96-well plates. CabAB (0.975 µM) or DMSO (0.00975%) was
575 added to wells and growth was recorded by measuring the OD_{595} every 10 min for 24 h using the
576 Tecan Infinite 200. Growth arrest was quantified by comparing the area under the curve (AUC)
577 between CabAB- and DMSO-treated cultures. All further assays using CabAB and DMSO treatments
578 were performed in the same conditions, unless specified otherwise.

579

580 **Construction of autolysis-deficient *S. pneumoniae* mutants**

581 The upstream and downstream regions of *lytA* and *lytC* were amplified from *S. pneumoniae* D39
582 gDNA. The PhunSweet cassette containing *pheS-sacB*-aph*A-3* which confers susceptibility to
583 chlorinated phenylalanine and sucrose, and resistance to kanamycin, was amplified from *S.*
584 *pneumoniae* D39 Δ*cps*::*PhunSweet* gDNA (71). DNAs were assembled using Gibson Assembly and
585 amplified with nested primers. *S. pneumoniae* D39 transformants were selected on BA with
586 kanamycin.

587 To remove the antibiotic resistance cassette, the flanking regions of *lytA* and *lytC* were
588 amplified, assembled with Gibson Assembly, and amplified with nested primers. Transformants were
589 recovered by counterselection on BA with 15 mM chlorinated phenylalanine and 10% sucrose.

590

591 **Scanning electron microscopy (SEM)**

592 *S. pneumoniae* D39 cultures (30 mL) were treated with DMSO or CabAB and incubated for 15 min at
593 37ºC. Cells were harvested by centrifugation (all centrifugations were carried out at 800 g for 10 min
594 at room temperature) and washed three times with PBS. Fixation was performed in 500 μL of 2.5%
595 glutaraldehyde and 1% paraformaldehyde in 0.1 M sodium cacodylate buffer for 30 min at room
596 temperature. Cells were washed three times with 0.1 M sodium cacodylate buffer and dehydrated in
597 increasingly higher ethanol concentrations (50%, 70%, 90%, 100%), by incubating 10 min in 500 μL
598 of each ethanol concentration. Ethanol was replaced with 500 μL tert-butyl alcohol and samples were
599 incubated at 30ºC for 1 h. Then, tert-butyl was removed and replaced with 500 μL of fresh tert-butyl
600 alcohol. Samples were kept at -20ºC overnight. Samples were then lyophilized under vacuum, gold-
601 sputtered using a Cressington 108 sputter coater, and imaged with a Hitachi SU-8010 scanning
602 electron microscope at 1.5kV.

603

604 **Transmission electron microscopy (TEM)**

605 *S. pneumoniae* D39 cultures (30 mL) were treated with DMSO or CabAB, incubated for 15 min at
606 37ºC, and recovered by centrifugation at 800 g. Cells were fixed with 2% formaldehyde, 2.5%
607 glutaraldehyde, 0.075% ruthenium red and 1.55 % lysine acetate in distilled water for 20 min at 4ºC.
608 Cells were washed twice in 0.075% ruthenium red, resuspended in 2% formaldehyde, 2.5%
609 glutaraldehyde and 0.075% ruthenium red, and incubated overnight at 4ºC. Cells were washed three
610 times with 0.075% ruthenium red and further processed at Instituto Gulbenkian de Ciência. Cells were
611 embedded in 2% low-melting point agarose and fixed with 1% osmium tetroxide and 0.06% ruthenium
612 red for 1 h at room temperature. Cells were washed once with 0.1 M sodium cacodylate buffer and
613 twice with distilled water. Dehydration was performed on ice using increasing concentrations of
614 ethanol (10%, 30%, 50%; 10 min each). Samples were stained overnight at 4ºC with 2% uranyl
615 acetate in 70% ethanol, followed by further dehydration with 90% ethanol and three times with 100%
616 ethanol. Infiltration was carried out with increasing concentrations of epoxy resin in ethanol (3:1, 1:1,

617 1:3), and 100% resin overnight, followed by two exchanges of 100% resin. Ultrathin sections were cut
618 and imaged on a Tecnai G2 Spirit BioTWIN Transmission Electron Microscope (FEI) equipped with
619 an Olympus-SIS Veleta CCD camera.

620 Large intracellular aggregates were observed in some CabAB-treated cells. To quantify these
621 structures, micrographs of CabAB- and DMSO-treated cells were blindly evaluated by two
622 researchers. Each researcher was first shown representative cells with and without aggregates, and
623 then independently counted the number of cells containing these structures. The final percentage of
624 cells with aggregates was calculated as the average between both researcher counts.

625

626 **Permeabilization and depolarization of *S. pneumoniae* membranes**

627 *S. pneumoniae* D39 cultures were treated with DMSO or CabAB. One-milliliter aliquots were taken at
628 0, 2, 5, 15, 30, 60, and 120 min post treatment and immediately chilled on ice. Cells were washed
629 twice with PBS and kept on ice. Cells were stained with 6 μM propidium iodide (Invitrogen) and 3 μM
630 $DiBAC_4(3)$ (Enzo Life Sciences) for 5 min at room temperature, protected from light. Cells were
631 centrifuged, resuspended in PBS, and added to black 96-well plates with clear bottoms (Nunc).
632 Fluorescence intensity was measured using a BioTek Neo2 Multimode Reader under the following
633 settings: shake for 5 s; propidium iodide – top reading, 535 ± 12 nm excitation, 617 ± 12 nm emission
634 and 120 gain; $DiBAC_4(3)$ – top reading, 492 ± 9 nm excitation, 518 ± 9 emission, 120 gain).
635 Fluorescent values were normalized to the OD_{595}.

636

637 **Efflux of ATP**

638 Cultures of *S. pneumoniae* were treated with DMSO or CabAB. Aliquots were taken at 0, 15 and 120
639 min post-treatment and kept on ice. Cells were centrifuged, and supernatants were filtered (0.22 μm)
640 and maintained on ice. Cells were permeabilized in DMSO for 10 min at room temperature. Both cells
641 and supernatants were diluted 1:10 in ddH_2O and kept on ice.

642 Extracellular and intracellular ATP was measured with the ATP Luminescent Cell Viability
643 Assay (Millipore) according to instructions. Luminescence was measured in a BioTek Neo2 Multimode

644 Reader using a gain of 150 and integration time of 10 s. An ATP standard curve confirmed linear
645 detection within the range of 0.2 μM to 2 mM ATP. Total ATP was calculated by summing
646 luminescence values from both the cell and supernatant fractions under each condition.
647
648 **Construction of *S. mitis* harboring HA-tagged bacteriocins**
649 DNAs containing HA (YPYDVPDYA)-tagged *cabA* and *cabB* were synthesized (Twist Bioscience).
650 The regions upstream (including the native promoter) and downstream (including a chloramphenicol
651 resistance cassette) of the *cab* operon were amplified from pJB11-*cabABC*. DNAs were assembled
652 by Gibson Assembly and amplified with nested primers. The resulting constructs were transformed
653 into the *S. mitis* Δ*cabABC* background, generating two mutant strains: *cabA-HA cabBC* and *cabA*
654 *cab-HA cabC.* Transformants were selected in BA with chloramphenicol.
655
656 **Confocal microscopy and immunofluorescence**
657 To quantify the percentage of cells that become membrane-permeable, *S. pneumoniae* was treated
658 with DMSO or CabAB. Cells were recovered by centrifugation (9600 g, 4ºC, 3 min) and washed three
659 times with PBS. Cells were stained with 30 μM propidium iodide and 5 μM SYTO 9 for 15 min at room
660 temperature, protected from light.
661 To determine whether large intracellular structures observed in CabAB-treated *S. pneumoniae*
662 cells corresponded to membranes, treated cells were washed three times with PBS and stained with
663 20 $\mu g.mL^{-1}$ FM4-64 and 15 $\mu g.mL^{-1}$ DAPI for 5 min at room temperature, protected from light.
664 For immunofluorescence of live competent bacteria, *S. mitis* harboring HA-tagged bacteriocins
665 were grown in acidic $C+Y_{YB}$ and diluted to OD_{600} = 0.1 in pre-warmed $C+Y_{YB}$. CSP_{G22} was added at 1
666 μM, and cells were incubated for 70 min at 37ºC and then chilled on ice. To retain the competent
667 status of cells, all subsequent steps were performed on ice using ice-cold solutions. Cells were
668 centrifuged (9600 g, 4ºC, 3 min) and washed twice in PBS. Blocking was performed in PBS with 5%
669 bovine serum albumin (BSA) for 1 h. Cells were pelleted and resuspended in 100 μL of primary rabbit
670 monoclonal anti-HA antibody (clone C29F4; Cell Signaling Technology) diluted 1:100 in PBS with 1%

671 BSA, and incubated for 1 h. Cells were washed twice in PBS with 0.1% Tween 20, resuspended in
672 100 µL of Alexa Fluor 488-conjugated goat anti-rabbit secondary antibody (Invitrogen) diluted 1:500
673 in PBS with 1% BSA, and incubated 1 h protected from light. Cells were washed twice with PBS
674 containing 0.1% Tween 20 and once with PBS. Cells were then stained with 20 µg.mL^{-1} FM4-64 and
675 15 µg.mL^{-1} DAPI for 5 at room temperature, covered from light.

676 Immediately before imaging, cells were mounted on thin 1.7% agarose pads. Fluorescence
677 imaging was performed using a Zeiss LSM 880 point scanning confocal microscope equipped with
678 an Airyscan detector. Samples were imaged with a Plan-Apochromat 63x/1.4 Oil DIC M27 objective
679 (Zeiss), using laser lines 405 nm (DAPI), 488 nm (SYTO 9 and Alexa Fluor 488), and 561 nm (FM4-
680 64 and propidium iodide). Imaging was performed at laser intensities of 2-3% and a gain of 700 for
681 DAPI, 700 for SYTO 9, 1000 for Alexa Fluor 488, 900 for FM4-64, and 700 for propidium iodide. The
682 Zeiss Zen v3.0 was used to control the microscope and for Airyscan processing. Image analysis was
683 conducted using ImageJ/FIJI v2.14 (72).

684

685 **Construction of a transformation-deficient *S. pneumoniae* mutant**

686 The upstream and downstream regions of *comGC* were amplified from *S. pneumoniae* D39 gDNA,
687 and *tetM* was amplified from *S. mitis* F22 gDNA. DNAs were ligated by Gibson Assembly and
688 amplified using nested primers. *S. pneumoniae* transformants were selected in BA with tetracycline.

689

690 **Horizontal gene transfer in biofilms**

691 Dual-species biofilms of *S. pneumoniae* D39-GFP Δ*comGC* (chloramphenicol and tetracycline
692 resistant; Chl^R Tet^R) and *S. mitis* (kanamycin resistant; Kan^R) were grown as described above, except
693 that C+Y_{YB} was adjusted to pH 6.6 to prevent natural competence induction. After 24h, non-adherent
694 cells were removed by aspiration, and 2 mL of fresh C+Y_{YB} (pH 7.4) containing catalase and 1 µM of
695 CSP_{G22} were added to biofilms. After 6 h of incubation at 34ºC with 5% CO_2, biofilm cells were
696 thoroughly resuspended in PBS and recovered by centrifugation.

697 Cells were plated on the following selective media: (i) BA with kanamycin to quantify total *S.*
698 *mitis* (Kan^R); (ii) BA with kanamycin and chloramphenicol to detect *S. mitis* transformants that have

699 acquired chloramphenicol resistance (Kan^R Chl^R), either with or without tetracycline resistance; (iii)
700 BA with kanamycin and tetracycline to detect *S. mitis* transformants that acquired tetracycline
701 resistance (Kan^R Tet^R), either with or without chloramphenicol resistance; (iv) BA with kanamycin,
702 chloramphenicol and tetracycline to identify *S. mitis* transformants that acquired both resistances
703 (Kan^R Chl^R Tet^R); (v) and BA with chloramphenicol and tetracycline (without kanamycin) to detect *S.*
704 *pneumoniae* loads.

705 Transformants were counted after 48 h of incubation. *S. mitis* transformation frequencies were
706 calculated as the ratio between the number of transformants (Kan^R colonies also resistant to
707 chloramphenicol and/or tetracycline) and the total number of Kan^R colonies. *S. mitis* G22 Δ*comE* was
708 used as a non-transformable control, in which acquisition of chloramphenicol and tetracycline
709 resistance should not occur via transformation.

710

711 **Statistical analyses**

712 The two-tailed unpaired *Mann-Whitney U* test with Benjamini and Hochberg correction for FDR was
713 used to compare bacterial loads. Student's *t*-test with Benjamini and Hochberg correction for FDR
714 was used to compare gene expression. The ratio paired *t*-test was used for the statistical analysis of
715 bacterial proportions in multi-species biofilms. All statistical analysis were computed using GraphPad
716 Prism 9.0 and considered significant at *P*-value ≤ 0.05.

717

718 **Data availability**

719 All data is available from the corresponding author upon reasonable request.

720

721 **Acknowledgements**

722 We are grateful to Jan-Willem Veening (University of Lausanne) and Morten Kjos (Norwegian
723 University of Life Sciences) for providing plasmids pPEP-LGZ and Jason Rosch (St. Jude Children's
724 Research Hospital) for providing *S. pneumoniae* strain harboring a PhunSweet cassette. We also

acknowledge Luisa N. Hiller (Carnegie Mellon University) and Adriano O. Henriques (ITQB NOVA) for fruitful discussions.

Funding

This work was supported by FCT – Fundação para a Ciência e Tecnologia, I.P., through project STOPneumo (PTDC/BIA-MIC/30703/2017), MOSTMICRO-ITQB R&D Unit (doi.org/10.54499/UID/04612/2025, UID/PRR/4612/2025), LS4FUTURE Associated Laboratory (DOI 10.54499/LA/P/0087/2020), and PPBI - Portuguese Platform of BioImaging (PPBI-POCI-01-0145-FEDER-022122) co-funded by national funds from OE - "Orçamento de Estado" and by european funds from FEDER - "Fundo Europeu de Desenvolvimento Regional". J. Borralho and J. Lança were supported by PhD fellowships (2021.07866.BD - doi.org/10.54499/2021.07866.BD and UI/BD/153385/2022 - doi.org/10.54499/UI/BD/153385/2022).

Author Contributions: R. Sá-Leão and J. Borralho contributed to the concept and design of the study. R. Sá-Leão contributed with reagents and materials. Data acquisition was performed by J. Borralho, J. Lança, J. Bryton and W. Antunes. Data was interpreted by J. Borralho, J. Lança, J. Bryton, W. Antunes and R. Sá-Leão. The manuscript was drafted by J. Borralho and R. Sá-Leão. All authors critically revised and approved the final version of the manuscript.

Competing Interest Statement: Universidade NOVA de Lisboa has filed a provisional patent application that covers pharmaceutical compositions comprising strain G22 and/or bacteriocin molecules, and derivatives thereof, which can inhibit the growth and persistence of the pathogen *S. pneumoniae* (PT119647).

References

1. Griffith F. 1928. The significance of pneumococcal types. J Hyg (Lond) 27:113-59.

751 2. Håvarstein LS, Coomaraswamy G, Morrison DA. 1995. An unmodified heptadecapeptide
752 pheromone induces competence for genetic transformation in *Streptococcus pneumoniae*.
753 Proc Natl Acad Sci U S A 92:11140-4.
754 3. Håvarstein LS, Gaustad P, Nes IF, Morrison DA. 1996. Identification of the streptococcal
755 competence-pheromone receptor. Mol Microbiol 21:863-9.
756 4. Hui FM, Morrison DA. 1991. Genetic transformation in *Streptococcus pneumoniae*: nucleotide
757 sequence analysis shows *comA*, a gene required for competence induction, to be a member
758 of the bacterial ATP-dependent transport protein family. J Bacteriol 173:372-81.
759 5. Pestova EV, Håvarstein LS, Morrison DA. 1996. Regulation of competence for genetic
760 transformation in *Streptococcus pneumoniae* by an auto-induced peptide pheromone and a
761 two-component regulatory system. Mol Microbiol 21:853-62.
762 6. Lee MS, Morrison DA. 1999. Identification of a new regulator in *Streptococcus pneumoniae*
763 linking quorum sensing to competence for genetic transformation. J Bacteriol 181:5004-16.
764 7. Peterson SN, Sung CK, Cline R, Desai BV, Snesrud EC, Luo P, Walling J, Li H, Mintz M,
765 Tsegaye G, Burr PC, Do Y, Ahn S, Gilbert J, Fleischmann RD, Morrison DA. 2004.
766 Identification of competence pheromone responsive genes in *Streptococcus pneumoniae* by
767 use of DNA microarrays. Mol Microbiol 51:1051-70.
768 8. Guiral S, Mitchell TJ, Martin B, Claverys JP. 2005. Competence-programmed predation of
769 noncompetent cells in the human pathogen *Streptococcus pneumoniae*: genetic
770 requirements. Proc Natl Acad Sci U S A 102:8710-5.
771 9. Moreno-Gámez S, Sorg RA, Domenech A, Kjos M, Weissing FJ, van Doorn GS, Veening JW.
772 2017. Quorum sensing integrates environmental cues, cell density and cell history to control
773 bacterial competence. Nat Commun 8:854.
774 10. Prudhomme M, Berge M, Martin B, Polard P. 2016. Pneumococcal competence coordination
775 relies on a cell-contact sensing mechanism. PLoS Genet 12:e1006113.
776 11. Prudhomme M, Johnston CHG, Soulet AL, Boyeldieu A, De Lemos D, Campo N, Polard P.
777 2024. Pneumococcal competence is a populational health sensor driving multilevel
778 heterogeneity in response to antibiotics. Nat Commun 15:5625.

779 12. Johnsborg O, Eldholm V, Bjørnstad ML, Håvarstein LS. 2008. A predatory mechanism
780 dramatically increases the efficiency of lateral gene transfer in *Streptococcus pneumoniae* and
781 related commensal species. Mol Microbiol 69:245-53.
782 13. Shen P, Lees JA, Bee GCW, Brown SP, Weiser JN. 2019. Pneumococcal quorum sensing
783 drives an asymmetric owner-intruder competitive strategy during carriage via the competence
784 regulon. Nat Microbiol 4:198-208.
785 14. Hohwy J, Reinholdt J, Kilian M. 2001. Population dynamics of *Streptococcus mitis* in its natural
786 habitat. Infect Immun 69:6055-63.
787 15. Salvadori G, Junges R, Morrison DA, Petersen FC. 2019. Competence in *Streptococcus*
788 *pneumoniae* and close commensal relatives: mechanisms and implications. Front Cell Infect
789 Microbiol 9:94.
790 16. Salvadori G, Junges R, Åmdal HA, Chen T, Morrison DA, Petersen FC. 2018. High-resolution
791 profiles of the *Streptococcus mitis* CSP signaling pathway reveal core and strain-specific
792 regulated genes. BMC Genomics 19:453.
793 17. Berg KH, Biørnstad TJ, Johnsborg O, Håvarstein LS. 2012. Properties and biological role of
794 streptococcal fratricins. Appl Environ Microbiol 78:3515-22.
795 18. Potgieter E, Chalkley LJ. 1995. Relatedness among penicillin-binding protein 2b genes of
796 *Streptococcus mitis*, *Streptococcus oralis*, and *Streptococcus pneumoniae*. Microb Drug
797 Resist 1:35-42.
798 19. Hakenbeck R. 2000. Transformation in *Streptococcus pneumoniae*: mosaic genes and the
799 regulation of competence. Res Microbiol 151:453-6.
800 20. Rieger M, Mauch H, Hakenbeck R. 2017. Long persistence of a *Streptococcus pneumoniae*
801 23F clone in a cystic fibrosis patient. mSphere 2.
802 21. Lessa FC, Milucky J, Rouphael NG, Bennett NM, Talbot HK, Harrison LH, Farley MM, Walston
803 J, Pimenta F, Gertz RE, Rajam G, Carvalho MDG, Beall B, Whitney CG. 2018. *Streptococcus*
804 *mitis* expressing pneumococcal serotype 1 capsule. Sci Rep 8:17959.
805 22. Pimenta F, Gertz RE, Park SH, Kim E, Moura I, Milucky J, Rouphael N, Farley MM, Harrison
806 LH, Bennett NM, Bigogo G, Feikin DR, Breiman R, Lessa FC, Whitney CG, Rajam G, Schiffer

807 J, da Gloria Carvalho M, Beall B. 2018. *Streptococcus infantis*, *Streptococcus mitis*, and
808 *Streptococcus oralis* strains with highly similar *cps5* loci and antigenic relatedness to serotype
809 5 pneumococci. Front Microbiol 9:3199.
810 23. Kalizang'oma A, Richard D, Kwambana-Adams B, Coelho J, Broughton K, Pichon B, Hopkins
811 KL, Chalker V, Beleza S, Bentley SD, Chaguza C, Heyderman RS. 2024. Population genomics
812 of *Streptococcus mitis* in UK and Ireland bloodstream infection and infective endocarditis
813 cases. Nat Commun 15:7812.
814 24. Skov Sørensen UB, Yao K, Yang Y, Tettelin H, Kilian M. 2016. Capsular polysaccharide
815 expression in commensal *Streptococcus* species: genetic and antigenic similarities to
816 *Streptococcus pneumoniae*. mBio 7.
817 25. Denapaite D, Brückner R, Nuhn M, Reichmann P, Henrich B, Maurer P, Schähle Y, Selbmann
818 P, Zimmermann W, Wambutt R, Hakenbeck R. 2010. The genome of *Streptococcus mitis* B6
819 - what is a commensal? PLoS One 5:e9426.
820 26. Ikryannikova LN, Malakhova MV, Lominadze GG, Karpova IY, Kostryukova ES, Mayansky
821 NA, Kruglov AN, Klimova EA, Lisitsina ES, Ilina EN, Govorun VM. 2017. Inhibitory effect of
822 streptococci on the growth of *M. catarrhalis* strains and the diversity of putative bacteriocin-
823 like gene loci in the genomes of *S. pneumoniae* and its relatives. AMB Express 7:218.
824 27. Borralho J, Handem S, Lança J, Ferreira B, Candeias C, Henriques AO, Hiller NL, Valente C,
825 Sá-Leão R. 2025. Inhibition of pneumococcal growth and biofilm formation by human isolates
826 of *Streptococcus mitis* and *Streptococcus oralis*. Appl Environ Microbiol 91:e0133624.
827 28. Lehtinen S, Croucher NJ, Blanquart F, Fraser C. 2022. Epidemiological dynamics of
828 bacteriocin competition and antibiotic resistance. Proc Biol Sci 289:20221197.
829 29. Håvarstein LS, Diep DB, Nes IF. 1995. A family of bacteriocin ABC transporters carry out
830 proteolytic processing of their substrates concomitant with export. Mol Microbiol 16:229-40.
831 30. Sati H, Carrara E, Savoldi A, Hansen P, Garlasco J, Campagnaro E, Boccia S, Castillo-Polo
832 JA, Magrini E, Garcia-Vello P, Wool E, Gigante V, Duffy E, Cassini A, Huttner B, Pardo PR,
833 Naghavi M, Mirzayev F, Zignol M, Cameron A, Tacconelli E, Group WBPPLA. 2025. The WHO

834 Bacterial Priority Pathogens List 2024: a prioritisation study to guide research, development,
835 and public health strategies against antimicrobial resistance. Lancet Infect Dis.
836 31. Kilian M, Poulsen K, Blomqvist T, Håvarstein LS, Bek-Thomsen M, Tettelin H, Sørensen UB.
837 2008. Evolution of *Streptococcus pneumoniae* and its close commensal relatives. PLoS One
838 3:e2683.
839 32. Pozzi G, Masala L, Iannelli F, Manganelli R, Havarstein LS, Piccoli L, Simon D, Morrison DA.
840 1996. Competence for genetic transformation in encapsulated strains of *Streptococcus*
841 *pneumoniae*: two allelic variants of the peptide pheromone. J Bacteriol 178:6087-90.
842 33. Nes IF, Diep DB, Holo H. 2007. Bacteriocin diversity in *Streptococcus* and *Enterococcus*. J
843 Bacteriol 189:1189-98.
844 34. Meza-Torres J, Lelek M, Quereda JJ, Sachse M, Manina G, Ershov D, Tinevez JY,
845 Radoshevich L, Maudet C, Chaze T, Giai Gianetto Q, Matondo M, Lecuit M, Martin-Verstraete
846 I, Zimmer C, Bierne H, Dussurget O, Cossart P, Pizarro-Cerdá J. 2021. Listeriolysin S: A
847 bacteriocin from *Listeria monocytogenes* that induces membrane permeabilization in a
848 contact-dependent manner. Proc Natl Acad Sci U S A 118.
849 35. García-Bayona L, Guo MS, Laub MT. 2017. Contact-dependent killing by
850 *Caulobacter crescentus* via cell surface-associated, glycine zipper proteins. Elife 6.
851 36. Oppegård C, Schmidt J, Kristiansen PE, Nissen-Meyer J. 2008. Mutational analysis of putative
852 helix-helix interacting GxxxG-motifs and tryptophan residues in the two-peptide bacteriocin
853 lactococcin G. Biochemistry 47:5242-9.
854 37. Ekblad B, Kyriakou PK, Oppegård C, Nissen-Meyer J, Kaznessis YN, Kristiansen PE. 2016.
855 Structure-function analysis of the two-peptide bacteriocin plantaricin EF. Biochemistry
856 55:5106-16.
857 38. Ekblad B, Kristiansen PE. 2019. NMR structures and mutational analysis of the two peptides
858 constituting the bacteriocin plantaricin S. Sci Rep 9:2333.
859 39. Moll G, Ubbink-Kok T, Hildeng-Hauge H, Nissen-Meyer J, Nes IF, Konings WN, Driessen AJ.
860 1996. Lactococcin G is a potassium ion-conducting, two-component bacteriocin. J Bacteriol
861 178:600-5.

862 40. McAuliffe O, Ryan MP, Ross RP, Hill C, Breeuwer P, Abee T. 1998. Lacticin 3147, a broad-
863 spectrum bacteriocin which selectively dissipates the membrane potential. Appl Environ
864 Microbiol 64:439-45.
865 41. Moll GN, van den Akker E, Hauge HH, Nissen-Meyer J, Nes IF, Konings WN, Driessen AJ.
866 1999. Complementary and overlapping selectivity of the two-peptide bacteriocins plantaricin
867 EF and JK. J Bacteriol 181:4848-52.
868 42. Zhang X, Wang Y, Liu L, Wei Y, Shang N, Li P. 2016. Two-peptide bacteriocin PlnEF causes
869 cell membrane damage to Lactobacillus plantarum. Biochim Biophys Acta 1858:274-80.
870 43. Wei H, Håvarstein LS. 2012. Fratricide is essential for efficient gene transfer between
871 pneumococci in biofilms. Appl Environ Microbiol 78:5897-905.
872 44. Steinmoen H, Knutsen E, Håvarstein LS. 2002. Induction of natural competence in
873 *Streptococcus pneumoniae* triggers lysis and DNA release from a subfraction of the cell
874 population. Proc Natl Acad Sci U S A 99:7681-6.
875 45. Ganaie F, Branche AR, Peasley M, Rosch JW, Nahm MH. 2022. Effect of oral streptococci
876 expressing pneumococcus-like cross-reactive capsule types on World Health Organization
877 recommended pneumococcal carriage detection procedure. Clin Infect Dis 75:647-656.
878 46. Peterson S, Cline RT, Tettelin H, Sharov V, Morrison DA. 2000. Gene expression analysis of
879 the *Streptococcus pneumoniae* competence regulons by use of DNA microarrays. J Bacteriol
880 182:6192-202.
881 47. Rimini R, Jansson B, Feger G, Roberts TC, de Francesco M, Gozzi A, Faggioni F, Domenici
882 E, Wallace DM, Frandsen N, Polissi A. 2000. Global analysis of transcription kinetics during
883 competence development in *Streptococcus pneumoniae* using high density DNA arrays. Mol
884 Microbiol 36:1279-92.
885 48. García E. 2025. Structure, function, and regulation of LytA: the N-acetylmuramoyl-L-alanine
886 amidase driving the "suicidal tendencies" of *Streptococcus pneumoniae-a review*.
887 Microorganisms 13.
888 49. Whatmore AM, Barcus VA, Dowson CG. 1999. Genetic diversity of the streptococcal
889 competence (*com*) gene locus. J Bacteriol 181:3144-54.

890 50. Carrolo M, Pinto FR, Melo-Cristino J, Ramirez M. 2009. Pherotypes are driving genetic
891 differentiation within *Streptococcus pneumoniae*. BMC Microbiol 9:191.
892 51. Vestrheim DF, Gaustad P, Aaberge IS, Caugant DA. 2011. Pherotypes of pneumococcal
893 strains co-existing in healthy children. Infect Genet Evol 11:1703-8.
894 52. Aras RA, Kang J, Tschumi AI, Harasaki Y, Blaser MJ. 2003. Extensive repetitive DNA
895 facilitates prokaryotic genome plasticity. Proc Natl Acad Sci U S A 100:13579-84.
896 53. Wang D, Li S, Guo F, Ning K, Wang L. 2017. Core-genome scaffold comparison reveals the
897 prevalence that inversion events are associated with pairs of inverted repeats. BMC Genomics
898 18:268.
899 54. Treangen TJ, Abraham AL, Touchon M, Rocha EP. 2009. Genesis, effects and fates of
900 repeats in prokaryotic genomes. FEMS Microbiol Rev 33:539-71.
901 55. Bogaardt C, van Tonder AJ, Brueggemann AB. 2015. Genomic analyses of pneumococci
902 reveal a wide diversity of bacteriocins - including pneumocyclicin, a novel circular bacteriocin.
903 BMC Genomics 16:554.
904 56. Puls JS, Winnerling B, Power JJ, Krüger AM, Brajtenbach D, Johnson M, Bilici K, Camus L,
905 Fließwasser T, Schneider T, Sahl HG, Ghosal D, Kubitscheck U, Heilbronner S, Grein F. 2024.
906 *Staphylococcus epidermidis* bacteriocin A37 kills natural competitors with a unique
907 mechanism of action. ISME J 18.
908 57. Borgeaud S, Metzger LC, Scrignari T, Blokesch M. 2015. The type VI secretion system of
909 *Vibrio cholerae* fosters horizontal gene transfer. Science 347:63-7.
910 58. Zhu L, Kuang Z, Wilson BA, Lau GW. 2013. Competence-independent activity of
911 pneumococcal EndA mediates degradation of extracellular DNA and nets and is important for
912 virulence. PLoS One 8:e70363.
913 59. Salvadori G, Junges R, Morrison DA, Petersen FC. 2016. Overcoming the barrier of low
914 efficiency during genetic transformation of *Streptococcus mitis*. Front Microbiol 7:1009.
915 60. Cowley LA, Petersen FC, Junges R, Jimson D Jimenez M, Morrison DA, Hanage WP. 2018.
916 Evolution via recombination: cell-to-cell contact facilitates larger recombination events in
917 *Streptococcus pneumoniae*. PLoS Genet 14:e1007410.

918 61. Marks LR, Reddinger RM, Hakansson AP. 2012. High levels of genetic recombination during
919 nasopharyngeal carriage and biofilm formation in *Streptococcus pneumoniae*. mBio 3.
920 62. Majewski J, Zawadzki P, Pickerill P, Cohan FM, Dowson CG. 2000. Barriers to genetic
921 exchange between bacterial species: *Streptococcus pneumoniae* transformation. J Bacteriol
922 182:1016-23.
923 63. Davison C, Tallman S, de Ste-Croix M, Antonio M, Oggioni MR, Kwambana-Adams B, Freund
924 F, Beleza S. 2024. Long-term evolution of *Streptococcus mitis* and *Streptococcus pneumoniae*
925 leads to higher genetic diversity within rather than between human populations. PLoS Genet
926 20:e1011317.
927 64. Stevens KE, Chang D, Zwack EE, Sebert ME. 2011. Competence in *Streptococcus*
928 *pneumoniae* is regulated by the rate of ribosomal decoding errors. mBio 2.
929 65. Campbell EA, Choi SY, Masure HR. 1998. A competence regulon in *Streptococcus*
930 *pneumoniae* revealed by genomic analysis. Mol Microbiol 27:929-39.
931 66. Grant CE, Bailey TL, Noble WS. 2011. FIMO: scanning for occurrences of a given motif.
932 Bioinformatics 27:1017-8.
933 67. Handem S, Ferreira B, Valente C, Sá-Leão R. 2025. Genomic and functional insights into
934 commensal streptococci with anti-pneumococcal activity. BMC Genomics 26:577.
935 68. Price MN, Dehal PS, Arkin AP. 2010. FastTree 2--approximately maximum-likelihood trees for
936 large alignments. PLoS One 5:e9490.
937 69. Letunic I, Bork P. 2024. Interactive Tree of Life (iTOL) v6: recent updates to the phylogenetic
938 tree display and annotation tool. Nucleic Acids Res 52:W78-W82.
939 70. Kjos M, Miller E, Slager J, Lake FB, Gericke O, Roberts IS, Rozen DE, Veening JW. 2016.
940 Expression of *Streptococcus pneumoniae* bacteriocins is induced by antibiotics via regulatory
941 interplay with the competence system. PLoS Pathog 12:e1005422.
942 71. Echlin H, Rosch JW. 2020. Advancing genetic tools in *Streptococcus pneumoniae*. Genes
943 (Basel) 11.
944 72. Schindelin J, Arganda-Carreras I, Frise E, Kaynig V, Longair M, Pietzsch T, Preibisch S,
945 Rueden C, Saalfeld S, Schmid B, Tinevez JY, White DJ, Hartenstein V, Eliceiri K, Tomancak

P, Cardona A. 2012. Fiji: an open-source platform for biological-image analysis. Nat Methods 9:676-82.

974 **Figure Legends**

975 **Fig. 1.** *Streptococcus mitis* genomes encode a plethora of competence-associated bacteriocins (*cab*).
976 (A) Core-SNP phylogeny of 253 *S. mitis* genomes and distribution of competence-induced
977 bacteriocins A and B (*cibAB*), dedicated immunity (*cibC*), and competence-associated bacteriocin
978 (*cab*) genes. (B) Prevalence of CibAB and 95 Cab variants in the *S. mitis* population. (C) Rarefaction
979 analysis of mature Cab amino acid sequences found in the *S. mitis* population.

980

981 **Fig. 2.** Cab bacteriocins are expressed at the late phase of competence. (A) Genetic organization of
982 *cab* cluster of strain *S. mitis* G22, containing two putative bacteriocin (*cabAB*) and an immunity protein
983 (*cabC*) upstream of the ABC-transporter *comAB* genes. The *cabABC* operon promoter (P*cabABC*)
984 contains five tandem copies of SigX-binding sites (SigX box; SigX is the alternative sigma factor that
985 controls gene expression during the late phase of competence). Expression of *comAB* is driven from
986 a different promoter and induced by ComE (represented as an orange circle). (B) Expression of
987 *cabABC* in *S. mitis* G22 containing a P*cabABC*-luciferase (*luc*) reporter, ectopically inserted in its
988 genome. Expression of *cabABC* was inferred by expression of *luc*. *S. mitis* was pre-grown in acidic
989 medium to avoid natural competence development and synthetic cognate competence-stimulating
990 peptide (CSP_{G22}) was added to wild-type *S. mitis* and mutants lacking competence regulators. (C)
991 Dose-response of *cabABC* expression across CSP_{G22} concentrations for the *S. mitis luc* reporter
992 containing either the full-length P*cabABC* promoter (which contains five SigX boxes), or a truncated
993 version containing only the most proximal SigX box. (D) Number of SigX boxes within *cab* clusters of
994 varied sizes. Data in panels B and C represent three to four independent experiments. Unpaired *t*-
995 tests were performed to compare *cab* expression. ** $P < 0.05$, *** $P < 0.001$, **** $P < 0.0001$.

996

997 **Fig. 3.** *S. mitis* and *S. pneumoniae* crosstalk through production of distinct CSP pheromones. (A)
998 Effect of CSP pheromones of close streptococci on *cabABC* expression in *S. mitis* G22 and alignment
999 of tested CSP variants (purple – Q14 amino acid residue, present only in inducing peptides). *S. mitis*
1000 G22 P*cabABC-luc* was pre-grown in acidic medium, to which exogenous CSP was added. (B) Effect

1001 of CSP with substitutions in residue 14 in the activation of *cabABC* expression in *S. mitis* G22. (C)
1002 Effect of CSP with substitutions in residue 14 in the activation of competence in *S. pneumoniae* of
1003 pherotype CSP-1 (P*comCDE-luc*). Dotted lines represent average luminescence value for nontreated
1004 controls. Experiments were repeated three times, independently. Unpaired *t*-tests were performed to
1005 compare *cab* expression. **** $P < 0.0001$. ns not significant.
1006
1007 **Fig. 4.** *S. mitis* bacteriocins CabAB mediate contact-dependent growth inhibition of *S. pneumoniae*.
1008 Experiments were done using *S. mitis* G22 Δ*blp4*Δ*blp1* and *S. pneumoniae* D39. The bacteriocin
1009 clusters *blp4* and *blp1* were first deleted from the genome of *S. mitis* G22 as they have anti-
1010 pneumococcal activity (27), which could obscure CabAB-mediated effects. (A) Proportion of *S. mitis*
1011 and *S. pneumoniae* in dual-species biofilm grown for 24 h in competence-permissive conditions in
1012 24-well plates. *S. mitis* mutant p(cab^+) contains the native *cabABC* copy, and an additional copy under
1013 constitutive regulation (promoter *p23*) in a multicopy plasmid. (B) *S. mitis* was grown in competence-
1014 permissive conditions. Cell-free supernatants (CFS) were recovered and cell pellets were boiled. CFS
1015 and heat-killed cells were added to *S. pneumoniae* cultures and growth was monitored. (C) Bacterial
1016 loads of *S. pneumoniae* grown in the presence of *S. mitis* in direct contact (left) or separated with a
1017 0.4 μm pore transwell membrane (right). Biofilms were grown in 12-well plates. As the surface area
1018 available for cell attachment is higher in 12-well plates than in 24-well plates, we hypothesize that this
1019 contributed to the observed differences in maximum cell counts for D39. (D) Corresponding bacterial
1020 loads of *S. mitis* G22 in experiment (C). (E) Representative images of CabA-HA and CabB-HA
1021 immunodetection on the surface of live competent *S. mitis* cells containing the native *cabABC*
1022 (negative control), *cabA-HA cabBC* or *cabA cabB-HA cabC* genotypes. *S. mitis* cultures were induced
1023 with CSP_{G22}, incubated with a primary anti-HA rabbit antibody, and then with an Alexa Fluor 488-
1024 conjugated goat anti-rabbit secondary antibody. Cells were stained with FM4-64 (membrane dye) and
1025 DAPI (nucleic acid dye). At least ten independent fields were detected per experiment/condition.
1026 Experiments were repeated at least three times, independently. The ratio paired *t*-test was used to

1027 compare bacterial proportions in dual-species biofilms. The two-tailed unpaired Mann-Whitney U test
1028 was used to compare bacterial loads. ** $P < 0.01$. *** $P < 0.001$. ns not significant.
1029
1030 **Fig. 5.** CabAB is a two-peptide bacteriocin with LytA-dependent bactericidal activity against *S.*
1031 *pneumoniae.* (A) *S. pneumoniae* was treated with synthetic CabA, CabB, an equimolar mixture of
1032 CabA and CabB (0.975 μM), or with DMSO (solvent where peptides were resuspended). Growth was
1033 recorded for 24 h. (B) Presence of GxxxG and GxxxG-like amino acid motifs in CabA and CabB
1034 sequences. (C) Exponential cultures of wild-type and autolysin-deficient *S. pneumoniae* were treated
1035 with DMSO (grey) or synthetic CabAB (purple). Growth was recorded for 24 h. For easier visualization
1036 of lysis (decrease in optical density), the first 12 h of growth is represented. Growth curves were
1037 repeated three times independently, and one representative experiment with two technical replicates
1038 per condition is shown.
1039
1040 **Fig. 6.** CabAB leads to permeabilization and depolarization of *S. pneumoniae* membranes, leading
1041 to metabolite leakage. (A) *S. pneumoniae* treated with DMSO or CabAB and imaged by scanning
1042 electron microscopy (SEM). (B) Quantification of membrane-permeable *S. pneumoniae* (stained with
1043 propidium iodide (PI)) upon treatment with DMSO (560 cells) or increasing concentrations of CabAB
1044 (0.975 μM – 481 cells; or 1.95 μM – 397 cells). (C-D) Quantification of populational membrane
1045 permeability (C) and depolarization (D) upon DMSO or CabAB treatment at several timepoints. (E)
1046 Proportion of extracellular *vs.* total ATP in wild-type and Δ*lytA S. pneumoniae* cultures upon DMSO
1047 or CabAB treatment. (F) Representative transmission electron microscopy (TEM) image and
1048 quantification of intracellular aggregates in DMSO- (n = 118 cells) or CabAB- treated *S. pneumoniae*
1049 (n = 138 cells). (G) Labeling of large intracellular aggregates by membrane dye FM4-64 in CabAB-
1050 treated *S. pneumoniae*. SEM and TEM were done once. Other data was taken from at least three
1051 independent experiments.
1052
1053 **Fig. 7.** Expression of *cabAB* facilitates horizontal gene transfer in dual-species biofilms. (A)
1054 Experimental setup to study gene transfer in dual-species biofilms. The *S. pneumoniae* DNA donor is

1055 nontransformable due to a *comGC* deletion, and contains chloramphenicol and tetracycline resistance
1056 cassettes at opposite ends of the chromosome (Chl^R and Tet^R); the *S. mitis* DNA receiver is labeled
1057 with a kanamycin resistance cassette (Kan^R); biofilms were pre-grown at a starting 1:1 ratio for 24 h
1058 in acidic medium to prevent natural competence induction; cells were aspirated and fresh medium
1059 containing CSP_{G22} was added to biofilms to transiently induce competence; after 6 h of incubation,
1060 cells were plated; *S. mitis* transformants were recovered and counted by selection in plates with
1061 kanamycin and combinations of chloramphenicol and/or tetracycline. (B-C) Acquisition of Chl^R and/or
1062 Tet^R by *S. mitis* in biofilms containing purified donor gDNA (B) or the strain itself (C). (D) Growth
1063 inhibition and lysis of 26 bacterial species when treated with 0.975 μM CabAB *vs.* DMSO during their
1064 exponential phase. Growth was recorded for 24 h. Lysis is shown when a decrease from the initial
1065 culture optical density was observed in all replicates. Experiments were repeated three times,
1066 independently. Transformation efficiencies were compared using unpaired *t*-tests. LOD limit of
1067 detection. * $P < 0.05$. ** $P < 0.01$.
1068
1069 **Fig. 8.** Model for the role of Cab bacteriocins in the acquisition of heterologous DNA. *S. mitis* produces
1070 the CSP precursor (preCSP) intracellularly, which is exported and processed by ComAB. Extracellular
1071 CSP(CSP_{G22}), as well as other CSP variants such as pneumococcal CSP-1, may be recognized by
1072 the membrane-bound histidine kinase ComD, leading to phosphorylation of the response regulator
1073 ComE. Phosphorylated ComE (ComE~P) activates expression of the early competence genes,
1074 establishing a positive feedback loop. This includes *sigX1 and sigX2*, which encode for the alternative
1075 sigma factor that drives expression of late competence genes. Among the late genes are the *cab*
1076 bacteriocins. Cab localize to the surface of producer cells. Surface-associated Cab mediate lysis of
1077 neighbouring *S. pneumoniae* cells in a cell contact- and LytA-dependent manner, resulting in the
1078 release of DNA. During the late competence phase, *S. mitis* cells also assemble a competence pilus
1079 responsible for the uptake of extracellular DNA, which can subsequently be integrated into the
1080 genome by homologous recombination.

Figure 1

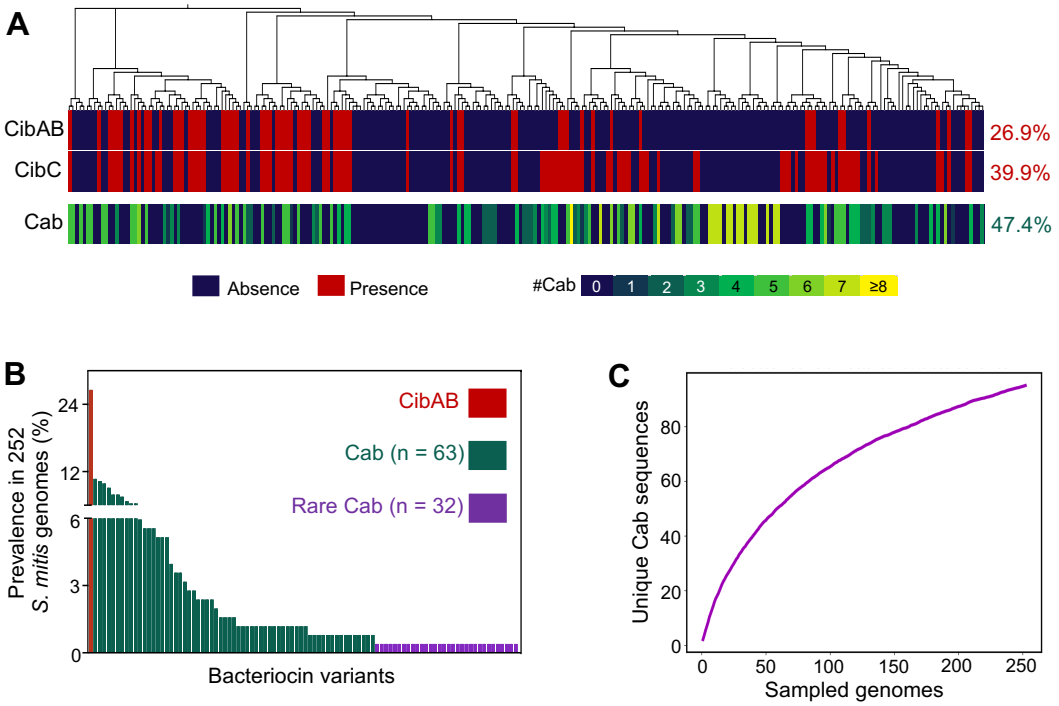
A
CibAB
CibC
Cab
26.9%
39.9%
47.4%
Absence
Presence
#Cab
0
1
2
3
4
5
6
7
≥8
B
Prevalence in 252 S. mitis genomes (%)
24
12
6
3
0
CibAB
Cab (n = 63)
Rare Cab (n = 32)
Bacteriocin variants
C
Unique Cab sequences
80
60
40
20
0
0
50
100
150
200
250
Sampled genomes

Figure 2

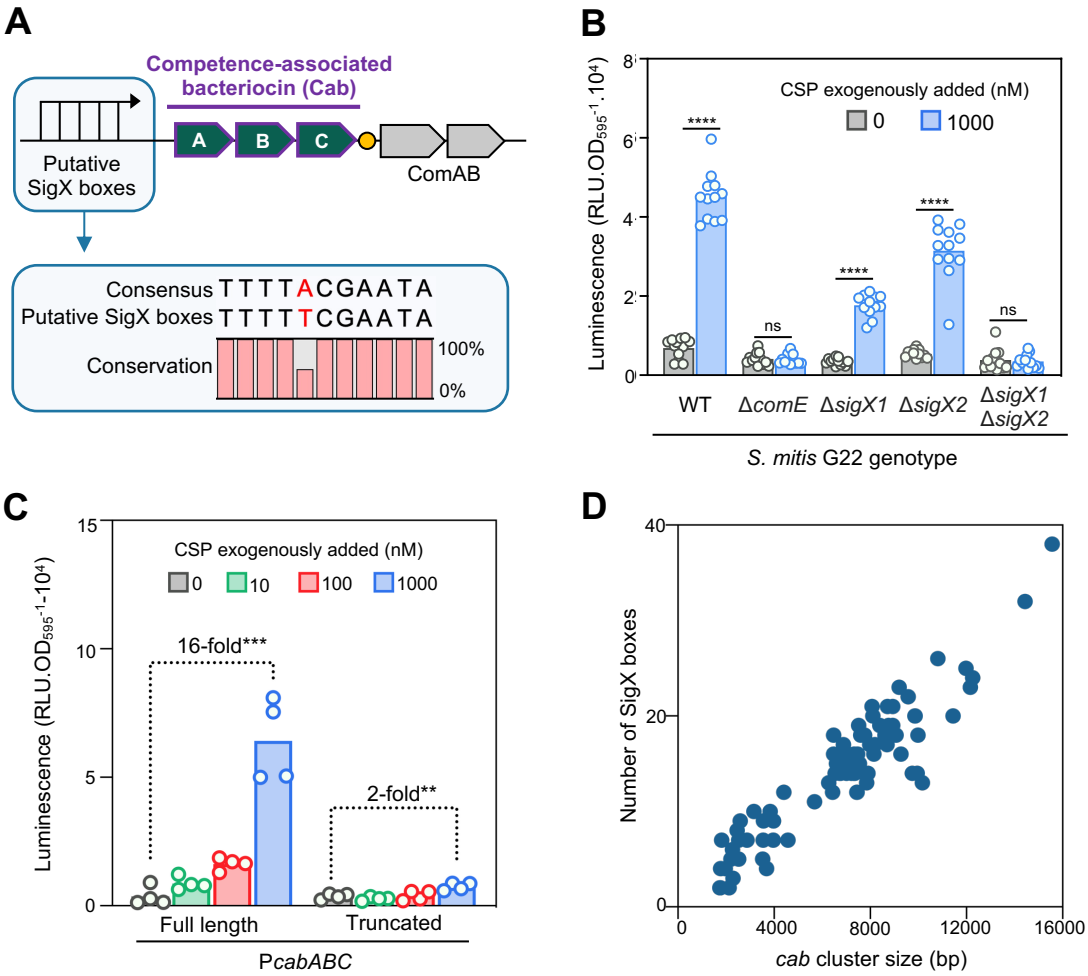
A
Competence-associated bacteriocin (Cab)
Putative SigX boxes
A
B
C
ComAB
Consensus TTTTTACGAATA
Putative SigX boxes TTTTTCGAATA
Conservation
100%
0%
B
CSP exogenously added (nM)
0
1000
Luminescence (RLU.OD595-1.10⁴)
****
ns
****
****
ns
WT
ΔcomE
ΔsigX1
ΔsigX2
ΔsigX1 ΔsigX2
S. mitis G22 genotype
C
CSP exogenously added (nM)
0
10
100
1000
Luminescence (RLU.OD595-1.10⁴)
16-fold***
2-fold**
Full length
Truncated
PcabABC
D
Number of SigX boxes
cab cluster size (bp)

Figure 3

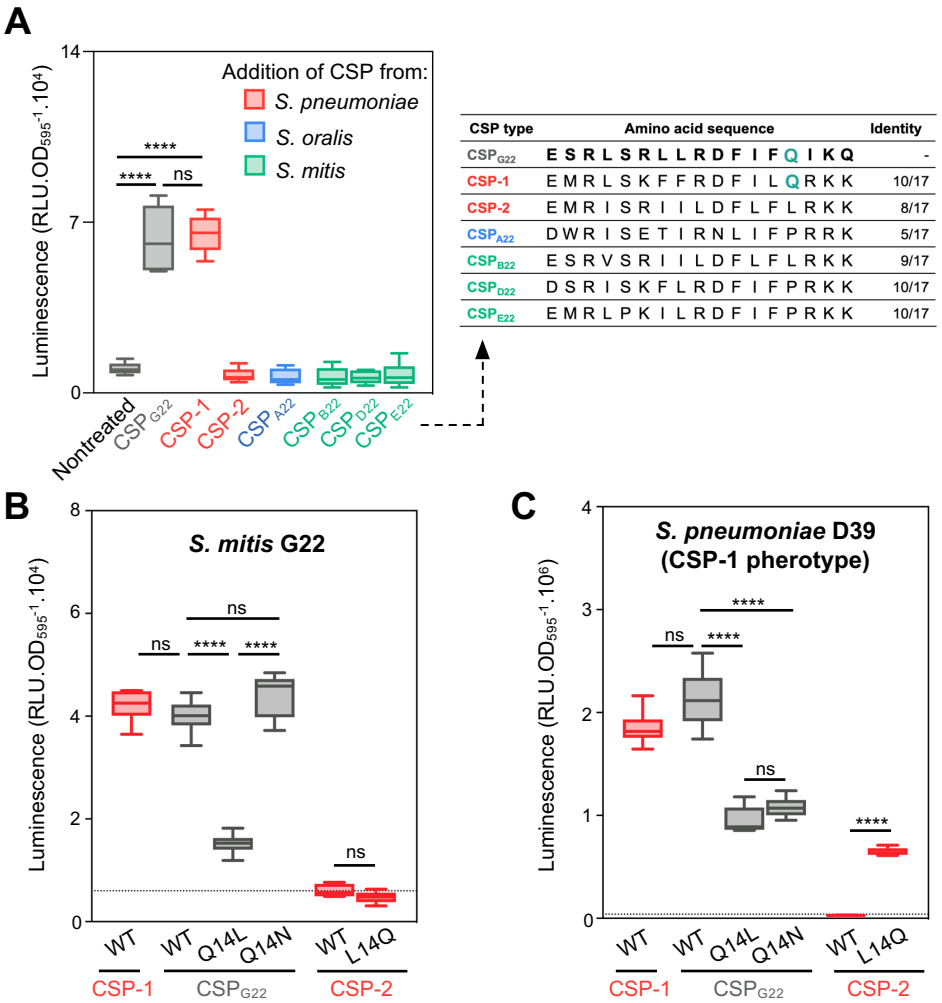

CSP type	Amino acid sequence	Identity
CSP_{G22}	**E S R L S R L L R D F I F Q I K Q**	-
CSP-1	E M R L S K F F R D F I L Q R K K	10/17
CSP-2	E M R I S R I I L D F L F L R K K	8/17
CSP_{A22}	D W R I S E T I R N L I F P R R K	5/17
CSP_{B22}	E S R V S R I I L D F L F L R K K	9/17
CSP_{D22}	D S R I S K F L R D F I F P R K K	10/17
CSP_{E22}	E M R L P K I L R D F I F P R K K	10/17

Figure 4

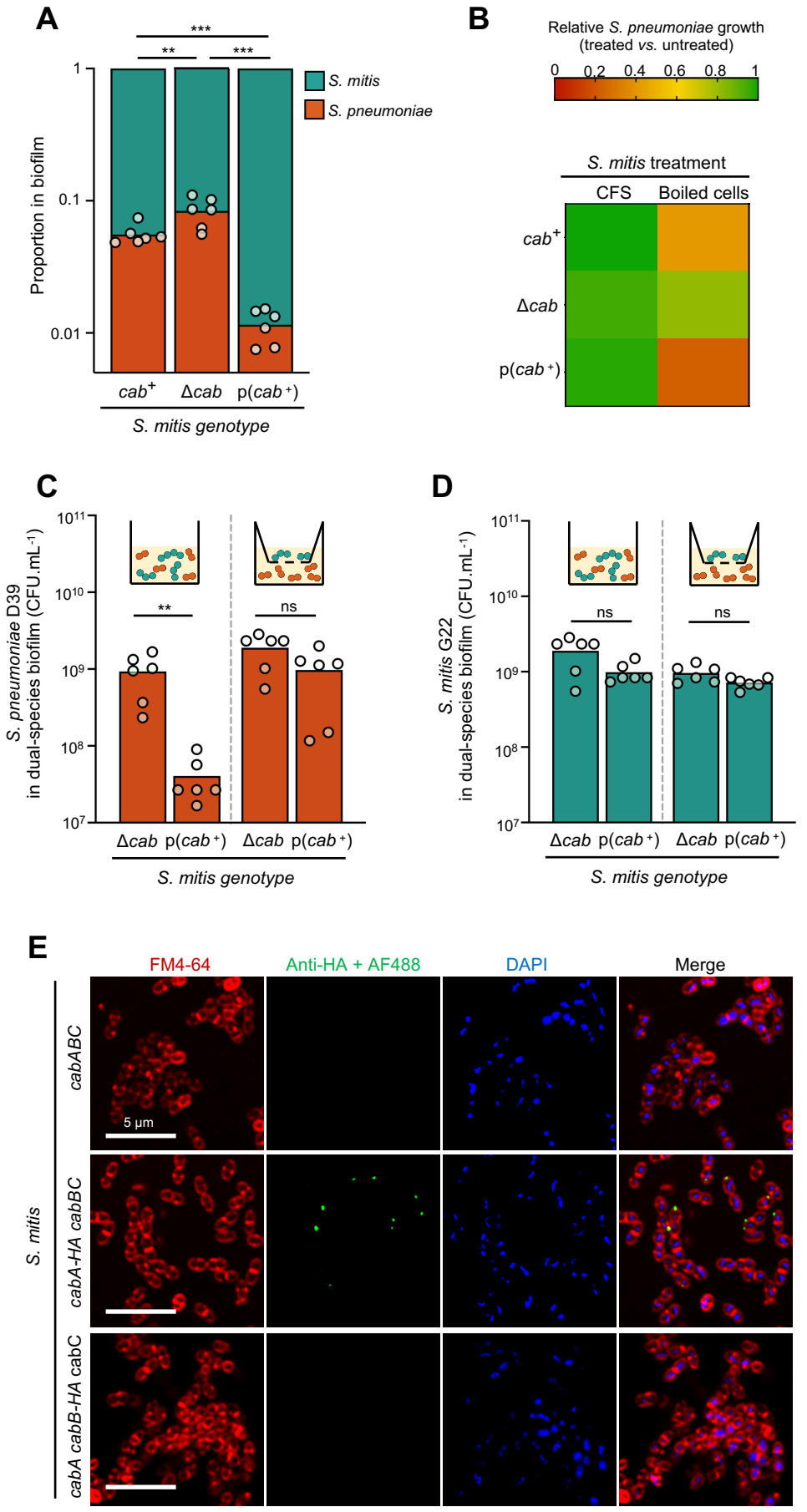
A
***
**
***
1
0.1
0.01
Proportion in biofilm
S. mitis
S. pneumoniae
cab+
Δcab
p(cab+)
S. mitis genotype
B
Relative S. pneumoniae growth
(treated vs. untreated)
0
0.2
0.4
0.6
0.8
1
S. mitis treatment
CFS
Boiled cells
cab+
Δcab
p(cab+)
C
S. pneumoniae D39
in dual-species biofilm (CFU.mL-1)
10^11
10^10
10^9
10^8
10^7
**
ns
Δcab
p(cab+)
Δcab
p(cab+)
S. mitis genotype
D
S. mitis G22
in dual-species biofilm (CFU.mL-1)
10^11
10^10
10^9
10^8
10^7
ns
ns
Δcab
p(cab+)
Δcab
p(cab+)
S. mitis genotype
E
FM4-64
Anti-HA + AF488
DAPI
Merge
S. mitis
cabABC
cabA-HA cabBC
cabA cabB-HA cabC
5 µm

Figure 5

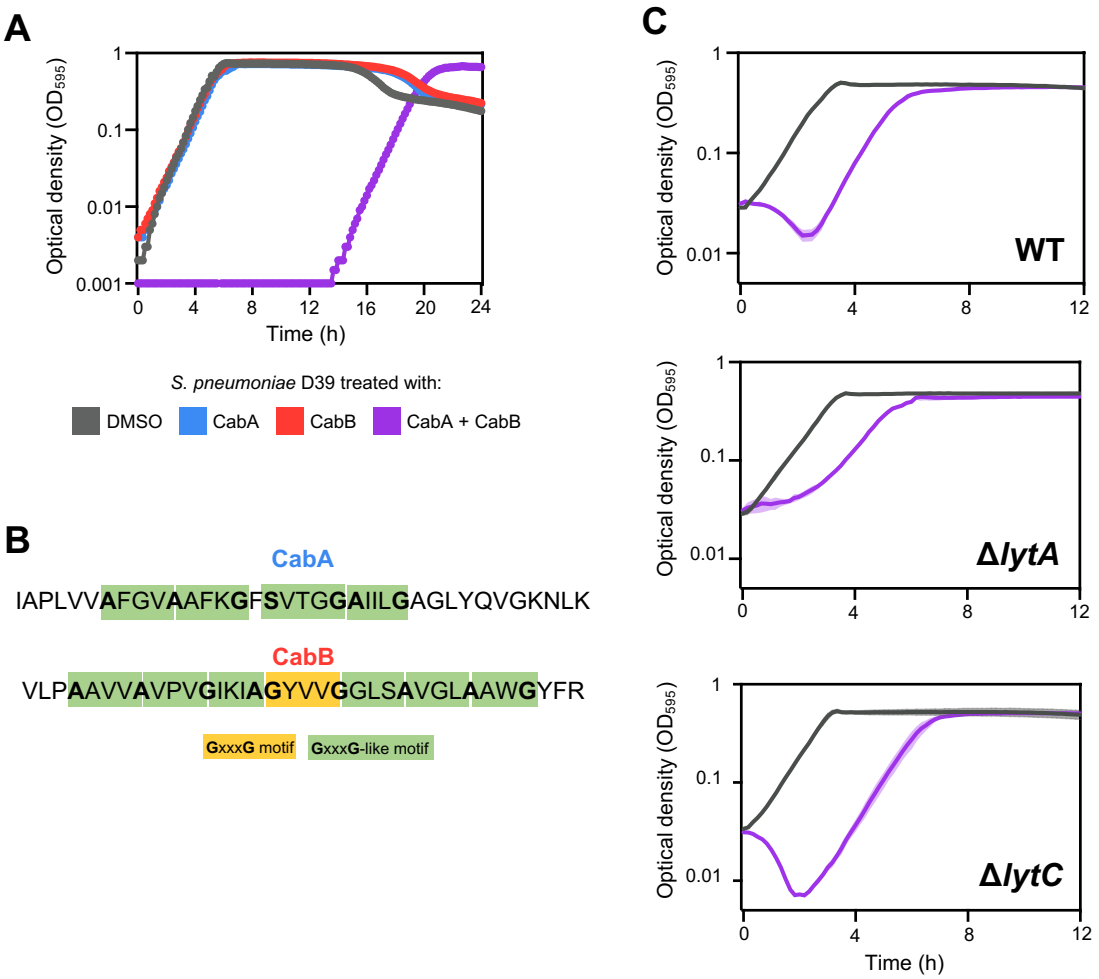
A
Optical density (OD595)
1
0.1
0.01
0.001
0
4
8
12
16
20
24
Time (h)
S. pneumoniae D39 treated with:
DMSO
CabA
CabB
CabA + CabB
B
CabA
IAPLVVAFGVAAFKGFSVTGGAIILGAGLYQVGKNLK
CabB
VLPAAVVAVPVGIKIAGYVVGGLSAVGLAAWGYFR
GxxxG motif
GxxxG-like motif
C
Optical density (OD595)
1
0.1
0.01
0
4
8
12
WT
ΔlytA
ΔlytC
Time (h)

Figure 6

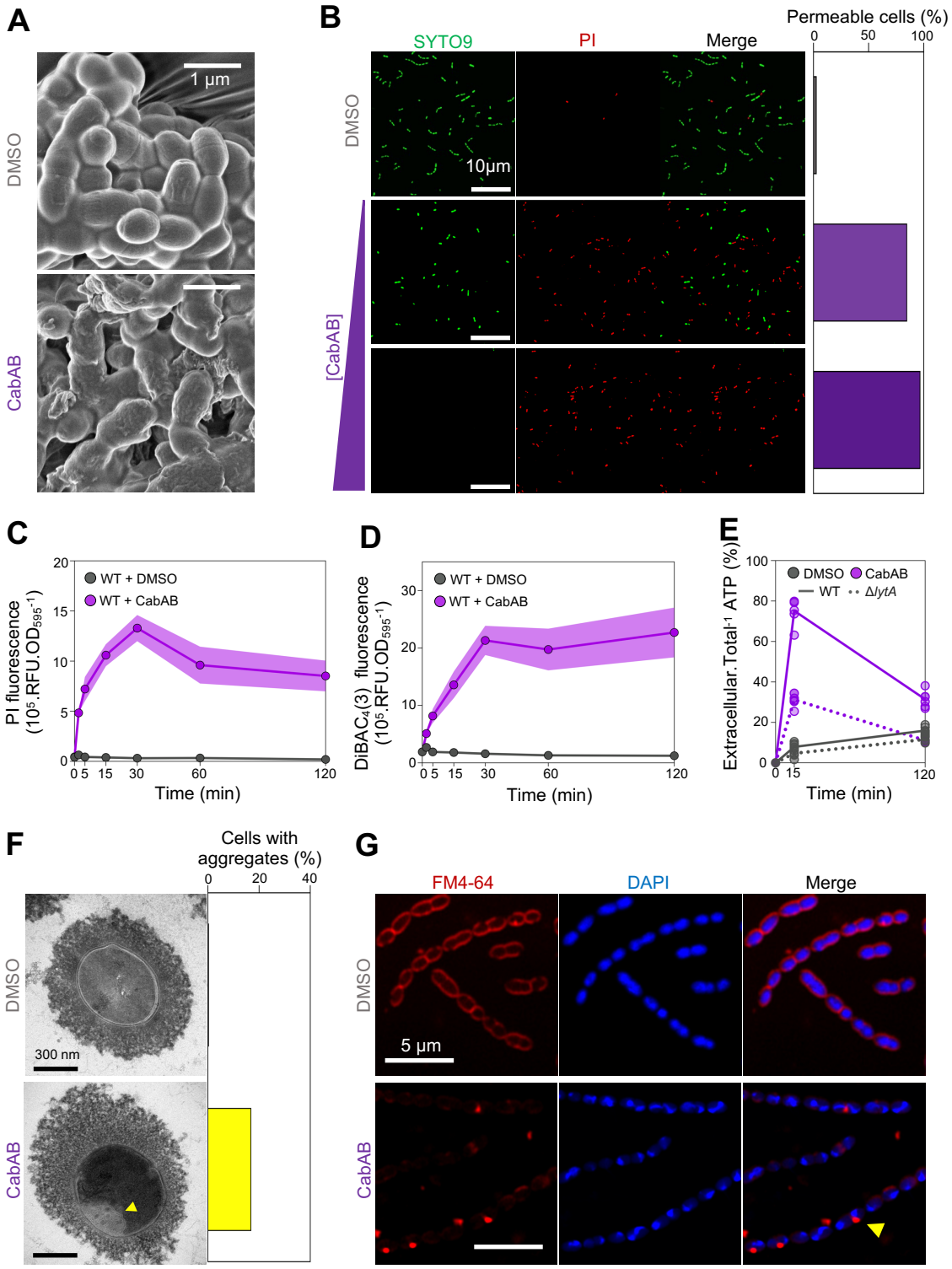
A
1 µm
DMSO
CabAB
B
SYTO9
PI
Merge
Permeable cells (%)
0
50
100
DMSO
10µm
[CabAB]
C
PI fluorescence
(10⁵.RFU.OD595⁻¹)
WT + DMSO
WT + CabAB
Time (min)
D
DiBAC4(3) fluorescence
(10⁵.RFU.OD595⁻¹)
WT + DMSO
WT + CabAB
Time (min)
E
Extracellular.Total⁻¹ ATP (%)
DMSO
CabAB
WT
ΔlytA
Time (min)
F
Cells with aggregates (%)
0
20
40
DMSO
300 nm
CabAB
G
FM4-64
DAPI
Merge
DMSO
5 µm
CabAB

Figure 7

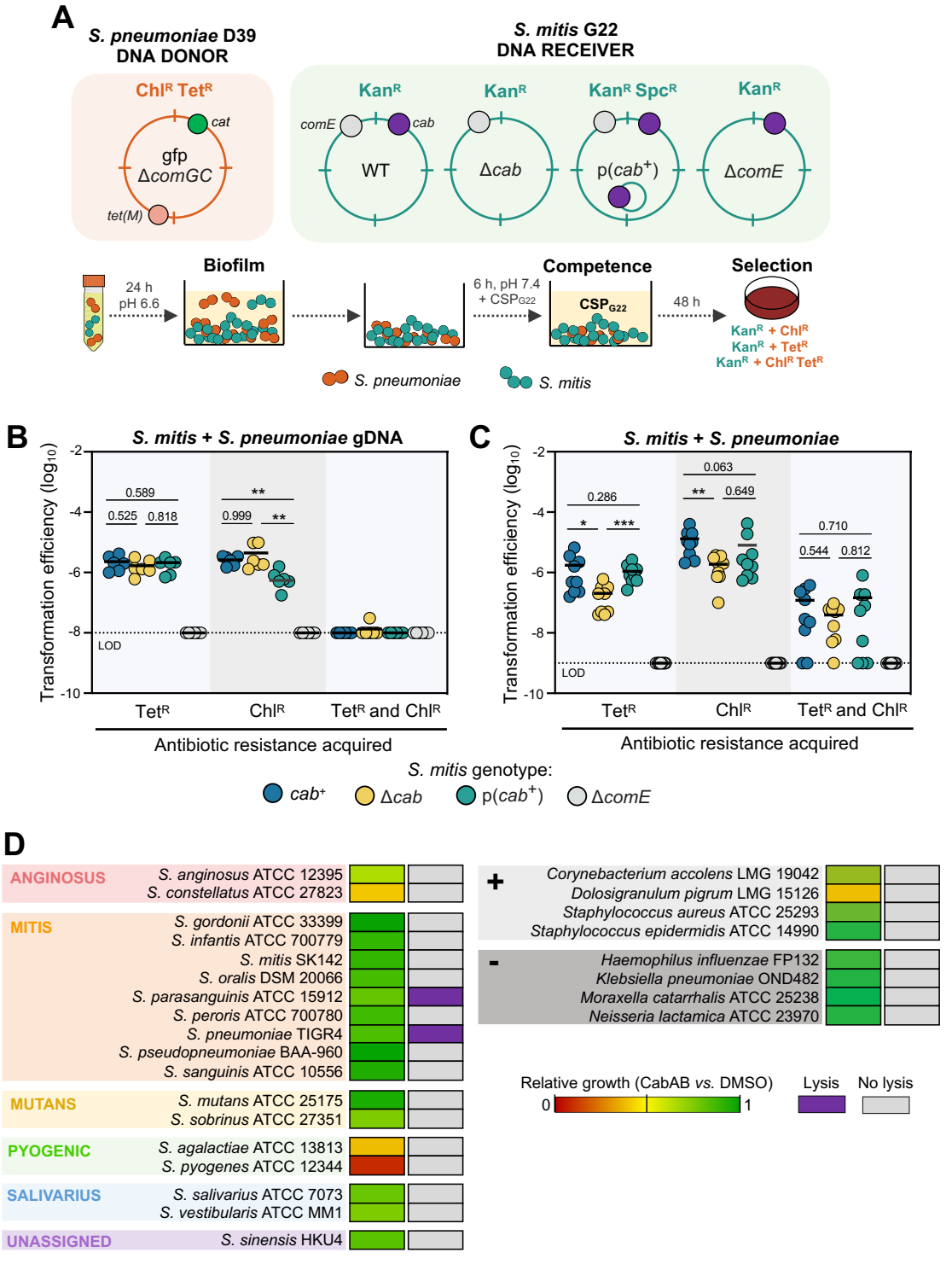
A
S. pneumoniae D39
DNA DONOR
ChlR TetR
cat
gfp
ΔcomGC
tet(M)
S. mitis G22
DNA RECEIVER
KanR
comE
cab
WT
KanR
Δcab
KanR SpcR
p(cab+)
KanR
ΔcomE
Biofilm
24 h
pH 6.6
Competence
6 h, pH 7.4
+ CSPG22
CSPG22
48 h
Selection
KanR + ChlR
KanR + TetR
KanR + ChlR TetR
S. pneumoniae
S. mitis
B
S. mitis + S. pneumoniae gDNA
Transformation efficiency (log10)
-2
-4
-6
-8
-10
0.589
0.525
0.818
**
0.999
**
LOD
TetR
ChlR
TetR and ChlR
Antibiotic resistance acquired
C
S. mitis + S. pneumoniae
0.286
*
***
0.063
**
0.649
0.710
0.544
0.812
LOD
TetR
ChlR
TetR and ChlR
Antibiotic resistance acquired
S. mitis genotype:
cab+
Δcab
p(cab+)
ΔcomE
D
ANGINOSUS
S. anginosus ATCC 12395
S. constellatus ATCC 27823
MITIS
S. gordonii ATCC 33399
S. infantis ATCC 700779
S. mitis SK142
S. oralis DSM 20066
S. parasanguinis ATCC 15912
S. peroris ATCC 700780
S. pneumoniae TIGR4
S. pseudopneumoniae BAA-960
S. sanguinis ATCC 10556
MUTANS
S. mutans ATCC 25175
S. sobrinus ATCC 27351
PYOGENIC
S. agalactiae ATCC 13813
S. pyogenes ATCC 12344
SALIVARIUS
S. salivarius ATCC 7073
S. vestibularis ATCC MM1
UNASSIGNED
S. sinensis HKU4
+
Corynebacterium accolens LMG 19042
Dolosigranulum pigrum LMG 15126
Staphylococcus aureus ATCC 25293
Staphylococcus epidermidis ATCC 14990
-
Haemophilus influenzae FP132
Klebsiella pneumoniae OND482
Moraxella catarrhalis ATCC 25238
Neisseria lactamica ATCC 23970
Relative growth (CabAB vs. DMSO)
0
1
Lysis
No lysis

Figure 8

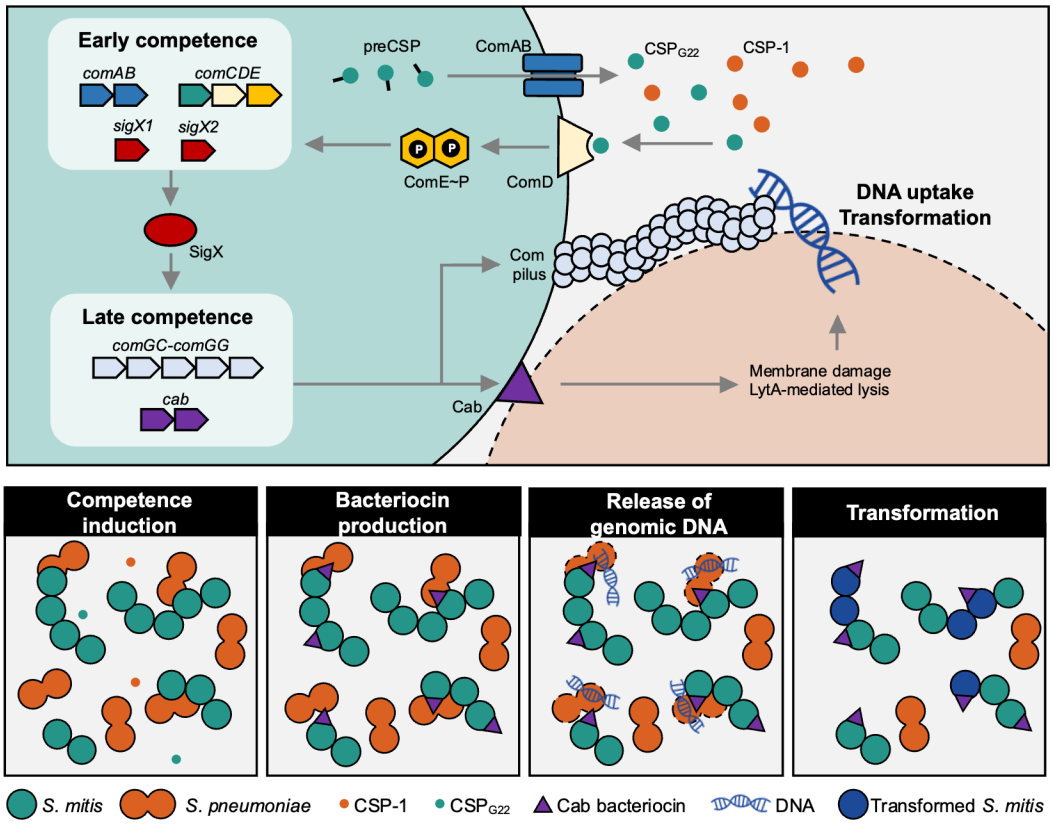
Early competence
comAB
comCDE
sigX1
sigX2
SigX
Late competence
comGC-comGG
cab
preCSP
ComAB
CSP$_{G22}$
CSP-1
ComE~P
ComD
Com pilus
Cab
DNA uptake
Transformation
Membrane damage
LytA-mediated lysis
Competence induction
Bacteriocin production
Release of genomic DNA
Transformation
S. mitis
S. pneumoniae
CSP-1
CSP$_{G22}$
Cab bacteriocin
DNA
Transformed S. mitis

Supplemental material

Streptococcus mitis bacteriocins drive contact-dependent lysis of *S. pneumoniae* facilitating transformation in multispecies environments

João Borralho[1], João Lança,[1], Joana Bryton[1], Wilson Antunes[2], Raquel Sá-Leão[1]*

[1] Laboratory of Molecular Microbiology of Human Pathogens, Instituto de Tecnologia Química e Biológica António Xavier, Universidade Nova de Lisboa, Oeiras, Portugal

[2] Centro de Investigação da Academia Militar (CINAMIL), Unidade Militar Laboratorial de Defesa Biológica e Química (UMLDBQ), Av. Dr. Alfredo Bensaúde, 1849-012, Lisboa, Portugal.

* Corresponding author: rsaleao@itqb.unl.pt

Keywords: Horizontal gene transfer, competence, interspecies interactions, predation, biofilms

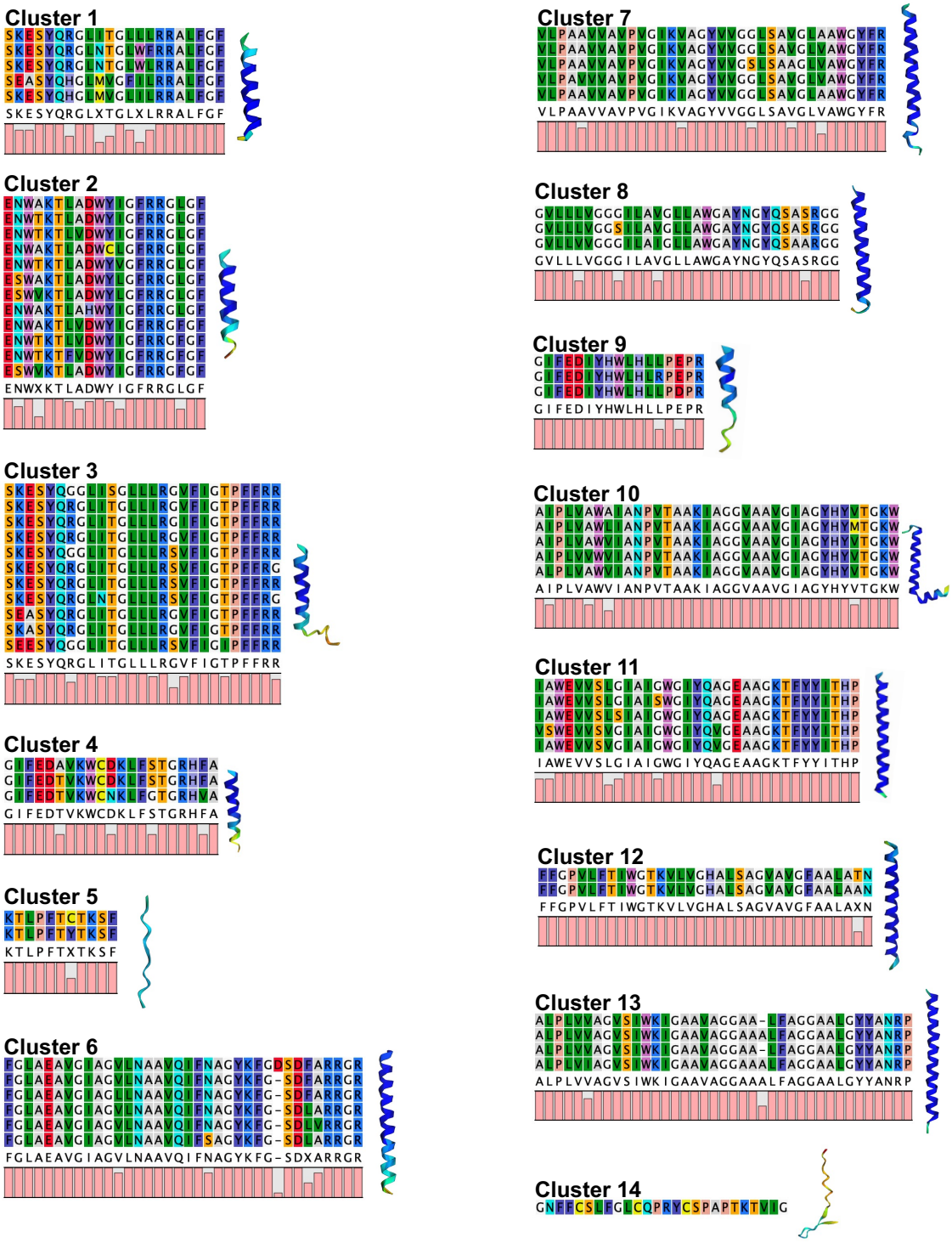

Fig. S1. Alignment-based clustering of Cab variants. The 95 Cab variants found *S. mitis* populations were clustered based on pairwise sequence alignments (see Materials and Methods). Alignments for Cab sequences within each cluster is shown, with associated Alphafold2 (ColabFold v1.5.5) structural model of the most prevalent variant. Amino acids are colored according to biochemical traits (RasMol coloring). Structures are colored according to plDDT (predicted local distance difference test) confidence.

(continues next page)

Fig. S1. (cont.)

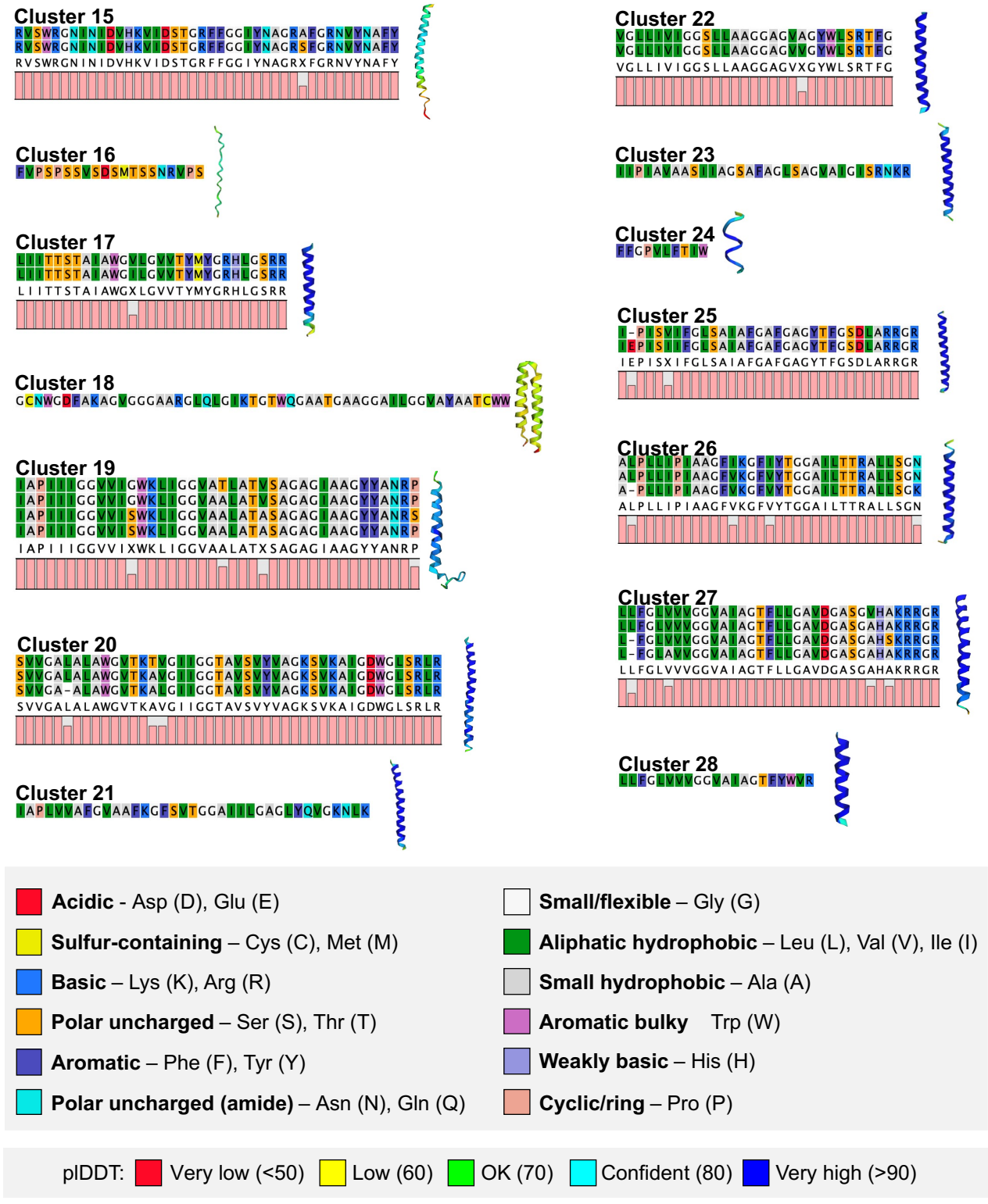
Cluster 15
Cluster 16
Cluster 17
Cluster 18
Cluster 19
Cluster 20
Cluster 21
Cluster 22
Cluster 23
Cluster 24
Cluster 25
Cluster 26
Cluster 27
Cluster 28
Acidic - Asp (D), Glu (E)
Sulfur-containing – Cys (C), Met (M)
Basic – Lys (K), Arg (R)
Polar uncharged – Ser (S), Thr (T)
Aromatic – Phe (F), Tyr (Y)
Polar uncharged (amide) – Asn (N), Gln (Q)
Small/flexible – Gly (G)
Aliphatic hydrophobic – Leu (L), Val (V), Ile (I)
Small hydrophobic – Ala (A)
Aromatic bulky Trp (W)
Weakly basic – His (H)
Cyclic/ring – Pro (P)
pIDDT: Very low (<50) Low (60) OK (70) Confident (80) Very high (>90)

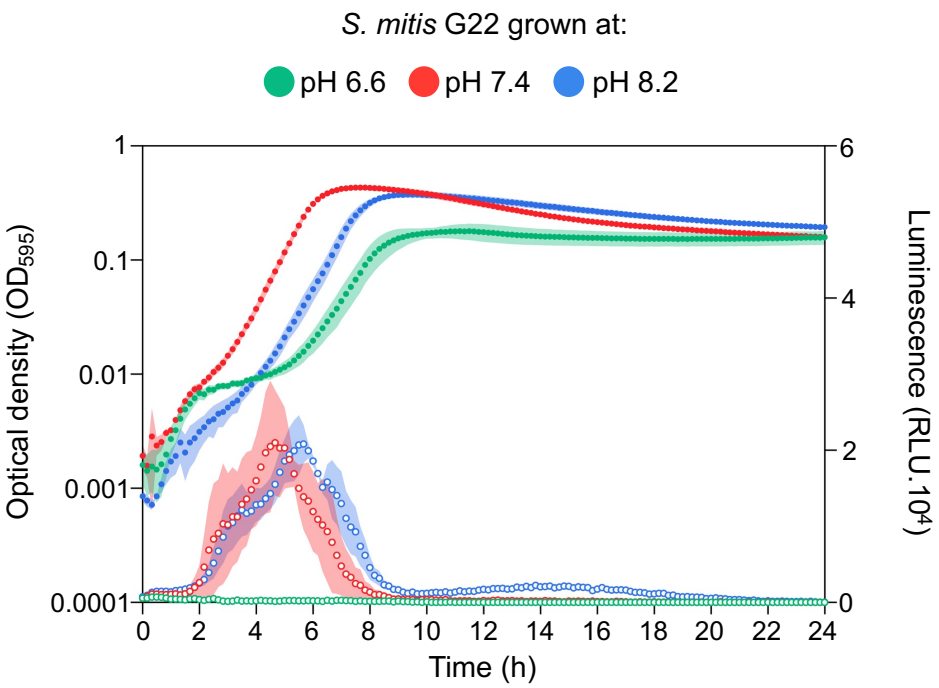

Fig. S2. *S. mitis* competence is inhibited in medium with acidic pH. *S. mitis* G22 harboring an early-competence reporter (P*comCDE-luc*) was pre-grown in medium at pH 6.6, before being diluted 1:100 in fresh medium at pH 6.6, 7.4, or 8.2. Optical density (closed circles) and luminescence (open circles) values were measured every 10 min for 24 h. Growth curves were repeated three times independently, and one representative experiment with two technical replicates per condition is shown.

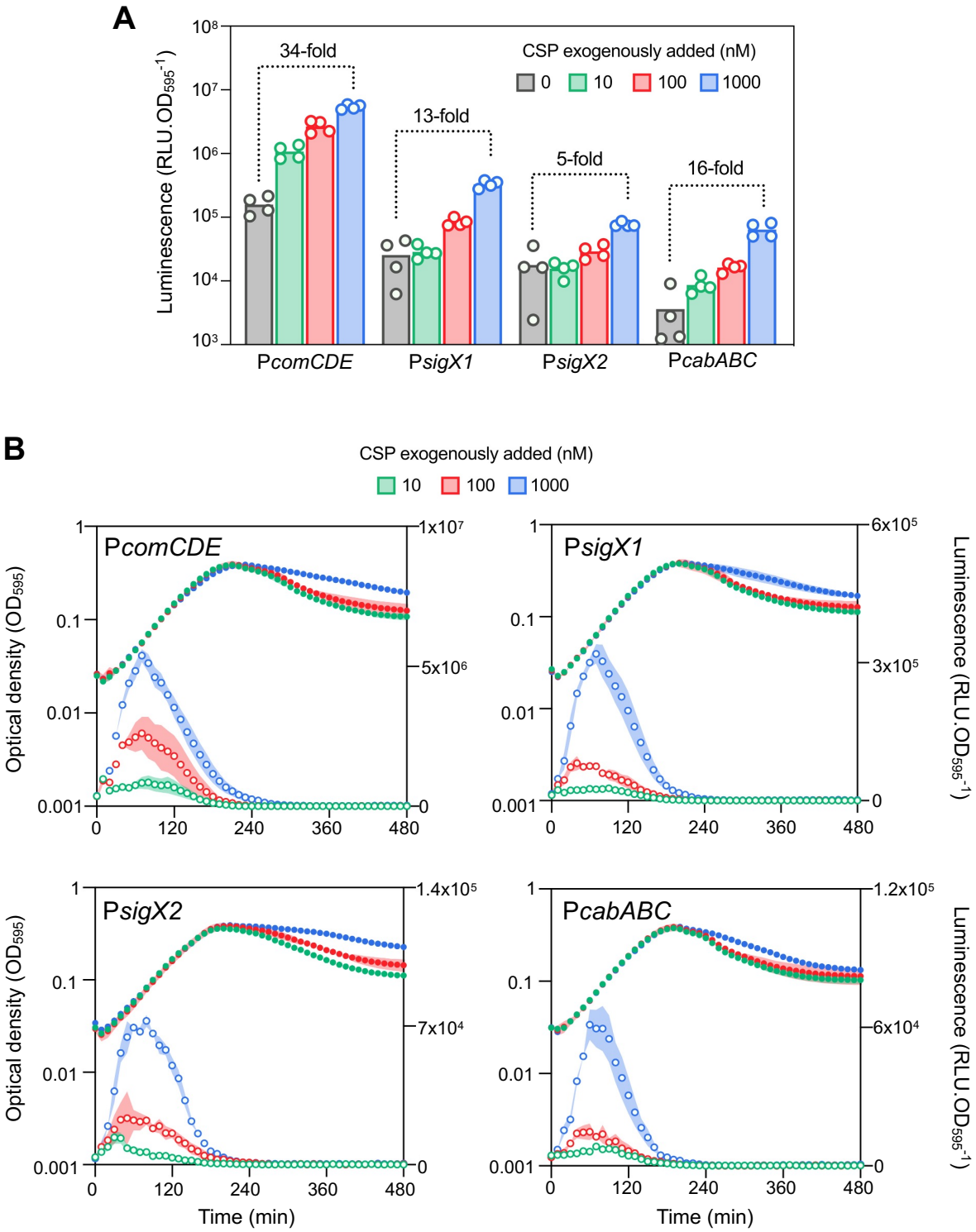

Fig. S3. Expression of *cabABC* follows the same dynamics of other competence genes. (A) Expression of *comCDE*, *sigX1*, *sigX2* and *cabABC* evaluated by luminescence produced by luminescent reporter *S. mitis*. Cells were pre-grown in acidic pH and diluted in fresh medium containing synthetic CSP_{G22}. Values represent the highest expression value ($RLU.OD_{595}^{-1}$) obtained during the 3 h post CSP_{G22} treatment. (B) Dynamics of *comCDE*, *sigX1*, *sigX2* and *cabABC* expression in *S. mitis*. Optical density – closed circles. Luminescence – open circles. Growth curves were repeated four times independently, and one representative experiment with two technical replicates per condition is shown. For clarity only the first 8 h of 24 h are shown, since there is no visible expression of the four reporters after this period.

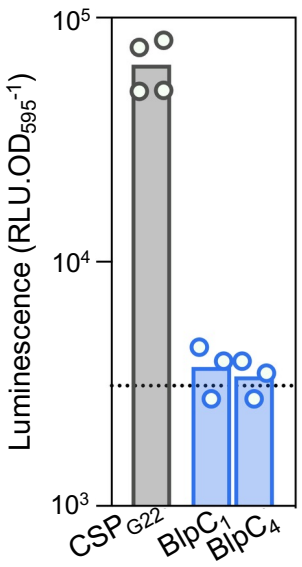

Fig. S4. Expression of *cabABC* is not induced by bacteriocin-like peptide pheromones (BlpC). *S. mitis* G22 harboring a P*cabABC-luc* reporter was pre-grown in acidic pH and diluted in fresh medium containing 1 µM of synthetic CSP_{G22} (grey), 1 µM of $BlpC_1$ or $BlpC_4$ pheromones (blue) or left untreated (dashed line). $BlpC_1$ or $BlpC_4$ are encoded in two *blp*-type bacteriocin clusters elsewhere in the genome of G22. Experiment were repeated four times independently.

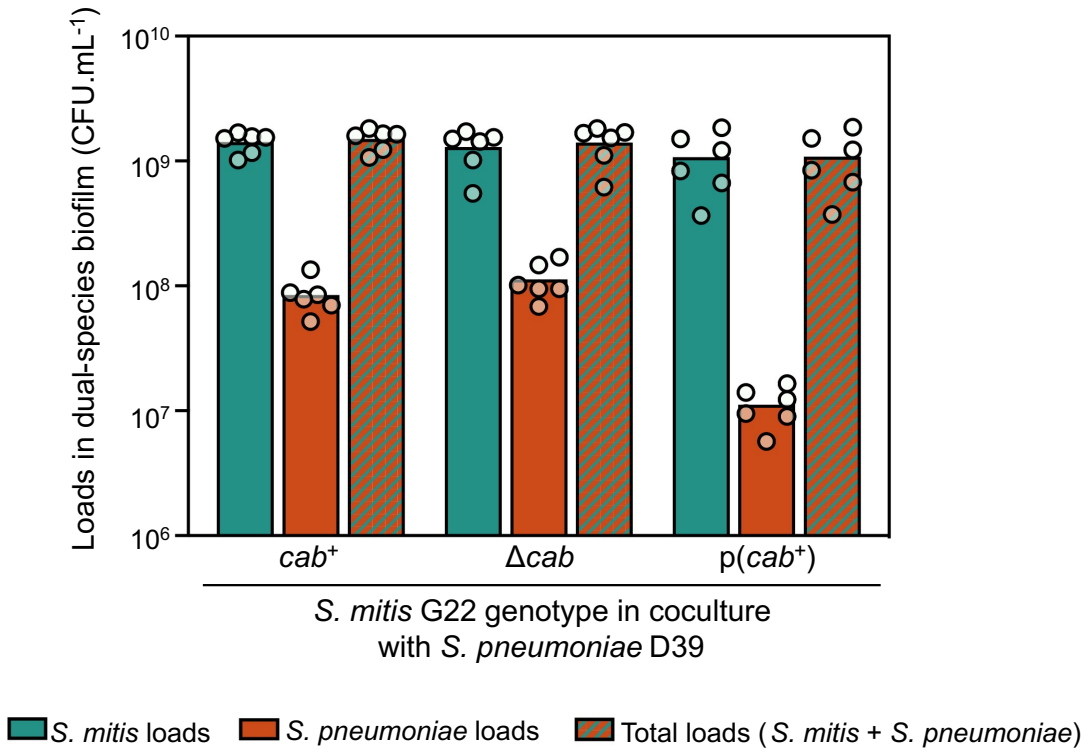

Fig. S5. Expression of *cab* by *S. mitis* reduces *S. pneumoniae* loads in dual-species biofilms. Individual and total bacterial loads of biofilm proportions presented in Figure 4A of the main text. *S. pneumoniae* and *S. mitis* of different *cab* genotypes were grown in 24 h biofilms in competence-permissive conditions. *S. mitis* and *S. pneumoniae* cell loads were enumerated by plating in BA with kanamycin or chloramphenicol, respectively. The experiment was repeated three times, independently.

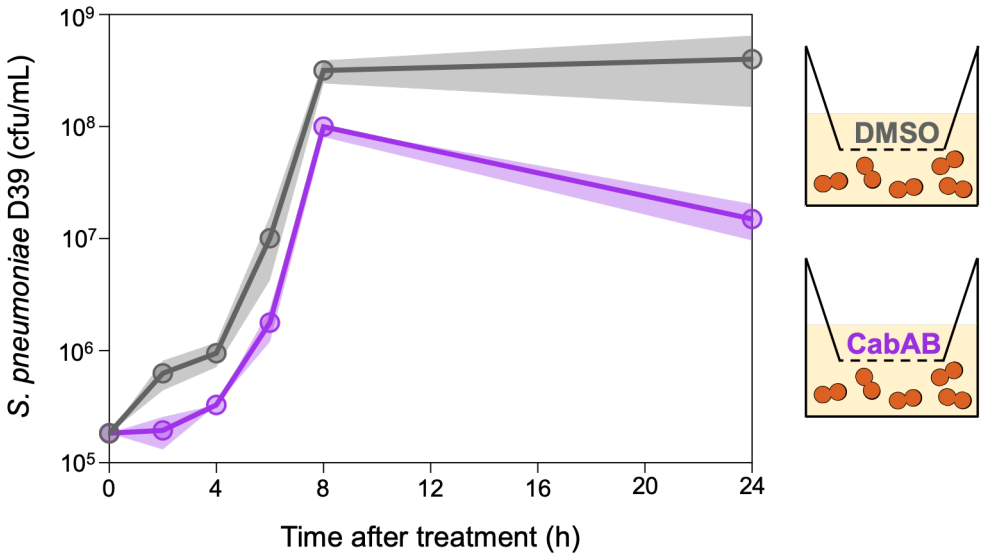

Fig. S6. Synthetic CabAB peptides can cross the transwell membrane. *S. pneumoniae* D39 cells were diluted to ~10^5 cfu/mL in C+Y_{YB} and 1.5 mL was added to 12-well plates. An insert containing a 0.4 µm pore polycarbonate membrane was placed on top and 0.5 mL of C+Y_{YB} with 0.975 µM CabAB or 0.00975% DMSO was added. Aliquots were taken from the bottom compartment at indicated timepoints and plated do assess *S. pneumoniae* loads. The experiments was repeated three times, independently.

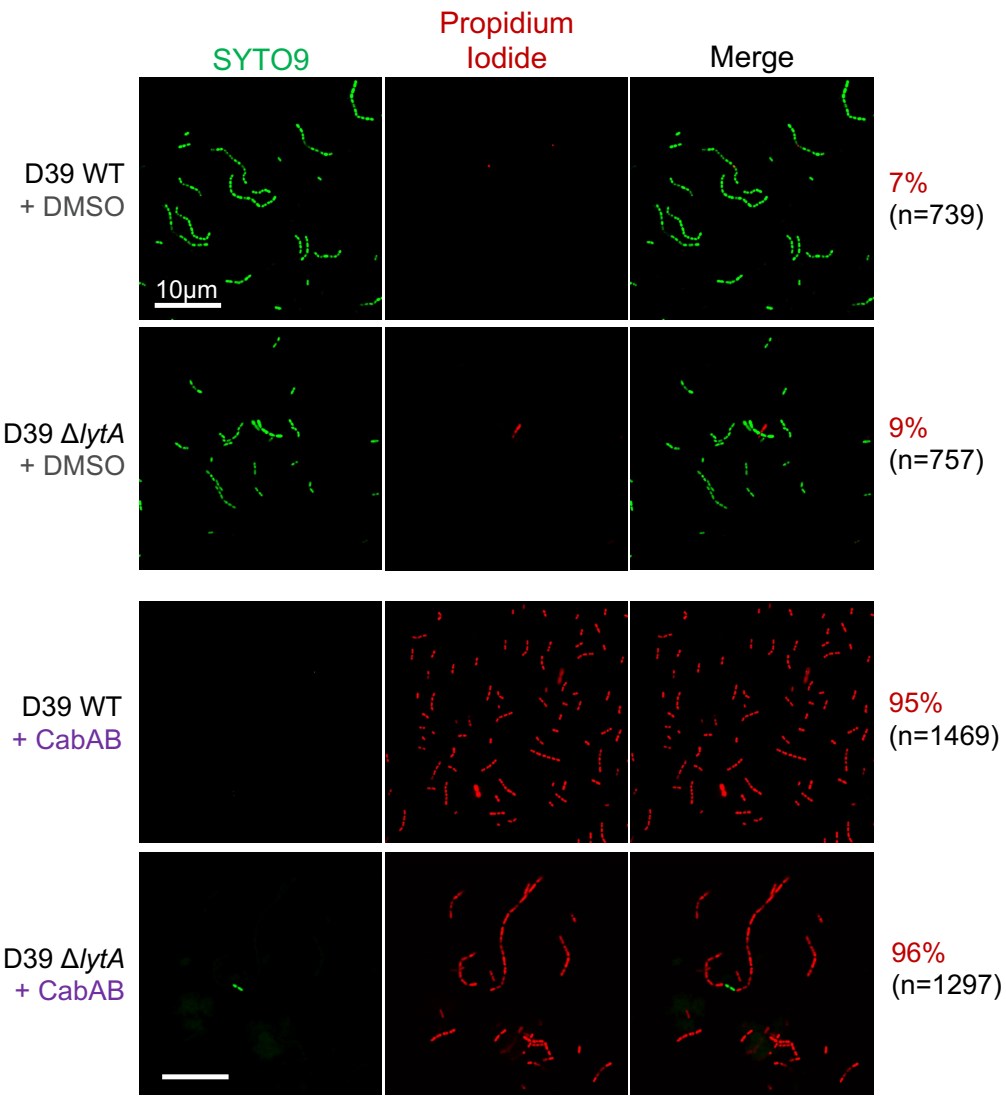

Fig. S7. Permeabilization of *S. pneumoniae* membranes does not depend on autolysin LytA. Confocal imaging of wild-type and Δ*lytA S. pneumoniae* treated with 0.00975% DMSO or 0.975 µM CabAB peptides. Membrane permeabilization is shown in red, by entry of propidium iodide. The total number and percentage of permeable cells is shown next to panels. Microscopy images are representative of three independent experiments.

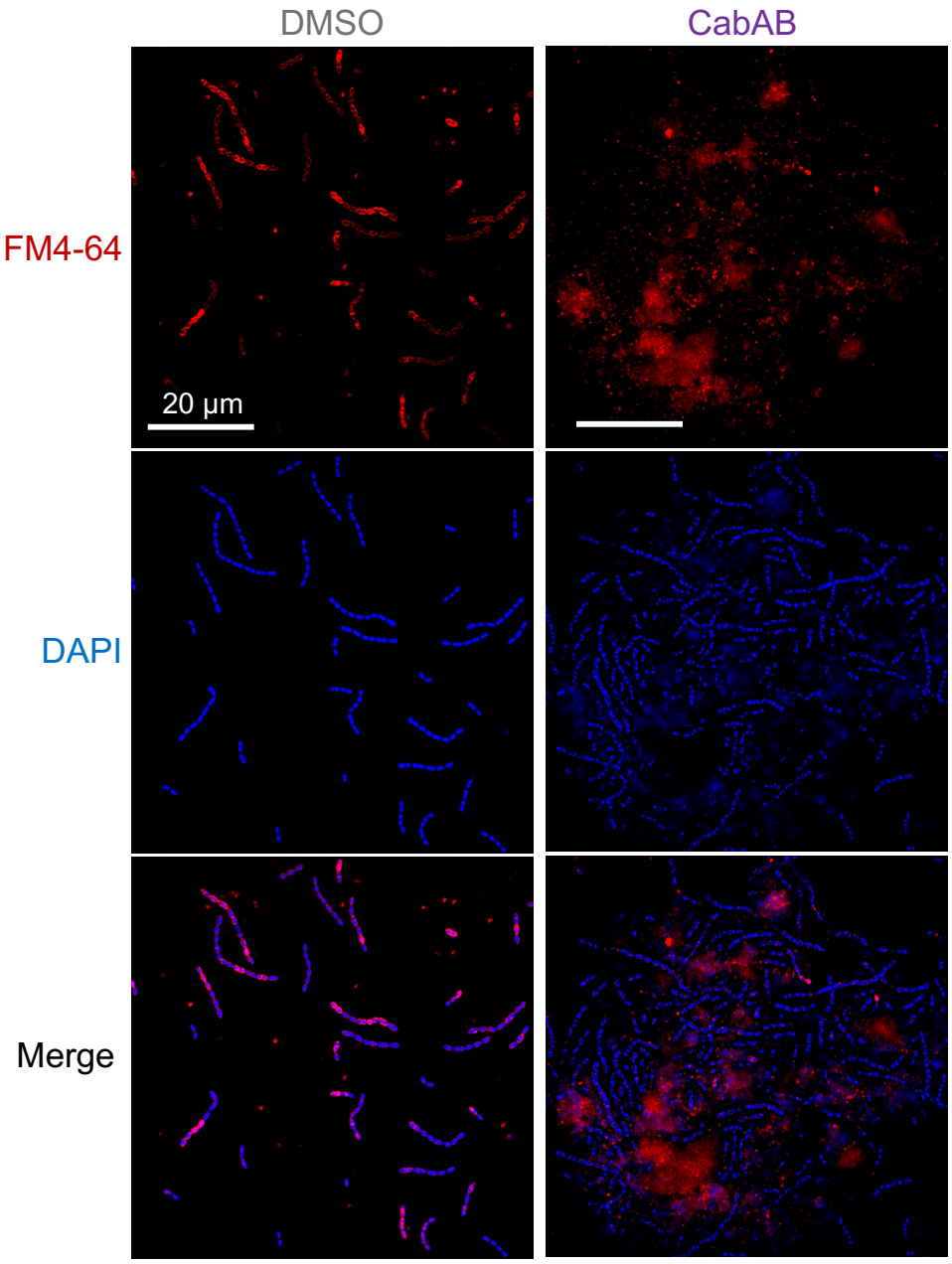

Fig. S8. CabAB treatment induces formation of large clumps of *S. pneumoniae* cells encased in a matrix of DNA and membrane material. *S. pneumoniae* D39 was treated with 0.00975% DMSO or 0.975 µM CabAB and stained with FM4-64 (membrane dye) and DAPI (nucleic acid dye), before being imaged in a confocal microscope. Experiment was repeated three times, independently.

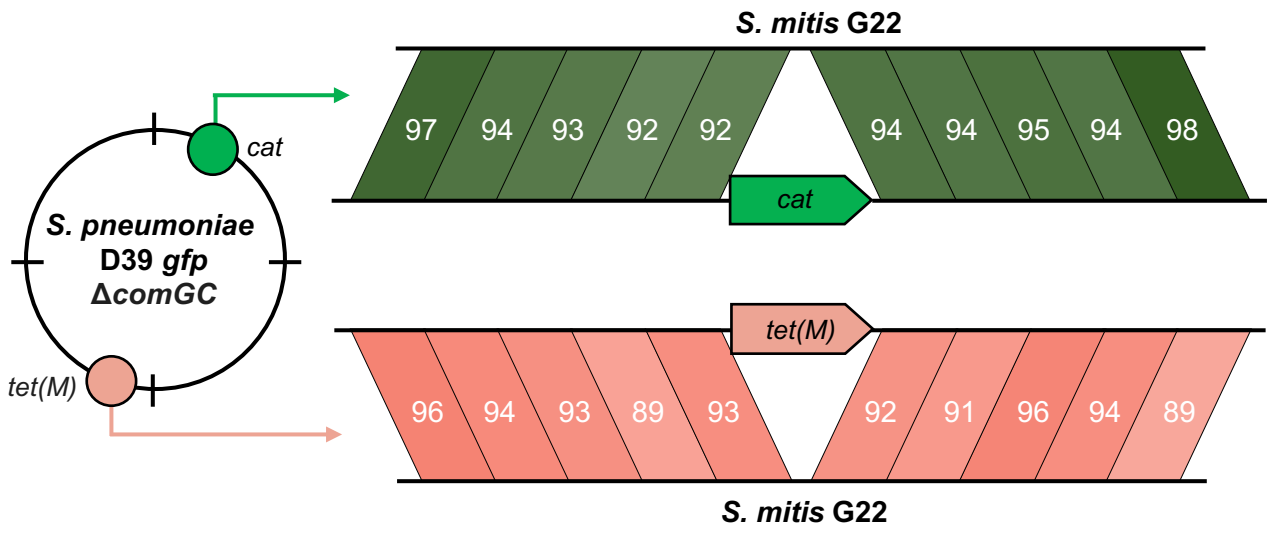

Fig. S9. Nucleotide sequence homology between *S. pneumoniae* D39 and *S. mitis* G22 flanking the sites of antibiotic resistance gene integration. Upstream and downstream regions of *cat* and *tet(M)* in the *S. pneumoniae* DNA donor were divided in five 1,000 bp blocks each and compared to the *S. mitis* G22 genome using BLASTn. Query coverage was consistently 100%, and the percentage of sequence identity is shown for each 1,000 bp block.

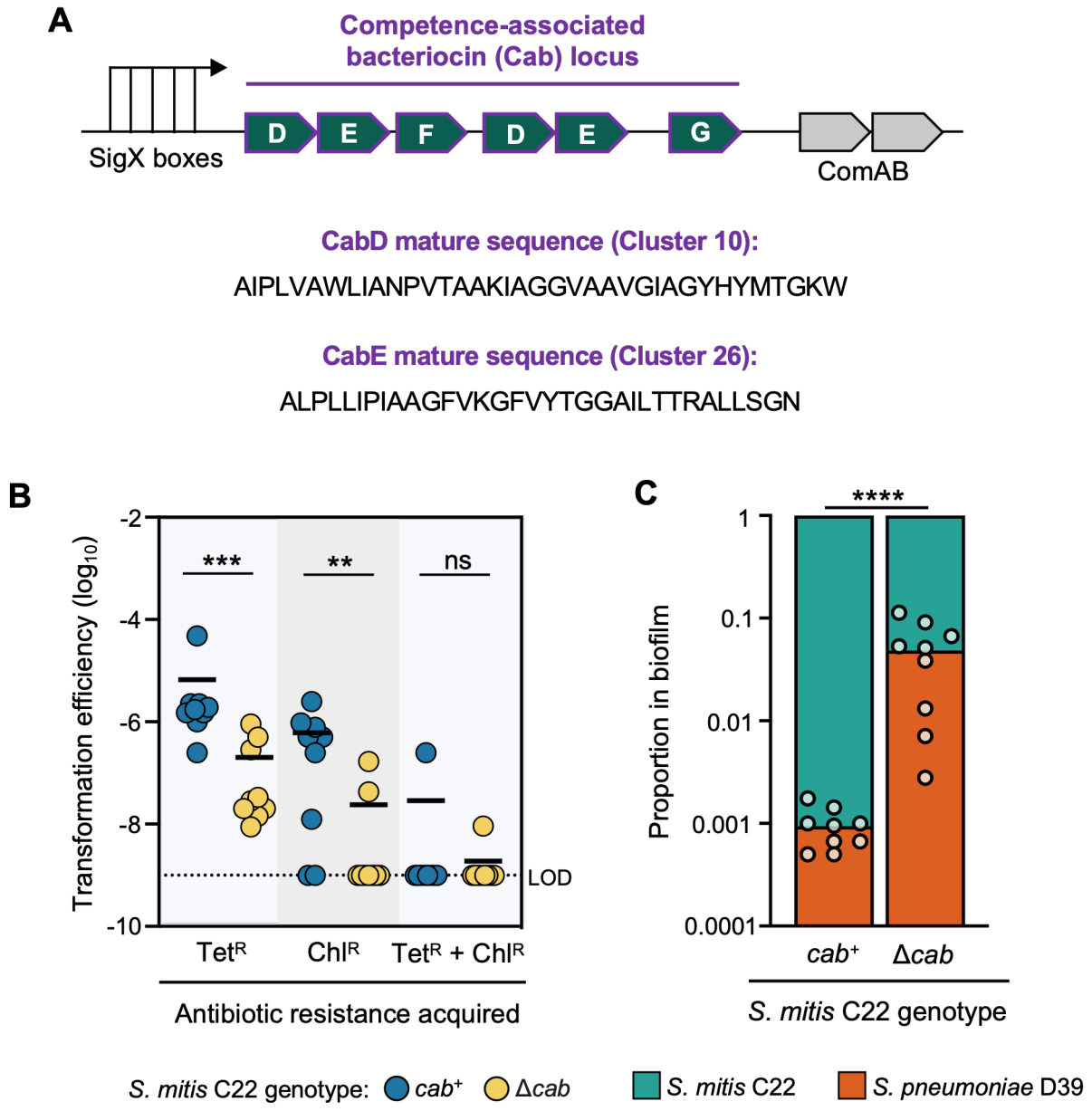

Fig. S10. The Cab bacteriocins of *S. mitis* C22 enhance HGT and mediate inhibition of *S. pneumoniae* in dual-species biofilms. (A) Genomic arrangement of the *S. mitis* C22 *cab* locus, which contains two copies of the bacteriocin *cabD*, two copies of the bacteriocin *cabE*, and the putative immunity proteins *cabF and cabG.* (B) Acquisition of Tet^R and Chl^R by *S. mitis* C22 when in 12-well biofilms with *S. pneumoniae* DNA donor (D39 *gfp* Δ*comGC*). (C) Proportion of *S. mitis* C22 and *S. pneumoniae* D39 when grown in dual-species biofilm. Experiments were repeated three times, independently. Results in panel C represent the proportion of each species in the dual-species biofilms of panel B. Transformation efficiencies were compared using unpaired t-tests. LOD limit of detection. ** $P < 0.01$. *** $P < 0.001$. **** $P < 0.0001$.

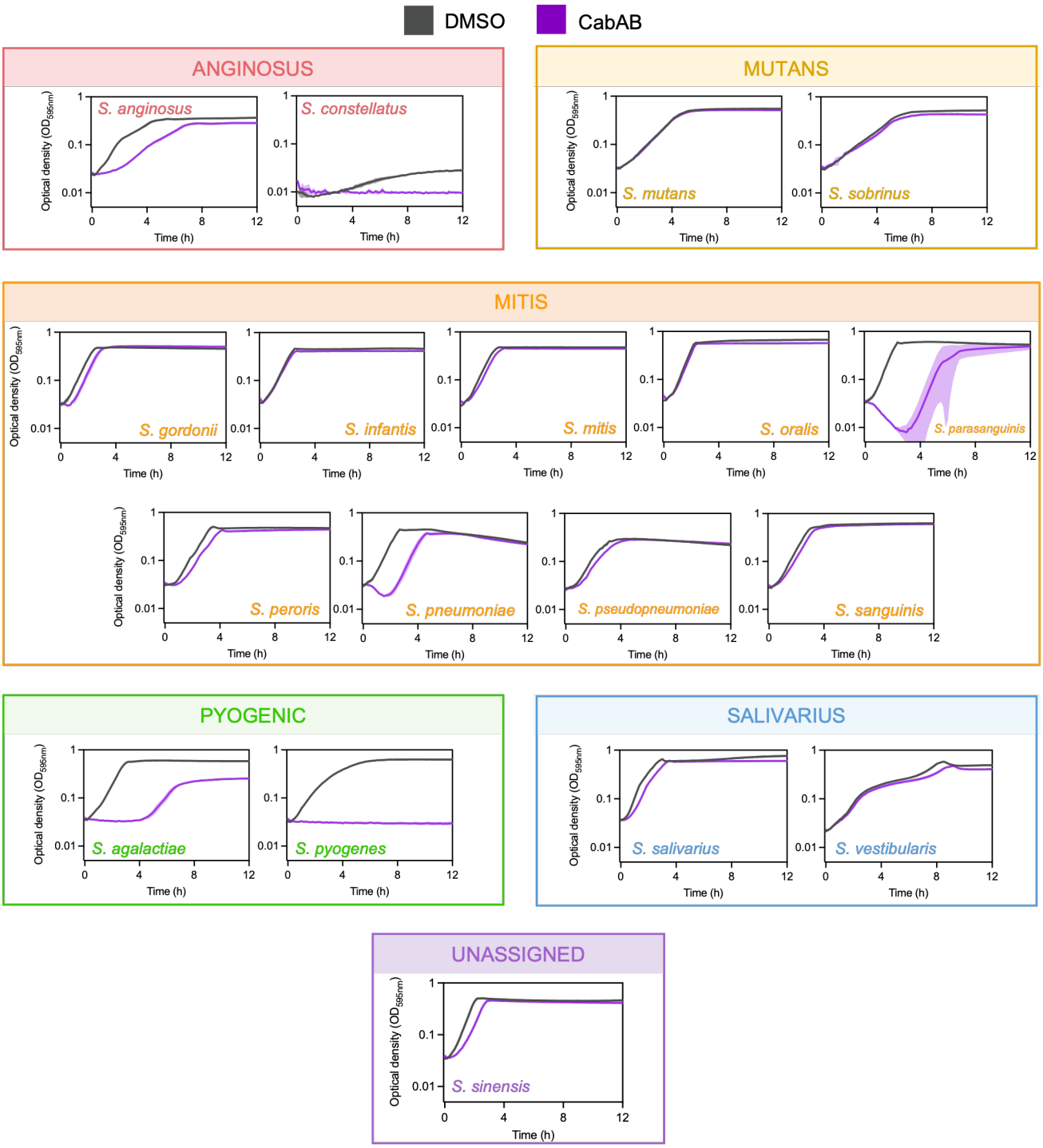

Fig. S11. Individual growth curves of 18 streptococcal species and their sensitivity to CabAB. Exponential cultures of streptococcal species were diluted to OD_{600} 0.1 in appropriate medium and treated with either DMSO or CabAB. Optical density was measured every 10 min for 24 h. For clarity, the first 12 h are shown. Species are colored according to streptococcal group. The experiment was repeated three times, independently. Summary data of the growth curves can be found in the main manuscript.

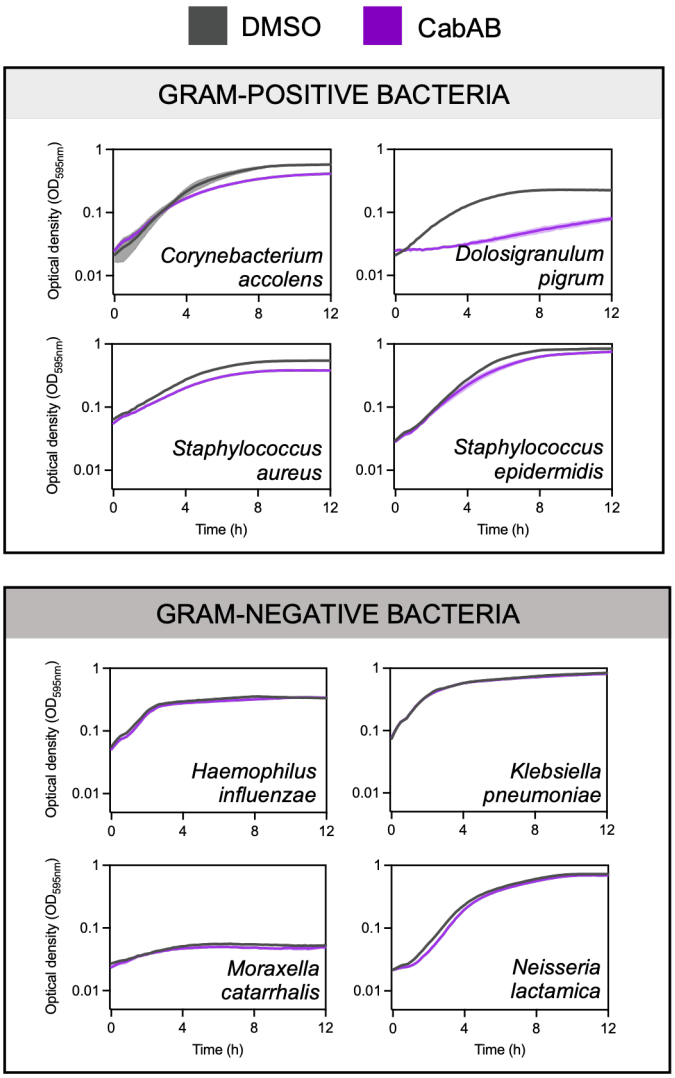

Fig. S12. Individual growth curves of 4 non-streptococcal Gram-positive and 4 Gram-negative bacteria and their sensitivity to CabAB. Exponential cultures of species were diluted to OD_{600} in appropriate medium and treated with either DMSO or CabAB. Optical density was measured every 10 min for 24 h. For clarity, the first 12 h are shown. Species are colored according to Gram staining. The experiment was repeated three times, independently. Summary data of the growth curves can be found in the main manuscript.

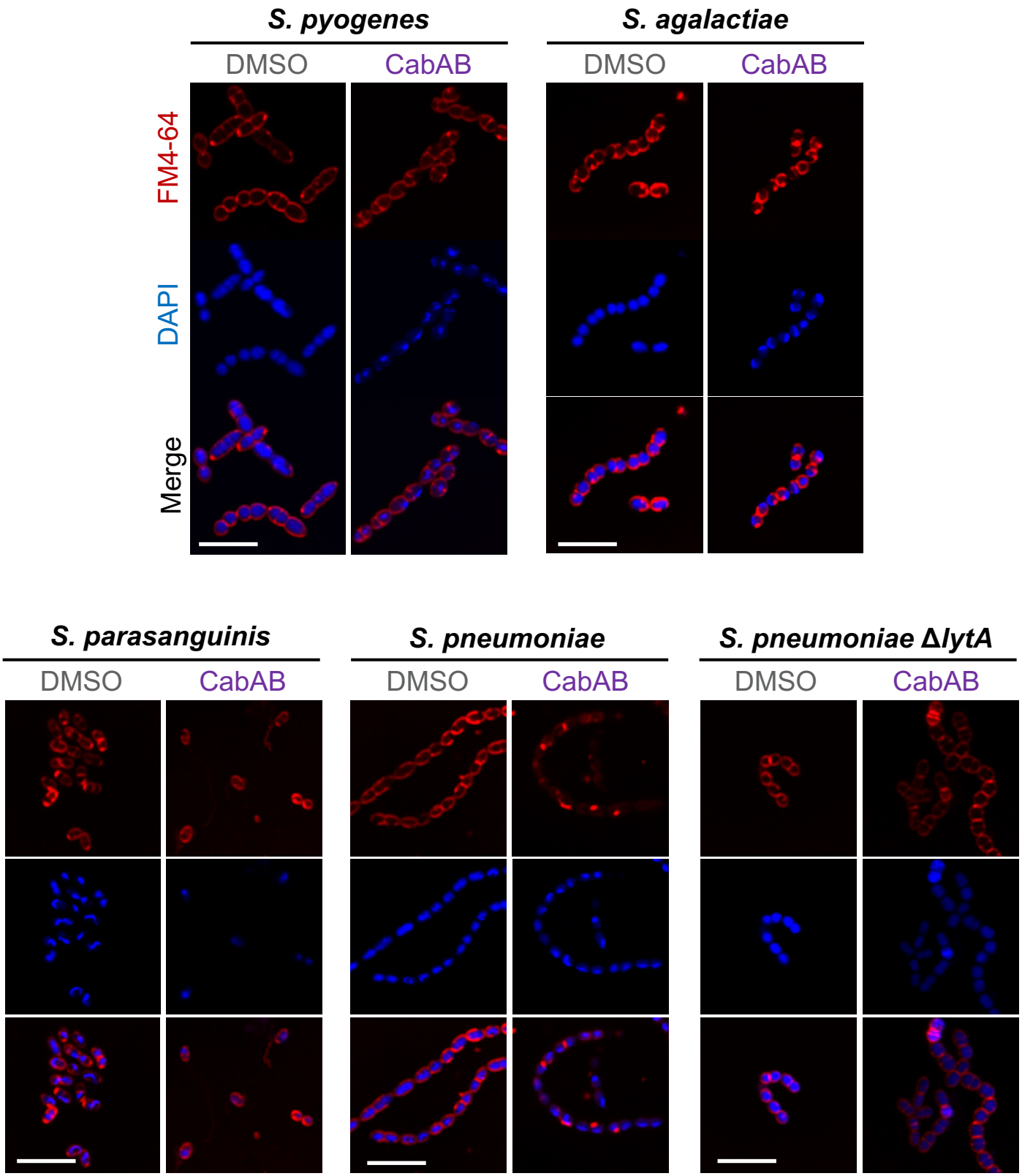

Fig. S13. CabAB treatment induces formation of membrane aggregates exclusively in *S. pneumoniae*. Cells were treated with 0.975 μM CabAB or 0.00975% DMSO for 15 min and stained with FM4-64 (membrane dye) and DAPI (nucleic acid dye), before being imaged in a confocal microscope. The experiment was repeated three times, independently. Scale – 5 μm.

Table S1. *Streptococcus mitis* genomes used in the study.

Strain	Region flanked by *plsX-acpP and* comAB recovered from genome (Y/N)	Presence of *cab* (Y/N)	*cab* locus length (bp)	Number of unique Cabs	Number of SigX boxes in *cab* locus	Presence of *cibAB* (Y/N)	Presence of *cibC* (Y/N)	Mature CSP sequence	4th last amino acid in CSP	Genbank accession	Location of region flanked by *plsX-acpP* and *comAB*
103U_S92	Y	Y	9862	4	20	Y	Y	EMRKPDGALFNLFRRR	F	GCA_946186075.1	23700 to 33569 (contig 5)
125U_S4	Y	N	-	-	-	N	N	EMRRSNNNFFNFLRRI	L	GCA_946184935.1	121366 to 123329 (contig 6)
128U_S6	N	-	-	-	-	-	-	-	-	GCA_946186995.1	-
12P_S5	Y	Y	6869	5	15	N	N	EIRQTHNIFFNFFKRR	F	GCA_946186085.1	27830 to 34698 (contig 6)
13P_S6	Y	Y	9282	5	16	Y	Y	EIRQTHNIFFNFFKRR	F	GCA_946187105.1	25159 to 34440 (contig 14)
14P_S7	Y	Y	2287	2	3	N	N	ESRVSDLILDFLFQRKK	Q	GCA_946186685.1	19479 to 21765 (contig 2)
161U_S19	Y	N	-	-	-	Y	Y	EMRKPDGALFNLFRRR	F	GCA_946188375.1	109310 to 116321 (contig 4)
1P_S1	Y	N	-	-	-	N	N	EIRIADKIFFNLFKRR	F	GCA_946183265.1	10854 to 17772 (contig 11)
22P_S11	N	-	-	-	-	-	-	-	-	GCA_946183395.1	-
27P_S14	Y	Y	7997	5	17	N	Y	EIRKTSNSLLNFFKRR	F	GCA_946184735.1	22263 to 30259 (contig 10)
32P_S19	Y	Y	6869	5	15	N	N	EIRQTHNIFFNFFKRR	F	GCA_946223905.1	28620 to 35488 (contig 11)
38P_S23	Y	Y	6883	3	17	N	N	ESRLSKLLRDFIFKIKQ	K	GCA_946183455.1	26015 to 32897 (contig 9)
3P_S2	N	-	-	-	-	-	-	-	-	GCA_946183495.1	-
44P_S26	Y	N	-	-	-	N	N	EIRIADKIFFNLFKRR	F	GCA_946186695.1	36560 to 43673 (contig 10)
50P_S29	Y	Y	7547	4	15	Y	Y	ESRLSRLLRDFIFQIKQ	Q	GCA_946188075.1	25384 to 32930 (contig 8)
52P_S30	N	-	-	-	-	-	-	-	-	GCA_946186135.1	-
61P_S37	N	-	-	-	-	-	-	-	-	GCA_946183505.1	-
62P_S38	Y	Y	7457	5	15	N	N	ESRLPKIRFDFIFPRKK	P	GCA_946183485.1	24444 to 24837 (contig 5)
68U_S84	Y	N	-	-	-	N	N	EIRQTHNIFFNFFKRR	F	GCA_946183445.1	13397 to 18312 (contig 11)
7P_S3	N	-	-	-	-	-	-	-	-	GCA_946185985.1	-
B1_S23	Y	Y	3685	6	4	N	Y	EMRKMNEKSFNFFNIFRRR	F	GCA_946189985.1	18059 to 21743 (contig 6)
B10_S32	N	-	-	-	-	-	-	-	-	GCA_946183015.1	-
B100_S21	N	-	-	-	-	-	-	-	-	GCA_946186585.1	-
B1015B24C5	Y	Y	8698	4	17	N	Y	EMRKSNSTFFHFLRRI	L	GCA_905220945.1	27478 to 36175 (contig 5)
B1015G24C3	Y	Y	3544	6	7	N	Y	ESRVSDLILDFLFQRKK	Q	GCA_905221115.1	3577 to 7120 (contig 16)
B1015H24C1	Y	Y	9990	4	18	Y	Y	ESRVSDLILDFLFQRKK	Q	GCA_905221235.1	24516 to 34505 (contig 8)
B1015H24C3	Y	N	-	-	-	N	N	ESRLPKILLDFLFLRKK	L	GCA_905221375.1	45744 to 49408 (contig 11)
B1015H24C4	Y	N	-	-	-	N	N	EMRRIGSVLLNFFKRR	F	GCA_905221455.1	110170 to 117841 (contig 8)
B102_S23	N	-	-	-	-	-	-	-	-	GCA_946183435.1	-
B105_S26	Y	Y	3557	4	9	N	Y	EMRKMNEKSFNFFNIFRR	I	GCA_946185425.1	22400 to 25956 (contig 13)
B106_S27	Y	Y	6472	5	16	N	N	ESRLSRLLRDFILQRKK	Q	GCA_946184175.1	27052 to 33524 (contig 3)
B107_S28	Y	N	-	-	-	N	N	EMRKMNEKSFNFFNIFRRR	F	GCA_946184385.1	73855 to 74301 (contig 3)
B110_S31	Y	N	-	-	-	N	N	ESRLPKIRFDFIFPRKK	P	GCA_946185245.1	58142 to 67806 (contig 5)
B111_S32	Y	N	-	-	-	Y	Y	EIRIADKIFFNLFKRR	F	GCA_946185595.1	35645 to 42337 (contig 8)
B112_S33	Y	Y	8000	5	17	N	Y	EMRLPKILRDFIFPRKK	P	GCA_946185795.1	16961 to 24960 (contig 6)
B113_S34	Y	Y	7352	5	14	N	N	EMRKPDGALFNLFRRR	F	GCA_946186035.1	28045 to 35396 (contig 4)
B114_S35	Y	Y	7477	1	16	Y	Y	ESRLPKILLDFIFPRKK	P	GCA_946184755.1	130119 to 137595 (contig 5)
B116_S37	Y	N	-	-	-	Y	Y	EMRRIDKMFINFLKRR	L	GCA_946186655.1	65112 to 74936 (contig 6)
B117_S38	Y	N	-	-	-	N	Y	EMRKMNEKSFNFFNIFRRR	F	GCA_946184245.1	112994 to 121923 (contig 7)
B119_S40	Y	N	-	-	-	N	N	ESRVSDLILDFLFQRKK	Q	GCA_946184705.1	31961 to 19319 (contig 13)
B12_S34	Y	Y	6838	5	15	N	N	EMRKPDGALFNLFRRR	F	GCA_946187535.1	27777 to 34614 (contig 5)
B121_S42	Y	N	-	-	-	N	Y	ESRVSDLILDFLFQRKK	Q	GCA_946184465.1	3398 to 5219 (contig 19)
B122_S43	Y	Y	9952	5	14	Y	Y	EIRQTHNIFFNFFKRR	F	GCA_946183295.1	27547 to 37498 (contig 7)
B124_S44	Y	N	-	-	-	N	N	EMRKMNEKSFNFFNIFRRR	F	GCA_946184765.1	33241 to 41252 (contig 13)
B125_S45	Y	Y	6733	3	14	Y	Y	EIRIADKIFFNLFKRR	F	GCA_946186825.1	10414 to 17146 (contig 9)
B126_S46	Y	Y	7012	5	14	Y	Y	EMRRIDKMFINFLKRR	L	GCA_946183535.1	26548 to 33559 (contig 6)
B128_S47	N	-	-	-	-	-	-	-	-	GCA_946187305.1	-
B129_S48	N	-	-	-	-	-	-	-	-	GCA_946183555.1	-
B13_S35	Y	N	-	-	-	Y	Y	EIRQTHNIFFNFFKRR	F	GCA_946184335.1	124084 to 131222 (contig 4)
B132_S51	Y	Y	5685	5	11	N	N	ESRVSDLILDFLFQRKK	Q	GCA_946188115.1	26091 to 31775 (contig 7)
B133-2_S52	N	-	-	-	-	-	-	-	-	GCA_946187925.1	-

(continues next page)

Table S1. (cont.)

B134_S53	N	-	-	-	-	-	-	-	-	GCA_946183695.1	-
B137_S55	Y	N	-	-	-	N	N	EMRKPDGALFNLFRRR	F	GCA_946183685.1	37817 to 47227 (contig 10)
B139_S57	Y	N	-	-	-	Y	Y	ESRMPKILRDFIFPRKK	P	GCA_946183965.1	129975 to 133398 (contig 6)
B14_S36	Y	N	-	-	-	Y	Y	DMRISESIRNLIFPRKKK	R	GCA_946188365.1	132557 to 140438 (contig 5)
B140_S58	Y	Y	7981	7	17	N	Y	EMRKMNEKSFNFFNIFRRR	F	GCA_946188035.1	21526 to 21918 (contig 7)
B146_S64	N	-	-	-	-	-	-	-	-	GCA_946184845.1	-
B147_S65	Y	N	-	-	-	Y	Y	EMRKMNEKSFNFFNIFRRR	F	GCA_946188285.1	33777 to 37954 (contig 129
B148_S66	N	-	-	-	-	-	-	-	-	GCA_946185855.1	-
B15_S37	Y	N	-	-	-	N	N	EMRKMNDKSFNLFNFFRRR	F	GCA_946188735.1	108533 to 116391 (contig 7)
B151_S69	N	-	-	-	-	-	-	-	-	GCA_946185905.1	-
B153_S71	Y	Y	10165	3	13	Y	Y	ESRLPKIRFDFIFPRKK	P	GCA_946188725.1	12287 to 22451 (contig 7)
B155_S73	N	-	-	-	-	-	-	-	-	GCA_946185295.1	-
B156_S74	N	-	-	-	-	-	-	-	-	GCA_946189305.1	-
B157_S75	Y	N	-	-	-	N	N	ESRLSRLLRDFIFQIKQ	Q	GCA_946188715.1	47861 to 48593 (contig 11)
B158_S76	N	-	-	-	-	-	-	-	-	GCA_946188825.1	-
B159_S77	Y	N	-	-	-	Y	Y	ESRLPKIRFDFIFPRKK	P	GCA_946188815.1	126333 to 135213 (contig 1)
B161_S79	Y	N	-	-	-	N	N	ESRLPKIRFDFIFPRKK	P	GCA_946188505.1	121745 to 133038 (contig 7)
B162_S80	N	-	-	-	-	-	-	-	-	GCA_946188645.1	-
B163_S81	N	-	-	-	-	-	-	-	-	GCA_946188665.1	-
B165_S83	Y	Y	7454	5	12	N	N	ESRLPKIRFDFIFPRKK	P	GCA_946188525.1	9840 to 17293 (contig 6)
B166_S84	N	-	-	-	-	-	-	-	-	GCA_946188555.1	-
B167_S85	Y	N	-	-	-	N	Y	ESRLPKILLDFLFLRKK	L	GCA_946188435.1	51984 to 55661 (contig 7)
B168_S86	Y	N	-	-	-	N	N	ESRLPKILLDFLFLRKK	L	GCA_946188425.1	129601 to 136812 (contig 5)
B169_S87	Y	N	-	-	-	N	Y	EMRLPKILRDFIFPRKK	P	GCA_946189595.1	100635 to 105207 (contig 7)
B170_S88	Y	Y	2522	2	7	N	N	EMRKMNEKSFNFFNIFRRR	F	GCA_946189625.1	16848 to 19369 (contig 119
B172_S90	N	-	-	-	-	-	-	-	-	GCA_946189565.1	-
B173_S91	N	-	-	-	-	-	-	-	-	GCA_946188785.1	-
B174_S92	Y	N	-	-	-	N	Y	EMRKPDGALFNLFRRR	F	GCA_946189255.1	44630 to 50769 (contig 13)
B176_S94	N	-	-	-	-	-	-	-	-	GCA_946188865.1	-
B19_S40	Y	Y	6430	2	12	N	Y	ESRVSDLILDFLFQRKK	Q	GCA_946190005.1	24129 to 30558 (contig 12)
B20_S41	N	-	-	-	-	-	-	-	-	GCA_946190035.1	-
B21_S42	N	-	-	-	-	-	-	-	-	GCA_946189125.1	-
B22_S43	Y	N	-	-	-	Y	Y	EMRKPDGALFNLFRRR	F	GCA_946189035.1	45816 to 51979 (contig 12)
B26_S45	Y	Y	7324	1	14	N	N	EMRRIDKIFINFLKRR	L	GCA_946189055.1	36560 to 43883 (contig 12)
B3_S25	Y	Y	6276	6	13	Y	Y	EMRKMNEKSFNFFNIFRRR	F	GCA_946189635.1	27034 to 33309 (contig 11)
B30_S48	Y	N	-	-	-	Y	Y	ESRVSDILLDFLFRRKK	R	GCA_946189895.1	13875 to 25318 (contig 11)
B31_S49	Y	Y	7447	5	12	Y	Y	EMRKMNDKSFNLFNFFRRR	F	GCA_946188485.1	24297 to 31743 (contig 13)
B33_S51	Y	Y	11446	5	20	Y	Y	ESRLPKIRFDFIFPRKK	P	GCA_946188605.1	9714 to 21159 (contig 14)
B34_S52	Y	N	-	-	-	N	N	EMRKMNEKSFNFFNIFNIFRR	F	GCA_946189235.1	27396 to 35035 (contig 17)
B37_S55	Y	N	-	-	-	N	Y	EIRKTSNSLLNFFKRR	F	GCA_946188755.1	8105 to 15978 (contig 6)
B38_S56	N	-	-	-	-	-	-	-	-	GCA_946188795.1	-
B4_S26	Y	N	-	-	-	N	N	EMRKMNEKSFNFFNIFRRR	F	GCA_946189945.1	13981 to 20965 (contig 29)
B42_S60	Y	N	-	-	-	Y	Y	ESRLPKIRFDFIFPRKK	P	GCA_946188675.1	147283 to 158055 (contig 5)
B43_S61	Y	Y	7325	4	16	Y	Y	EIRQTHNIFFNFFKRR	F	GCA_946188595.1	23294 to 30618 (contig 15)
B44_S62	Y	Y	6767	5	14	Y	Y	ESRLPKIRFDFIFPRKK	P	GCA_946188765.1	24640 to 31406 (contig 5)
B45_S63	Y	N	-	-	-	Y	Y	EIRQTHNIFFNFFKRR	F	GCA_946189355.1	8513 to 9245 (contig 6)
B46_S64	N	-	-	-	-	-	-	-	-	GCA_946188655.1	-
B47_S65	Y	N	-	-	-	N	Y	EMRKSNNNFFHFLRRI	L	GCA_946188745.1	43466 to 50055 (contig 7)
B49_S67	N	-	-	-	-	-	-	-	-	GCA_946188965.1	-
B5_S27	N	-	-	-	-	-	-	-	-	GCA_946189025.1	-
B50_S68	Y	N	-	-	-	Y	Y	ESRLPKIRFDFIFPRKK	P	GCA_946188955.1	126680 to 135327 (contig 7)

(continues next page)

Table S1. (cont.)

B52_S70	Y	N	-	-	-	N	N	ETRKTINSLLNLFKRR	F	GCA_946189865.1	13665 to 14681 (contig 16)
B54_S72	N	-	-	-	-	-	-	-	-	GCA_946188925.1	-
B55_S73	Y	N	-	-	-	N	N	ESRLSRLLRDFIFQIKQ	Q	GCA_946188895.1	49166 to 58656 (contig 9)
B56_S74	N	-	-	-	-	-	-	-	-	GCA_946188995.1	-
B57_S75	Y	N	-	-	-	N	Y	EMRRIDKMFINFLKRR	L	GCA_946188985.1	117917 to 125697 (contig 4)
B59_S77	N	-	-	-	-	-	-	-	-	GCA_946188875.1	-
B60_S78	Y	N	-	-	-	N	N	EMRKPDGALFNLFRRR	F	GCA_946189965.1	124476 to 131218 (contig 4)
B61_S79	Y	N	-	-	-	Y	Y	EIRKSNSALVNFFKRR	F	GCA_946188855.1	55573 to 66461 (contig 10)
B63_S81	Y	Y	7221	5	14	N	Y	ESRVSDLILDFLFQRKK	Q	GCA_946189015.1	10888 to 18108 (contig 15)
B65_S83	Y	N	-	-	-	N	N	ESRVSDILLDFLFRRKK	R	GCA_946189955.1	118327 to 122899 (contig 3)
B67_S85	Y	Y	3156	4	10	Y	Y	EMRKSNNTFFNFLRRI	L	GCA_946188885.1	7767 to 10922 (contig 13)
B69_S87	N	-	-	-	-	-	-	-	-	GCA_946188945.1	-
B73_S91	Y	Y	8931	3	19	N	N	ESRVSDILLDFLFRRKK	R	GCA_946188935.1	13555 to 22485 (contig 9)
B74_S92	Y	N	-	-	-	N	N	EIRQTHNIFFNFFKRR	F	GCA_946188975.1	10138 to 10870 (contig 11)
B76_S94	Y	Y	7437	4	12	N	N	ESRLSRLLRDFIFQIKQ	Q	GCA_946189935.1	30822 to 38258 (contig 8)
B77_S95	Y	N	-	-	-	N	Y	EIRKTSNSLLNFFKRR	F	GCA_946189755.1	118938 to 126810 (contig 5)
B78_S96	Y	Y	8714	4	21	Y	Y	EMRRIDKMFINFLKRR	L	GCA_946189875.1	25049 to 33762 (contig 5)
B79_S1	Y	Y	3832	6	10	Y	Y	EMRKMNEKSFNFFNIFRRR	F	GCA_946188405.1	8778 to 12609 (contig 18)
B82_S4	Y	N	-	-	-	N	N	EMRKMNEKSFNFFNIFRRR	F	GCA_946188465.1	68030 to 72644 (contig 9)
B85_S7	Y	N	-	-	-	N	N	ESRLPKIRFDFIFPRKK	P	GCA_946189515.1	124429 to 125974 (contig 6)
B88_S10	Y	N	-	-	-	N	Y	EMRLPKILRDFIFPRKK	P	GCA_946189785.1	67460 to 77667 (contig 6)
B89L_S11	Y	Y	8758	4	19	Y	Y	EMRKPDGALFNLFRRR	F	GCA_946188455.1	23760 to 32517 (contig 5)
B9_S31	Y	N	-	-	-	N	N	EMRKMNEKSFNFFNIFRRR	F	GCA_946189075.1	32842 to 41229 (contig 13)
B91_S12	Y	N	-	-	-	Y	Y	EMRLSKFLRDFILQRKN	Q	GCA_946189535.1	19728 to 28296 (contig 10)
B93_S14	N	-	-	-	-	-	-	-	-	GCA_946189095.1	-
B95_S16	Y	N	-	-	-	N	N	MKNTVKLEQFVALKEKTCRR FEVGKLEKQLIVYLISSKEDK	K	GCA_946188475.1	57945 to 58714 (contig 10)
B96_S17	Y	Y	7329	1	16	N	N	EIRIADKIFFNLFKRR	F	GCA_946189115.1	35203 to 42531 (contig 12)
B97_S18	Y	N	-	-	-	N	N	EIRQTHNIFFNFFKRR	F	GCA_946189825.1	102775 to 103025 (contig 4)
B99_S20	N	-	-	-	-	-	-	-	-	GCA_946189005.1	-
GCF_000027165.1_ASM2716v1	Y	Y	9068	5	18	Y	Y	EMRKPDGALFNLFRRR	F	GCA_000027165.1_ASM2716v1	53854 to 62921 (contig 1)
GCF_000148505.1_ASM14850v1	N	-	-	-	-	-	-	-	-	GCA_000148505.1_ASM14850v1	-
GCF_000148525.1_ASM14852v1	Y	Y	4573	7	7	N	N	ESRVSDILLDFLFRRKK	R	GCA_000148525.1_ASM14852v1	23154 to 27726 (contig 22)
GCF_000148545.1_ASM14854v1	N	-	-	-	-	-	-	-	-	GCA_000148545.1_ASM14854v1	-
GCF_000148585.2_ASM14858v3	Y	Y	8195	5	17	Y	Y	EIRQTHNIFFNFFKRR	F	GCA_000148585.2_ASM14858v3	46590 to 54784 (contig 1)
GCF_000220045.1_ASM22004v2	Y	N	-	-	-	N	N	ESRLSRLLRDFIFQIKQ	Q	GCA_000220045.1_ASM22004v2	113804 to 121511 (contig 10)
GCF_000220085.1_ASM22008v2	Y	Y	7601	3	18	N	N	EMRRIDKIFNFLKRR	L	GCA_000220085.1_ASM22008v2	33312 to 40912 (contig 6)
GCF_000222785.1_ASM22278v2	Y	N	-	-	-	Y	Y	EMRLPKILRDFIFPRKK	P	GCA_000222785.1_ASM22278v2	80829 to 88913 (contig 17)
GCF_000257805.1_ASM25780v1	Y	N	-	-	-	N	N	EMRRIDKIFINFLKRR	L	GCA_000257805.1_ASM25780v1	30349 to 36794 (contig 56)
GCF_000257865.1_ASM25786v1	Y	N	-	-	-	N	N	EMRKMNEKSFNFFNIFRRR	F	GCA_000257865.1_ASM25786v1	108462 to 111048 (contig 56)
SK579v1.0	Y	N	-	-	-	N	N	EIRKSNSALVNFFKRR	F	GCA_000257905.1_SmitisSK579v1.0	51648 to 53976 (contig 13)
GCF_000385815.1_ASM38581v1	N	-	-	-	-	-	-	-	-	GCA_000385815.1_ASM38581v1	-
Smit.str17_34_v1.0	Y	Y	8147	3	16	N	N	ESRISDLLLDFLFQRKK	Q	GCA_000430305.1_Smit.str17_34_v1.	24690 to 32836 (contig 5)
Smit.str18_56_v1.0	Y	N	-	-	-	N	N	ETRKTINSLLNLFKRR	F	GCA_000430345.1_Smit.str18_56_v1.	6585 to 7319 (contig 12)
Smit.str29_42_v1.0	Y	N	-	-	-	Y	Y	EIRQTHNIFFNFFKRR	F	GCA_000430365.1_Smit.str29_42_v1.	28257 to 34755 (contig 8)
Sm.str21_39_v1.0	Y	N	-	-	-	N	N	EMRLPKILRDFIFPRKK	P	GCA_000506725.1_Sm.str21_39_v1.0	107853 to 111953 (contig 6)
Sm.str27_7_v1.0	Y	N	-	-	-	N	N	EIRQTHNIFFNFFKRR	F	GCA_000506765.1_Sm.str27_7_v1.0	48091 to 54587 (contig 8)
GCF_000722685.1_ASM72268v1	Y	Y	6593	3	15	N	N	EIRKSNSALVNFFKRR	F	GCA_000722685.1_ASM72268v1	33237 to 39817 (contig 3)
GCF_000722695.1_ASM72269v1	Y	Y	8106	4	20	N	Y	EMRLPKILRDFIFPRKK	P	GCA_000722695.1_ASM72269v1	28640 to 36745 (contig 2)
GCF_000722705.1_ASM72270v1	Y	Y	7521	3	19	N	Y	EMRRIDKMFINFLKRR	L	GCA_000722705.1_ASM72270v1	26310 to 33830 (contig 1)
GCF_000722755.1_ASM72275v1	Y	N	-	-	-	N	N	ETRKTINSLLNLFKRR	F	GCA_000722755.1_ASM72275v1	19662 to 20232 (contig 8)

(continues next page)

Table S1. (cont.)

GCF_000722765.2_ASM72276v2	Y	Y	7760	4	18	N	Y	EMRKSNNNFFHFLRRI	L	GCA_000722765.2 ASM72276v2	49608 to 57367 (contig 1)
GCF_000722775.1_ASM72277v1	Y	Y	8930	3	21	N	N	EIRKTSNSLLNFFKRR	F	GCA_000722775.1 ASM72277v1	27763 to 36692 (contig 6)
GCF_000722815.1_ASM72281v1	Y	Y	1789	3	4	N	N	EMRRSNNNFFNFLRRI	L	GCA_000722815.1 ASM72281v1	20061 to 21849 (contig 1)
GCF_000722835.1_ASM72283v1	N	-	-	-	-	-	-	-	-	GCA_000722835.1 ASM72283v1	-
GCF_000724165.1_ASM72416v1	Y	N	-	-	-	N	N	Not found	-	GCA_000724165.1 ASM72416v1	438770 to 446249 (contig 12)
GCF_000960005.1_ASM96000v1	Y	Y	8611	2	18	Y	Y	EMRKPDGALFNLFRRR	F	GCA_000960005.1 ASM96000v1	29135 to 37745 (contig 1)
GCF_000960025.1_ASM96002v1	Y	Y	12265	4	24	N	N	ESRLPKIRFDFIFPRKK	P	GCA_000960025.1 ASM96002v1	32833 to 45097 (contig 3)
GCF_000960065.1_ASM96006v1	Y	N	-	-	-	N	N	DMRISESIRNLIFPRKKK	R	GCA_000960065.1 ASM96006v1	33075 to 43002 (contig 5)
GCF_001070035.1_ASM107003v1	N	-	-	-	-	-	-	-	-	GCA_001070035.1 ASM107003v1	-
GCF_001070205.1_ASM107020v1	N	-	-	-	-	-	-	-	-	GCA_001070205.1 ASM107020v1	-
GCF_001070375.1_ASM107037v1	N	-	-	-	-	-	-	-	-	GCA_001070375.1 ASM107037v1	-
GCF_001070705.1_ASM107070v1	Y	N	-	-	-	N	N	ESRLSKLLRDFIFKIKQ	K	GCA_001070705.1 ASM107070v1	91104 to 97864 (contig 13)
GCF_001070985.1_ASM107098v1	Y	N	-	-	-	Y	Y	EMRKPDGALFNLFRRR	F	GCA_001070985.1 ASM107098v1	125336 to 135287 (contig 33)
GCF_001074635.1_ASM107463v1	N	-	-	-	-	-	-	-	-	GCA_001074635.1 ASM107463v1	-
GCF_001281025.1_ASM128102v1	Y	N	-	-	-	Y	Y	EMRKSNNNFFNFLRRI	L	GCA_001281025.1 ASM128102v1	326587 to 336055 (contig 1)
GCF_001546795.1_ASM154679v1	N	-	-	-	-	-	-	-	-	GCA_001546795.1 ASM154679v1	-
GCF_001560895.1_ASM156089v1	Y	Y	2200	2	5	N	N	EMRKSNNTFFNFLRRI	-	GCA_001560895.1 ASM156089v1	73674 to 75873 (contig 1)
GCF_001579045.1_ASM157904v1	Y	N	-	-	-	Y	Y	EMRLPKILRDFIFPRKK	P	GCA_001579045.1 ASM157904v1	416341 to 423519 (contig 63)
GCF_001588595.1_ASM158859v1	Y	N	-	-	-	N	N	ETRKTINSLLNLFKRR	F	GCA_001588595.1 ASM158859v1	14693 to 15462 (contig 4)
GCF_001588605.1_ASM158860v1	Y	N	-	-	-	N	N	ETRKTINSLLNLFKRR	F	GCA_001588605.1 ASM158860v1	34154 to 34922 (contig 15)
GCF_001588625.1_ASM158862v1	Y	Y	9205	5	23	N	N	EMRKPDGALFNLFRRR	F	GCA_001588625.1 ASM158862v1	9739 to 18943 (contig 27)
GCF_002005545.1_ASM200554v1	Y	Y	3980	6	9	N	N	EMRLPKILRDFIFPRKK	P	GCA_002005545.1 ASM200554v1	495219 to 499198 (contig 1)
GCF_002014755.1_ASM201475v1	Y	N	-	-	-	N	N	EIRQTHNIFFNFFKRR	F	GCA_002014755.1 ASM201475v1	115535 to 123729 (contig 6)
GCF_002014795.1_ASM201479v1	Y	Y	8075	4	21	N	Y	EMRKPDGALFNLFRRR	F	GCA_002014795.1 ASM201479v1	26394 to 34468 (contig 6)
GCF_002014875.1_ASM201487v1	Y	N	-	-	-	Y	Y	EIRQTHNIFFNFFKRR	F	GCA_002014875.1 ASM201487v1	63548 to 69821 (contig 7)
GCF_002096735.1_ASM209673v1	Y	Y	9752	2	14	N	N	EMRKSNNNFFNFLRRI	L	GCA_002096735.1 ASM209673v1	14476 to 24227 (contig 13)
GCF_002096755.1_ASM209675v1	N	-	-	-	-	-	-	-	-	GCA_002096755.1 ASM209675v1	-
GCF_002096765.1_ASM209676v1	Y	Y	6682	6	16	Y	Y	EMRKPDGALFNLFRRR	F	GCA_002096765.1 ASM209676v1	26701 to 33382 (contig 48)
GCF_002096775.1_ASM209677v1	Y	N	-	-	-	Y	Y	ESRLPKIRFDFIFPRKK	P	GCA_002096775.1 ASM209677v1	23754 to 24138 (contig 24)
GCF_002096815.1_ASM209681v1	Y	N	-	-	-	Y	Y	EMRRIDKMFINFLKRR	L	GCA_002096815.1 ASM209681v1	14082 to 19251 (contig 18)
GCF_002096835.1_ASM209683v1	Y	N	-	-	-	Y	Y	ESRVSDILLDFLFRRKK	R	GCA_002096835.1 ASM209683v1	4746 to 5469 (contig 19)
GCF_002096845.1_ASM209684v1	N	-	-	-	-	-	-	-	-	GCA_002096845.1 ASM209684v1	-
GCF_002096895.1_ASM209689v1	Y	N	-	-	-	N	N	DSRISKYLRDFIFPRKK	P	GCA_002096895.1 ASM209689v1	125698 to 126269 (contig 19)
GCF_002096925.1_ASM209692v1	N	-	-	-	-	-	-	-	-	GCA_002096925.1 ASM209692v1	-
GCF_002096935.1_ASM209693v1	Y	Y	6733	3	14	N	N	EIRIADKIFFNLFKRR	F	GCA_002096935.1 ASM209693v1	24923 to 31655 (contig 25)
GCF_002860825.1_ASM286082v1	Y	Y	3524	6	5	N	N	EMRKSNNTFFNFLRRI	L	GCA_002860825.1 ASM286082v1	18587 to 22110 (contig 13)
GCF_002860865.1_ASM286086v1	Y	Y	2525	2	5	N	N	ESRVSDLILDFLFQRKK	Q	GCA_002860865.1 ASM286086v1	58524 to 61048 (contig 3)
GCF_002860905.1_ASM286090v1	Y	Y	3156	4	10	Y	Y	EMRRIDKIFINFLKRR	L	GCA_002860905.1 ASM286090v1	18653 to 21808 (contig 8)
GCF_002871315.1_ASM287131v1	Y	Y	3524	6	5	N	N	EMRKSNNTFFNFLRRI	L	GCA_002871315.1 ASM287131v1	18509 to 22032 (contig 13)
GCF_003942775.1_ASM394277v1	N	-	-	-	-	-	-	-	-	GCA_003942775.1 ASM394277v1	-
GCF_003942885.1_ASM394288v1	N	-	-	-	-	-	-	-	-	GCA_003942885.1 ASM394288v1	-
GCF_003942965.1_ASM394296v1	Y	N	-	-	-	N	N	Not found	-	GCA_003942965.1 ASM394296v1	11262 to 11512 (contig 3)
GCF_003942995.1_ASM394299v1	Y	N	-	-	-	Y	Y	ESRVSDILLDFLFRRKK	R	GCA_003942995.1 ASM394299v1	30869 to 40944 (contig 14)
GCF_003943915.1_ASM394391v1	N	-	-	-	-	-	-	-	-	GCA_003943915.1 ASM394391v1	-
GCF_003943965.1_ASM394396v1	Y	N	-	-	-	N	Y	EMRRSNNNFFNFLRRI	L	GCA_003943965.1 ASM394396v1	40655 to 42425 (contig 16)
GCF_005144795.1_ASM514479v1	Y	Y	1780	2	4	Y	Y	ESRLSKIFLDFIFPRKK	P	GCA_005144795.1 ASM514479v1	13402 to 15181 (contig 16)
GCF_005844455.1_ASM584445v1	N	-	-	-	-	-	-	-	-	GCA_005844455.1 ASM584445v1	-
GCF_008763935.1_FS623	Y	Y	6780	5	16	Y	Y	ESRLPKIRFDFIFPRKK	P	GCA_008763935.1 FS623	107171 to 113950 (contig 5)
GCF_009495695.1_ASM949569v1	N	-	-	-	-	-	-	-	-	GCA_009495695.1 ASM949569v1	-
GCF_009495705.1_ASM949570v1	Y	Y	7465	7	16	N	N	EIRKTSNSLLNFFKRR	F	GCA_009495705.1 ASM949570v1	23517 to 30981 (contig 17)

(continues next page)

Table S1. (cont.)

GCF_009495735.1_ASM949573v1	Y	N	-	-	-	N	N	ESRVSDLILDFLFQRKK	Q	GCA_009495735.1 ASM949573v1	88623 to 96087 (contig 8)
GCF_009495895.1_ASM949589v1	Y	Y	7465	7	16	N	N	EIRKTSNSLLNFFKRR	F	GCA_009495895.1 ASM949589v1	23636 to 31100 (contig 8)
GCF_009495955.1_ASM949595v1	Y	N	-	-	-	N	N	EIRKTSNSLLNFFKRR	F	GCA_009495955.1 ASM949595v1	58616 to 66080 (contig 10)
GCF_009496035.1_ASM949603v1	Y	N	-	-	-	N	N	EIRKTSNSLLNFFKRR	F	GCA_009496035.1 ASM949603v1	88623 to 96087 (contig 9)
GCF_009496045.1_ASM949604v1	Y	N	-	-	-	N	N	EIRKTSNSLLNFFKRR	F	GCA_009496045.1 ASM949604v1	88615 to 96079 (contig 9)
GCF_009496065.1_ASM949606v1	Y	Y	7465	7	16	N	N	EIRKTSNSLLNFFKRR	F	GCA_009496065.1 ASM949606v1	23577 to 31041 (contig 10)
GCF_009496075.1_ASM949607v1	Y	Y	7465	7	16	N	N	EIRKTSNSLLNFFKRR	F	GCA_009496075.1 ASM949607v1	23517 to 30981 (contig 11)
GCF_009496165.1_ASM949616v1	Y	Y	7465	7	16	N	N	EIRKTSNSLLNFFKRR	F	GCA_009496165.1 ASM949616v1	23517 to 30981 (contig 8)
GCF_009496185.1_ASM949618v1	N	-	-	-	-	-	-	-	-	GCA_009496185.1 ASM949618v1	-
GCF_009496205.1_ASM949620v1	N	-	-	-	-	-	-	-	-	GCA_009496205.1 ASM949620v1	-
GCF_009496295.1_ASM949629v1	Y	N	-	-	-	Y	Y	ESRLPKIRFDFIFPRKK	P	GCA_009496295.1 ASM949629v1	124953 to 131821 (contig 6)
GCF_009496335.1_ASM949633v1	Y	N	-	-	-	N	N	EIRKTSNSLLNFFKRR	F	GCA_009496335.1 ASM949633v1	88622 to 96086 (contig 8)
GCF_009496355.1_ASM949635v1	Y	N	-	-	-	N	N	EIRKTSNSLLNFFKRR	F	GCA_009496355.1 ASM949635v1	88623 to 96087 (contig 7)
GCF_009496385.1_ASM949638v1	Y	Y	2273	2	6	N	N	EMRKSNNTFFNFLRRI	L	GCA_009496385.1 ASM949638v1	111359 to 113631 (contig 5)
GCF_009496395.1_ASM949639v1	Y	Y	7465	7	16	N	N	EIRKTSNSLLNFFKRR	F	GCA_009496395.1 ASM949639v1	23577 to 31041 (contig 8)
GCF_009496435.1_ASM949643v1	Y	N	-	-	-	N	N	EIRKTSNSLLNFFKRR	F	GCA_009496435.1 ASM949643v1	88623 to 96087 (contig 8)
GCF_009496505.1_ASM949650v1	Y	Y	7465	7	16	N	N	EIRKTSNSLLNFFKRR	F	GCA_009496505.1 ASM949650v1	23517 to 30981 (contig 6)
GCF_009496725.1_ASM949672v1	Y	Y	7465	7	16	N	N	EIRKTSNSLLNFFKRR	F	GCA_009496725.1 ASM949672v1	23577 to 31041 (contig 7)
GCF_009496735.1_ASM949673v1	Y	Y	7465	7	16	N	N	EIRKTSNSLLNFFKRR	F	GCA_009496735.1 ASM949673v1	23577 to 31041 (contig 7)
GCF_009496755.1_ASM949675v1	Y	N	-	-	-	N	N	EIRKTSNSLLNFFKRR	F	GCA_009496755.1 ASM949675v1	18419 to 25883 (contig 15)
GCF_009496795.1_ASM949679v1	Y	Y	7465	7	16	N	N	EIRKTSNSLLNFFKRR	F	GCA_009496795.1 ASM949679v1	23577 to 31041 (contig 8)
GCF_009496805.1_ASM949680v1	Y	Y	7465	7	16	N	N	EIRKTSNSLLNFFKRR	F	GCA_009496805.1 ASM949680v1	23577 to 31041 (contig 8)
GCF_009496815.1_ASM949681v1	Y	Y	7465	7	16	N	N	EIRKTSNSLLNFFKRR	F	GCA_009496815.1 ASM949681v1	23577 to 31041 (contig 9)
GCF_009496825.1_ASM949682v1	N	-	-	-	-	-	-	-	-	GCA_009496825.1 ASM949682v1	-
GCF_009496835.1_ASM949683v1	Y	Y	7465	7	16	N	N	EIRKTSNSLLNFFKRR	F	GCA_009496835.1 ASM949683v1	23577 to 31041 (contig 9)
GCF_009496895.1_ASM949689v1	Y	Y	7465	7	16	N	N	EIRKTSNSLLNFFKRR	F	GCA_009496895.1 ASM949689v1	23517 to 30981 (contig 15)
GCF_009496905.1_ASM949690v1	Y	N	-	-	-	N	N	EIRKTINGLLNFFKRR	F	GCA_009496905.1 ASM949690v1	51468 to 56727 (contig 9)
GCF_009730515.1_ASM973051v1	Y	Y	8195	5	17	N	N	EIRQTHNIFFNFFKRR	-	GCA_009730515.1 ASM973051v1	31493 to 39687 (contig 1)
GCF_900459425.1_42042_B02	Y	N	-	-	-	N	N	EIRQTHNIFFNFFKRR	F	GCA_900459425.1 42042_B02	116797 to 124991 (contig 2)
MSCx	Y	Y	8886	4	18	Y	Y	DSRISKYLRDFIFPRKK	P	GCA_905187535.1	25487 to 34372 (contig 11)
NM2_1	Y	N	-	-	-	N	N	EIRKTSNSLLNFFKRR	F	GCA_905187515.1	32077 to 39698 (contig 13)
NM4_2	Y	N	-	-	-	N	Y	EIRKTSNSLLNFFKRR	F	GCA_905187545.1	32687 to 40308 (contig 13)
NM5_2	N	-	-	-	-	-	-	-	-	GCA_905187495.1	-
P11_S4	Y	N	-	-	-	N	N	EMRKPDGALFNLFRRR	F	GCA_946189525.1	42441 to 48870 (contig 6)
P164_S40	N	-	-	-	-	-	-	-	-	GCA_946189105.1	-
P21_S10	Y	Y	7902	6	14	N	N	EMRKPDGALFNLFRRR	F	GCA_946189045.1	26201 to 34102 (contig 7)
P28_S15	Y	N	-	-	-	Y	Y	ESRLPKIRFDFIFPRKK	P	GCA_946188915.1	120578 to 128595 (contig 6)
P42_S25	N	-	-	-	-	-	-	-	-	GCA_946189085.1	-
P55_S33	Y	Y	7359	5	16	Y	Y	EMRKPDGALFNLFRRR	F	GCA_946189995.1	28034 to 35392 (contig 7)
P59_S35	Y	N	-	-	-	Y	Y	ESRLPKIRFDFIFPRKK	P	GCA_946189495.1	151368 to 161798 (contig 4)
P60_S36	N	-	-	-	-	-	-	-	-	GCA_946190025.1	-
S1071B24C1	Y	Y	2587	2	9	N	N	ESRISDLLLDFLFQRKK	Q	GCA_905221505.1	3951 to 6537 (contig 12)
S1071B24C2	Y	Y	2461	2	8	N	N	ESRISDLLLDFLFQRKK	Q	GCA_905221525.1	3630 to 6090 (contig 13)
S1071G24C1	Y	N	-	-	-	N	N	EMRKIDDALFNLFNFFRRR	F	GCA_905221535.1	47372 to 58002 (contig 11)
S1071G24C2	Y	N	-	-	-	N	N	EMRKIDDALFNLFNFFRRR	F	GCA_905221545.1	47372 to 58002 (contig 11)
S1071G24C3	Y	Y	2461	2	8	N	N	ESRISDLLLDFLFQRKK	Q	GCA_905221005.1	3630 to 6090 (contig 12)
S1071G24C4	N	-	-	-	-	-	-	-	-	GCA_905221035.1	-
S1071G24C5	N	-	-	-	-	-	-	-	-	GCA_905221045.1	-
S1072B24C4	Y	Y	2873	4	7	N	N	EMRMLKSPFSFLFPRKK	P	GCA_905221065.1	23060 to 25952 (contig 4)
S1072B24C5	Y	Y	2873	4	7	N	N	EMRMLKSPFSFLFPRKK	P	GCA_905221055.1	23060 to 25952 (contig 4)

(continues next page)

Table S1. (cont.)

S1072G24C4	Y	N	-	-	-	N	N	ESRISDLLLDFLFQRKK	Q	GCA_905221105.1	26882 to 35329 (contig 7)
S1075M24C2	Y	N	-	-	-	Y	Y	ESRVADLLLDFLFQRKK	Q	GCA_905221085.1	103323 to 113219 (contig 6)
S1075M24C3	Y	N	-	-	-	N	N	ESRISDLLLDFLFQRKK	Q	GCA_905221095.1	31726 to 42537 (contig 11)
S1075M24C5	Y	Y	10812	2	26	N	N	ESRISDLLLDFLFQRKK	Q	GCA_905221075.1	27291 to 37102 (contig 8)
S1086G24C1	N	-	-	-	-	-	-	-	-	GCA_905221125.1	-
S1088B24C2	Y	Y	6473	2	18	N	Y	ESRVSDLILDFLFQRKK	Q	GCA_905221135.1	26672 to 33144 (contig 6)
S1088M24C1	Y	N	-	-	-	N	N	EMRIADKIFFNLFKRR	F	GCA_905221145.1	54156 to 65018 (contig 7)
S1091B24C4	Y	N	-	-	-	N	N	EMRKPDGALFNLFRRR	F	GCA_905221155.1	125261 to 134199 (contig 4)
S1092G24C1	Y	Y	1740	2	2	N	N	DMRISGSIRNLIFPRKKK	R	GCA_905221165.1	12912 to 14651 (contig 9)
S1092G24C3	Y	Y	1768	2	2	N	N	EIRKKSNSLLNFFKRR	F	GCA_905221175.1	13104 to 14871 (contig 5)
S1092G24C4	N	-	-	-	-	-	-	-	-	GCA_905221185.1	-
S1093G24C1	Y	Y	8698	4	17	N	Y	EMRKSNSTFFHFLRRI	L	GCA_905221195.1	27478 to 36175 (contig 5)
S1093G24C2	Y	N	-	-	-	N	N	ESRLPKILRDFIFPRKK	P	GCA_905221205.1	66159 to 73603 (contig 4)
S1093G24C3	Y	N	-	-	-	N	N	EMRKTSYSLLNLFKRR	F	GCA_905221225.1	104898 to 109878 (contig 7)
S1096G24C5	N	-	-	-	-	-	-	-	-	GCA_905221215.1	-
S1096M24C3	Y	Y	9580	5	22	N	N	EIRKTSNSLFNFFKRR	F	GCA_905221245.1	11901 to 21480 (contig 6)
S1096M24C5	N	-	-	-	-	-	-	-	-	GCA_905221285.1	-
U10_S50	Y	N	-	-	-	Y	Y	EMRRIDKMFINFLKRR	L	GCA_946188615.1	136100 to 146454 (contig 6)
U104_S93	Y	Y	9859	4	20	Y	Y	EMRKPDGALFNLFRRR	F	GCA_946188685.1	23700 to 33558 (contig 6)
U105_S94	N	-	-	-	-	-	-	-	-	GCA_946188575.1	-
U109_S95	Y	N	-	-	-	N	N	EIRKTSNSLFNFFKRR	F	GCA_946188695.1	67998 to 77255 (contig 5)
U114_S96	Y	N	-	-	-	Y	Y	EMRRIDKMFINFLKRR	L	GCA_946188415.1	84542 to 94928 (contig 4)
U117_S1	Y	N	-	-	-	N	N	DSRISKYLRDFIFPRKK	P	GCA_946188585.1	15202 to 15765 (contig 7)
U12_S51	Y	N	-	-	-	Y	Y	ESRLPKIRFDFIFPRKK	P	GCA_946224775.1	52874 to 63087 (contig 6)
U122_S2	Y	N	-	-	-	N	Y	EIRKTSNSLLNFFKRR	F	GCA_946189145.1	149195 to 157067 (contig 2)
U123_S3	Y	N	-	-	-	N	N	ESRVSDILLNFLFRRKK	R	GCA_946190065.1	49685 to 50417 (contig 16)
U126_S5	Y	Y	8396	4	19	Y	Y	ESRVSDLILDFLFQRKK	Q	GCA_946190085.1	25538 to 25928 (contig 3)
U13_S52	Y	N	-	-	-	N	N	ESRLSKLLRDFIFKIKQ	K	GCA_946190075.1	21460 to 34396 (contig 12)
U131_S7	Y	N	-	-	-	N	N	ESRVSDLILDFLFQRKK	Q	GCA_946190095.1	127239 to 129511 (contig 5)
U134_S8	Y	Y	1964	3	4	N	N	EMRRSNNNFFNFLRRI	L	GCA_946190055.1	12955 to 14918 (contig 6)
U135_S9	Y	Y	1964	3	4	N	N	EMRRSNNNFFNFLRRI	L	GCA_946190045.1	12955 to 14918 (contig 6)
U14_S53	N	-	-	-	-	-	-	-	-	GCA_946190385.1	-
U143_S13	Y	N	-	-	-	N	N	EIRKKSNSLLNFFKRR	F	GCA_946190395.1	13391 to 14114 (contig 3)
U144_S14	Y	N	-	-	-	N	Y	EMRKMNEKSFNFFNIFRRR	F	GCA_946190245.1	31975 to 35539 (contig 15)
U148_S15	Y	Y	1964	3	4	N	N	EMRRSNNNFFNFLRRI	L	GCA_946190215.1	12955 to 14918 (contig 6)
U15_S54	Y	Y	3970	1	7	N	N	ESRVSDLILDFLFQRKK	Q	GCA_946190375.1	44742 to 48711 (contig 14)
U16_S55	Y	N	-	-	-	Y	Y	ESRLPKIRFDFIFPRKK	P	GCA_946190205.1	52874 to 63087 (contig 9)
U164_S21	Y	N	-	-	-	N	N	DSRISKYLRDFIFPRKK	P	GCA_946190365.1	56909 to 62429 (contig 9)
U165-2_S22	N	-	-	-	-	-	-	-	-	GCA_946186005.1	-
U23_S57	Y	N	-	-	-	N	N	EMRRIDKMFINFLKRR	L	GCA_946190355.1	34140 to 39308 (contig 18)
U24_S58	Y	N	-	-	-	N	N	EMRRIDKMFINFLKRR	L	GCA_946190345.1	13215 to 18383 (contig 16)
U25_S59	N	-	-	-	-	-	-	-	-	GCA_946224995.1	-
U28_S60	N	-	-	-	-	-	-	-	-	GCA_946225005.1	-
U32_S62	Y	Y	6537	3	14	N	N	EMRRIDKIFINFLKRR	L	GCA_946224725.1	25517 to 32053 (contig 4)
U35_S65	Y	N	-	-	-	N	N	EMRRIDKIFINFLKRR	L	GCA_946224685.1	125817 to 132353 (contig 5)
U36_S66	N	-	-	-	-	-	-	-	-	GCA_946224705.1	-
U39_S69	N	-	-	-	-	-	-	-	-	GCA_946224645.1	-
U40_S70	Y	Y	1815	3	7	N	N	EIRKTINGLLNFFKRR	F	GCA_946190305.1	49454 to 51267 (contig 3)
U48_S72	N	-	-	-	-	-	-	-	-	GCA_946224865.1	-
U52_S74	N	-	-	-	-	-	-	-	-	GCA_946190225.1	-

(continues next page)

Table S1. (cont.)

U54_S75	Y	N	-	-	-	N	N	EMRRIDKMFINFLKRR	L	GCA_946190185.1	18384 to 28422 (contig 12)
U56_S76	Y	N	-	-	-	N	N	ETRKTINSLLNLFKRR	F	GCA_946190325.1	71434 to 73220 (contig 5)
U57_S77	Y	N	-	-	-	N	N	ETRKTINSLLNLFKRR	F	GCA_946190235.1	37034 to 38822 (contig 12)
U61_S78	N	-	-	-	-	-	-	-	-	GCA_946190115.1	-
U63_S79	Y	N	-	-	-	N	N	ETRKTINSLLNLFKRR	F	GCA_946190175.1	37034 to 38822 (contig 15)
U65_S81	Y	N	-	-	-	N	N	EMRRIDKMFINFLKRR	L	GCA_946190125.1	10058 to 15226 (contig 20)
U67_S83	Y	Y	7327	1	14	Y	Y	EMRRIDKMFINFLKRR	L	GCA_946190165.1	35610 to 42936 (contig 11)
U8_S49	Y	N	-	-	-	Y	Y	ESRLPKIRFDFIFPRKK	P	GCA_946190315.1	52874 to 63087 (contig 6)
U92_S86	Y	N	-	-	-	N	N	ETRKTINSLLNLFKRR	F	GCA_946190145.1	58367 to 59135 (contig 6)
U98_S90	Y	N	-	-	-	N	N	EIRIADKIFFNLFKRR	F	GCA_946190155.1	14745 to 15455 (contig 11)
U99_S91	Y	N	-	-	-	N	N	EIRIADKIFFNLFKRR	F	GCA_946190155.1	14745 to 15455 (contig 12)
WTCHG_774611_72895361	N	-	-	-	-	-	-	-	-	GCA_946190255.1	-
WTCHG_774611_72965368	Y	N	-	-	-	N	N	ESRVSDILLDFLFRRKK	R	GCA_946190195.1	114512 to 120897 (contig 4)
WTCHG_774611_73005372	Y	Y	12164	2	23	N	N	EMRKMNDKSFNLFNFFRRR	F	GCA_946190135.1	24172 to 36335 (contig 6)
WTCHG_774611_73015373	N	-	-	-	-	-	-	-	-	GCA_946190275.1	-
WTCHG_774611_73075379	Y	N	-	-	-	Y	Y	EMRKPDGALFNLFRRR	F	GCA_946190295.1	119791 to 129649 (contig 6)
WTCHG_774611_73095381	Y	N	-	-	-	N	N	EMRKMNDKSFNLFNFFRRR	F	GCA_946190335.1	118632 to 130795 (contig 6)
WTCHG_774611_73775353	Y	Y	11984	5	25	N	N	EIRLSKFLRDFILQRKK	Q	GCA_946190285.1	28199 to 40182 (contig 5)
WTCHG_774611_73825358	Y	Y	11984	5	25	N	N	EIRLSKFLRDFILQRKK	Q	GCA_946190255.1	28199 to 40182 (contig 5)
WTCHG_774611_73845360	Y	N	-	-	-	N	N	EMRKMNDKSFNLFNFFRRR	F	GCA_946185975.1	118632 to 130795 (contig 6)
B22	Y	Y	15566	11	38	N	Y	ESRVSRIILDFLFLRKK	L	GCA_965111745.1	61443 to 77008 (contig 1)
C22	Y	Y	7274	3	15	N	Y	ESRLSRLLRDFIFQIKQ	Q	GCA_965111725.1	50761 to 58034 (contig 1)
D22	Y	Y	2127	2	2	N	N	DSRISKFLRDFIFPRKK	P	GCA_965111735.1	34443 to 36569 (contig 1)
E22	Y	Y	14434	1	32	Y	Y	EMRLPKILRDFIFPRKK	P	GCA_965111705.1	263852 to 278285 (contig 1)
F22	Y	Y	7848	5	13	Y	Y	ESRVSRIILDFLFLRKK	L	GCA_965111715.1	42896 to 50743 (contig 1)
G22	Y	Y	4404	2	12	N	Y	ESRLSRLLRDFIFQIKQ	Q	GCA_965111695.1	57304 to 61707 (contig 1)
B6	Y	Y	9068	5	18	Y	Y	EMRKPDGALFNLFRRR	F	GCA_000027165.1	53854 to 62921 (contig 1)
FDA684	Y	Y	8195	5	17	N	N	EIRQTHNIFFNFFKRR	F	GCA_009730515.1	31493 to 39687 (contig 1)
SK637	Y	Y	7760	4	18	N	Y	EMRKSNNNFFHFLRRI	L	GCA_000722765.2	49608 to 57367 (contig 1)
SVGS061	Y	Y	2200	2	5	N	N	EMRKSNNTFFNFLRRI	L	GCA_001560895.1	73674 to 75873 (contig 1)

The genomic region between *plsX-acpP* and *comAB* was extracted from publicly available *S. mitis* genomes. Of the 332 genomes analyzed, this region was successfully retrieved from 253; the remaining genomes contained contig breaks and were excluded from further analyses. The 253 genomes were screened for the presence of competence-associated bacteriocin (*cab*), competence-induced bacteriocins A and B (*cibAB*), and the cognate immunity protein (*cibC*) genes. The number of SigX boxes in *cab* loci was determined. Mature CSP sequences of each strain was predicted by identifying small ORFs upstream of *comDE* that contained a double-glycine cleavage motif.

Table S2. Bacterial strains, plasmids, peptides and oligonucleotides used in the study.

Bacterial strain, plasmid, oligonucleotide or peptide	Relevant genotype or sequence	Note	Source
Bacterial strains			
Corynebacterium accolens LMG 19042	Wild type	-	BCCM/LMG
Dolosigranulum pigrum LMG 15126	Wild type	-	BCCM/LMG
Escherichia coli DH5α	Wild type	-	Thermo Fisher
Escherichia coli DH10B	Wild type	-	Thermo Fisher
Haemophilus influenzae FP7132	Wild type		P. Lavado
Klebsiella pneumoniae OND482	Wild type	-	Simões *et al* ., 2022
Moraxella catarrhalis ATCC 25238	Wild type	-	ATCC
Neisseria lactamica ATCC 23970	Wild type	-	ATCC
Staphylococcus aureus ATCC 25293	Wild type	-	ATCC
Staphylococcus epidermidis ATCC 14990	Wild type	-	ATCC
Streptococcus agalactiae ATCC 13813	Wild type	-	ATCC
Streptococcus anginosus ATCC 12395	Wild type	-	ATCC
Streptococcus constellatus ATCC 27823	Wild type	-	ATCC
Streptococcus gordonii ATCC 33399	Wild type	-	ATCC
Streptococcus infantis ATCC 700779	Wild type	-	ATCC
Streptococcus mitis SK142	Wild type	-	ATCC
Streptococcus mitis C22	Wild type	-	Borralho, Handem and Lança *et al.,* 2025
Streptococcus mitis C22 Δ*cab*	Δ*cab* ::*aphA-3*	kan^R	Borralho, Handem and Lança *et al.,* 2025
Streptococcus mitis C22 kan^R	*ZIP::aphA-3*	kan^R	This study
Streptococcus mitis F22	Wild type	-	Borralho, Handem and Lança *et al.,* 2025
Streptococcus mitis G22	Wild type	-	Borralho, Handem and Lança *et al.,* 2025
Streptococcus mitis G22 P*comCDE* -pJB11	*CIL* ::P*comCDE* -mNeonGreen-luciferase *cat*	chl^R	This study
Streptococcus mitis G22 *PsigX1-pJB11*	*CIL::PsigX1-mNeonGreen-luciferase cat*	chl^R	This study
Streptococcus mitis G22 *PsigX2-pJB11*	*CIL::PsigX2-mNeonGreen-luciferase cat*	chl^R	This study
Streptococcus mitis G22 *PcabABC-pJB11*	*CIL::PcabABC-mNeonGreen-luciferase cat*	chl^R	This study
Streptococcus mitis G22 *PcabABC* (truncated)-*pJB11*	*CIL::P* cabABC(truncated)-*mNeonGreen-luciferase cat*	chl^R	This study
Streptococcus mitis G22 Δ*comE PcabABC-pJB11*	Δ*comE::aphA-3 CIL::PcabABC-mNeonGreen-luciferase cat*	kan^R chl^R	This study
Streptococcus mitis G22 Δ*sigX1 PcabABC-pJB11*	Δ*sigX1::aphA-3 CIL::PcabABC-mNeonGreen-luciferase cat*	kan^R chl^R	This study
Streptococcus mitis G22 Δ*sigX2 PcabABC-pJB11*	Δ*sigX2::ant(9) CIL::PcabABC-mNeonGreen-luciferase cat*	spc^R chl^R	This study
Streptococcus mitis G22 Δ*sigX1* Δ*sigX2 PcabABC-*	Δ*sigX1* ::*aphA-3* Δ*sigX2* ::*ant(9) CIL* ::P*cabABC-mNeonGreen-luciferase cat*	kan^R spc^R chl^R	This study
Streptococcus mitis G22 Δ*blp4* Δ*blp1*	Δ*blp4* ::*lox72* Δ*blp1::aphA-3*	kan^R	Borralho, Handem and Lança *et al.,* 2025
Streptococcus mitis G22 Δ*blp4* Δ*blp1* (markerless)	Δ*blp4* ::*lox72* Δ*blp1::lox72*	-	This study
Streptococcus mitis Δ*blp4* Δ*blp1* Δ*cabABC*	Δ*blp4* ::*lox72* Δ*blp1::lox72* Δ*cabABC* ::*aphA-3*	kan^R	This study
Streptococcus mitis G22 p(*cab* $^+$)	Δ*blp4* ::*lox72* Δ*blp1::lox72* Δ*cabABC* ::*aphA-3* pJB09-P23-*cabABC*	spc^R kan^R	This study

(continues next page)

Table S2. (cont.)

Streptococcus mitis G22 *cabA-HA*	*Δblp4 ::lox72 Δblp1 ::lox72 ΔcabABC ::aphA-3 CIL::cabA-HA cabBC cat*	kan^R chl^R	This study
Streptococcus mitis G22 *cabB-HA*	*Δblp4 ::lox72 Δblp1 ::lox72 ΔcabABC ::aphA-3 CIL::cabA cabB-HA cabC cat*	kan^R chl^R	This study
Streptococcus mitis G22 *Δblp4 Δblp1 ΔcomE*	*Δblp4 ::lox72 Δblp1 ::lox72 ΔcomE ::aphA-3*	kan^R	This study
Streptococcus mutans ATCC 25175	Wild type	-	ATCC
Streptococcus oralis DSM 20066	Wild type	-	DSMZ
Streptococcus parasanguinis ATCC 15912	Wild type	-	ATCC
Streptococcus peroris ATCC 700780	Wild type	-	ATCC
Streptococcus pneumoniae D39	Wild type	-	Avery *et al.*, 1944
Streptococcus pneumoniae D39 PhunSweet	*Δcps ::pheS-sacB-aphA-3*	kan^R	Echlin and Rosch, 2020
Streptococcus pneumoniae D39 P*comCDE*-pJB11	*CIL* ::P*comCDE*-mNeonGreen-luciferase *cat*	chl^R	This study
Streptococcus pneumoniae D39 *ΔlytA*	*ΔlytA ::pheS-sacB-aphA-3*	kan^R	This study
Streptococcus pneumoniae D39 *ΔlytA* (markerless)	*ΔlytA*	-	This study
Streptococcus pneumoniae D39 *ΔlytC*	*ΔlytC ::pheS-sacB-aphA-3*	kan^R	This study
Streptococcus pneumoniae D39 *ΔlytC* (markerless)	*ΔlytC*	-	This study
Streptococcus pneumoniae D39-GFP	P*hlpA-hlpA-gfp cat*	chl^R	Valente *et* al., 2022
Streptococcus pneumoniae D39-GFP ΔcomGC	P*hlpA-hlpA-gfp cat ΔcomGC ::tet(M)*	tet^R	This study
Streptococcus pneumoniae TIGR4	Wild type	-	ATCC
Streptococcus pseudopneumoniae BAA-960	Wild type	-	ATCC
Streptococcus pyogenes ATCC 12344	Wild type	-	ATCC
Streptococcus salivarius ATCC 7073	Wild type	-	ATCC
Streptococcus sanguinis ATCC 10556	Wild type	-	ATCC
Streptococcus sinensis HKU4	Wild type	-	DSMZ
Streptococcus sobrinus ATCC 27351	Wild type	-	ATCC
Streptococcus vestibularis ATCC MM1	Wild type	-	ATCC
Plasmids			
pDL278-P23-DsRed-Express2	*P23-dsRed-Express2 pMB1 pVA380-1 ant(9)*	*E. coli*-streptococcal	Plasmid #121505 (Addgene)
pJB09-cabABC	pDL278-P23-DsRed-Express2 but *ΔdsRed-Express2 ::cabABC*	*E. coli*-streptococcal	This study
pBIR	*p15A aphA-3 tdTomato cat*	Integrates in *CIL* locus	This study (Twist Bioscience)
pPEP-LGZ	*luc sfGFP lacZ cat p15A ant(9)*	Integrates in *CEP* locus	Kjos *et al* ., 2016
pJB10	pBIR but *ΔtdTomato ::hlpA-mNeonGreen*	Integrates in *CIL* locus	This study
pJB11	pJB10 but *luc*	Integrates in *CIL* locus	This study
pJB11-PcomCDE(G22)	pJB11 but P*comCDE* reporter (*S. mitis* G22)	Integrates in *CIL* locus	This study
pJB11-PcomCDE(D39)	pJB11 but P*comCDE* reporter (S. *pneumoniae* D39)	Integrates in *CIL* locus	This study
pJB11-PsigX1	pJB11 but P*sigX1* reporter	Integrates in *CIL* locus	This study
pJB11-PsigX2	pJB11 but P*sigX2* reporter	Integrates in *CIL* locus	This study

(continues next page)

Table S2. (cont.)

pJB11-PcabABC	pJB11 but P*cabABC* reporter	Integrates in *CIL* locus	This study
pJB11-PcabABC(truncated)	pJB11 but P*cabABC* (truncated) reporter	Integrates in *CIL* locus	This study
pKan	*pMB1 lox66-p3-aphA-3-lox71*	Integrates in *cab* locus	Borralho, Handem and Lança *et al.*, 2025
Peptides			
$BlpC_1$	GLWEELYETITTPLKLRTTFKP	-	NZYTech
$BlpC_4$	GWWEELLHETILSKFKITKALELPVQL	-	NZYTech
CSP-1	EMRLSKFFRDFILQRKK	-	NZYTech
CSP-2	EMRISRIILDFLFLRKK	-	NZYTech
CSP-2(L14Q)	EMRISRIILDFLFQRKK	-	NZYTech
CSP_{A22}	DWRISETIRNLIFPRRK	-	NZYTech
CSP_{B22}	ESRVSRIILDFLFLRKK	-	NZYTech
CSP_{D22}	DSRISKFLRDFIFPRKK	-	NZYTech
CSP_{E22}	EMRLPKILRDFIFPRKK	-	NZYTech
CSP_{G22}	ESRLSRLLRDFIFQIKQ	-	NZYTech
CSP_{G22}(Q14L)	ESRLSRLLRDFIFLIKQ	-	NZYTech
CSP_{G22}(Q14N)	ESRLSRLLRDFIFNIKQ	-	NZYTech
Oligonucleotides			
P1F_cab7_OE	ATGACAAATTTTGACAAAATGGAAC	Construction of plasmid pJB09-cabABC	This study
P1R_cab7_OE	CCCTATAGAACGTCTACTACCTC		
P1F_pDL278_OE	CTCGGTACCAAATTCCAGAAAAG		
P1F_pDL278_OE	GTTTGTCCTCCTTAACTAGTAATTAATAC		
P1F_hlpA_mNG_twist	AAAGCACTCAAAAGTTTACCTTATGG	Construction of plasmid pJB10	This study
P1R_hlpA_mNG_twist	CGCAAAAAACCCCGCTTCGGCGGGGTTTTTTCGCTTATTTATAC		
P1F_pBIR_backbone	ATCGGAGAAATTGGACACACC		
P1R_pBIR_backbone	CCCTATCAAAAGAATCTTGCTTGGC		
PF_luc_pPEP	GCTGAAGGAGGAATAATGAGATCC	Construction of plasmid pJB11	This study
PR_luc_pPEP	TTACAATTTGGGCTTTCCGCC		
PF_pJB10_backbone	GAATGGACGAGTTGTATAAG		
PR_pJB10_backbone	TTATTTATACAATTCATCCATACCC		
PF_reporter_PcomCDE(G22)	AGCTGGTCTCTGACTATATAGTAGCAAAGCTGGG	Construction of plasmid pJB11-PcomCDE (G22)	This study
PR_reporter_PcomCDE(G22)	CGATGGTCTCAAGTCAATAAAATCTCCTAAAATGTTTTTTTC		
PF_reporter_PcomCDE(D39)	AGCTGGTCTCTGACTATATAATAGCAAAGCTGGG	Construction of plasmid pJB11-PcomCDE (D39)	This study
PR_reporter_PcomCDE(D39)	CGATGGTCTCAAGTCAATAAAATCTCCTAAAATGTTTTTTC		
PF_reporter_PsigX1	AGCTGGTCTCTGACTCCCAAAGAGAGGCAAGACC	Construction of plasmid pJB11-PsigX1	This study
PR_reporter_PsigX1	CGATGGTCTCAAGTCTCTTTTCCCCTTTCTGTGTAC		

(continues next page)

Table S2. (cont.)

PF_reporter_PsigX2	AGCTGGTCTCTGACTCCCTGAGAGAGGCCCGTC	Construction of plasmid pJB11-PsigX2	This study
PR_reporter_PsigX2	CGATGGTCTCAAGTCAGTCTTCCCCTTTCTGTGTAC		
PF_reporter_PcabABC	AGCTGGTCTCTGACTAAATAACATCTTCACAACTAATCG	Construction of plasmid pJB11-PcabABC	This study
PR_reporter_PcabABC	CGATGGTCTCAAGTCCTTTTTTCTCCTTTATTTCTATTTTTTAG		
PF_reporter_PcabABC_trunc	AGCTGGTCTCTGACTTTTAGTTGTGTATTTTCGAATTG	Construction of plasmid pJB11-PcabABC (truncated)	This study
PR_reporter_PcabABC_trunc	CGATGGTCTCAAGTCCTTTTTTCTCCTTTATTTCTATTTTTTAG		
P1F_comE_G22	GGATTAAACAGTATGAGAGG	Deletion of *comE* in *S. mitis* G22	This study
P1F_comE_G22	GTCAATACCGTTCGTATAGCATACATTATACGAAGTTATTCATTCAAATTCCCTCTTAAATC		
P2F_comE_G22_pKan	CAAATTATTAGATTTAAGAGGGAATTTGAATGAATAACTTCGTATAATGTATGC		
P2R_comE_G22_pKan	CATTATATCAATTTCTTGCTAATTGTCAATCACTATAACTTCGTATAGCATAC		
P3F_comE_G22	GTTTTAGTACCGTTCGTATAATGTATGCTATACGAAGTTATAGTGATTGACAATTAGCAAGAAATTG		
P3R_comE_G22	TATTACCATTATAGGAAGCC		
P4F_comE_G22	TATAACAGGAGATAATTTTG		
P4R_comE_G22	ACAGAGCTGGAATAAGAGAAATCC		
P1F_sigX1_G22	ATTGTCATCGCTGCGACAAAC	Deletion of *sigX1* in *S. mitis* G22	This study
P1R_sigX1_G22	GTCAATACCGTTCGTATAGCATACATTATACGAAGTTATCATTCTTTTCCCCTTTCTGTGTACAG		
P2F_sigX1_G22_pKan	GACTGTACACAGAAAGGGGAAAAGAATGATAACTTCGTATAATGTATGC		
P2R_sigX1_G22_pKan	CTTTTTTGCATGAATTCCTAATGGGTACGATAACTTCGTATAGCATAC		
P3F_sigX1_G22	GTTTTAGTACCGTTCGTATAATGTATGCTATACGAAGTTATCGTACCCATTAGGAATTCATGC		
P3R_sigX1_G22	CGCTACACATGGAATTCCAC		
P4F_sigX1_G22	AGCAATCTTGAAAGTTCATGCTAAG		
P4R_sigX1_G22	ATCCGGACAACGCTCGGGACCTAC		
P1F_sigX2_G22	TGCTTGTCAAAGCCTGGCTTTCTTG	Deletion of *sigX2* in *S. mitis* G22	This study
P1F_sigX2_G22	CATGCAAAACAATGAATAGGCATAGTCTTCCCCTTTCTGTGTAC		
P2F_sigX2_G22_pPEP	GACTGTACACAGAAAGGGGAAGACTATGCATGCAAAACAATGAATAGG		
P2R_sigX2_G22_pPEP	CTTTTTTGCATGAATTCCTAATGAGTACGCTAATTGAGAGAAGTTTCTATAG		
P3F_sigX2_G22	CTAATTGAGAGAAGTTTCTATAGCGTACTCATTAGGAATTCATGCAAA		
P3R_sigX2_G22	CCGCTACACATGGAATTCCACTC		
P4F_sigX2_G22	CTATTCAATCAAGATTAGTGGAAAC		
P4R_sigX2_G22	TAGTTAGCCGTCCCTTTCTGGTAAG		

(continues next page)

Table S2. (cont.)

P1F_PS_lytA_D39	GGTTTATCAGCGGTTCTCTGC	Deletion of *lytA* in *S. pneumoniae D39*	This study
P1R_PS_lytA_D39	CGGATCGATCCTTAATAGTGGGTTCCATATTCTACTCCTTATCAA		
P2F_PS_lytA_D39	GTTTTAATTGATAAGGAGTAGAATATGGAACCCACTATTAAGGATCGATC		
P2R_PS_lytA_D39	CTGTTCTGATTTGAAAGACATTCCATTATTACTAAAACAATTCATCCAGTAAAATATAAT		
P3F_PS_lytA_D39	CTGGATGAATTGTTTTATAATAATGGAATGTCTTTCAAATCAG		
P3R_PS_lytA_D39	TTTTACTTTCTGACAAAGGACG		
P4F_PS_lytA_D39	TTCAATTGTATCTATCGGCAG		
P4R_PS_lytA_D39	TTCCTCAATCTATATAACATAGCTTTATG		
P5F_PS_lytA_D39	GTTTTAATTGATAAGGAGTAGAATATGGAATAATAATGGAATGTCTTTCAAATCAG		
P5R_PS_lytA_D39	CTGTTCTGATTTGAAAGACATTCCATTATTATTCCATATTCTACTCCTTATCAA		
P1F_PS_lytC_D39	ACTAAAGGAAGATGGAACCAG	Deletion of *lytC* in *S. pneumoniae D39*	This study
P1R_PS_lytC_D39	CGGATCGATCCTTAATAGTGGGAGACATCTGAATGCTGTTCC		
P2F_PS_lytC_D39	CTAGGTGGAACAGCATTCAGATGTCTCCCACTATTAAGGATCGATC		
P2R_PS_lytC_D39	CACATCCCTCTTTCAAATCATCGCTTACTAAAACAATTCATCCAGTAAAATATAAT		
P3F_PS_lytC_D39	CTGGATGAATTGTTTTATAAGCGATGATTTGAAAGAGGG		
P3R_PS_lytC_D39	TTCTTAGTCATGCTTCCATCC		
P4F_PS_lytC_D39	CTCAAATTGAGGCCAAGAGAG		
P4R_PS_lytC_D39	GTCCAAGTTCGGCTGCAAG		
P5F_PS_lytC_D39	CTAGGTGGAACAGCATTCAGATGTCTTAAGCGATGATTTGAAAGAGGG		
P5R_PS_lytC_D39	CACATCCCTCTTTCAAATCATCGCTTAAGACATCTGAATGCTGTTCC		
P1F_comGC_del	AATCGTTGACTTTGCAAGCAG	Deletion of *comGC* in *S. pneumoniae* D39	This study
P1R_comGC_del	TAATTTTCCTCCTATTTAGATCTTGCATGTATAGTTATTATACCAGGGGGACAGTGCAATGTCAATTTAAAAATTTACCTCCATATTTTGATACATG		
P2F_comGC_del	TTGACATTGCACTGTCCCCCTGGTATAATAACTATACATGCAAGATCTAAATAGGAGGAAAATTAATGAAAATTATTAATATTGGAGTTTTAGC		
P2R_comGC_del	CATTGACTTTACGATTTGCTCCTCCATTCTAAGTTATTTTATTGAACATATATCG		
P3F_comGC_del	GTACGATATATGTTCAATAAAATAACTTAGAATGGAGGAGCAAATCGTAAAGTC		
P3R_comGC_del	GTGACTGCGTAGAGGAGAAC		
P4F_comGC_del	TTCAGGCTGAGACGGAAAAAATTAG		
P4R_comGC_del	CAGATTTGAGTCCATAAACC		
P1F_cabAB_HA	CAAGCGCCAGGGTTTTCC	Construction of *S. mitis* harboring HA-tagged bacteriocins	This study
P1R_cabAB_HA	GTTCTGTTCCATTTTGTCAAAATTTGTCATCTTTTTTCTCCTTTATTTCTATTTTTTAG		
P2F_cabAB_HA	GTAAACTAAAAAATAGAAATAAAGGAGAAAAAAGATGACAAATTTTGACAAAATGGAAC		
P2F_cabAB_HA	CCAGGGGGACAGTGCAATGTCAATTATCCATTCTTTTTTTCTTTACTTC		
P3F_cabAB_HA	CATTCTTTTATATAGAAGTAAAGAAAAAAAGAATGGATAATTGACATTGCACTGTCCCC		
P3F_cabAB_HA	GCCCTCTGAGCGGATAACAATTTC		
P4F_cabAB_HA	ATCGGAGAAATTGGACACACC		
P4R_cabAB_HA	TTCGCAAATAGCGAAACCAATG		

(continues next page)

Table S2. (cont.)

P1F_C22_kan_ZIP	GCTGAACAACAGTGTGTCATA	Construction of *S. mitis* C22 mutant with kanamycin resistance	This study
P1R_C22_kan_ZIP	CAGGGGGACAGTGCAATGTCAATAGCTCAATTTGACACTTTTCTTC		
P2F_C22_kan_ZIP	CGAAGAAGAAAAGTGTCAAATTGAGCTATTGACATTGCACTGTCC		
P2R_C22_kan_ZIP	CTATGCAGGTCATTTCTACTCTTATAGCTAAAACAATTCATCCAGTAAAATA		
P3F_C22_kan_ZIP	TATTATATTTTACTGGATGAATTGTTTTAGCTATAAGAGTAGAAATGACCTGC		
P3R_C22_kan_ZIP	TCCCTTCCTATCAATTAGGTC		
P4F_C22_kan_ZIP	AGATAGATCAGCTATTGGAGAC		
P4R_C22_kan_ZIP	TATTTAAGTCCATCATAGCTTGG		

chl^R - chloramphenicol resistant; kan^R - kanamycin resistant; tet^R - tetracycline resistant; spc^R - spectinomycin resistant.

Supplementary references

Simões AS, Touret T, Faria NA, Peres Ladeiro S, Costa J, Bispo S, Serrano M, Palos C, Miragaia M, Bastos Leite R, Sá-Leão R. Using whole genome sequencing to investigate a mock-outbreak of carbapenem-resistant *Klebsiella pneumoniae* in real-time. *Acta Med Port*. 2022 Jan 3;35(1):36–41. doi: 10.20344/amp.15174. Epub 2021 Nov 10. PMID: 34755594.

Borralho J, Handem S, Lança J, Ferreira B, Candeias C, Henriques AO, Hiller NL, Valente C, Sá-Leão R. Inhibition of pneumococcal growth and biofilm formation by human isolates of *Streptococcus mitis* and *Streptococcus oralis*. *Appl Environ Microbiol*. 2025 Mar 19;91(3):e0133624. doi: 10.1128/aem.01336-24. Epub 2025 Feb 26. PMID: 40008876; PMCID: PMC11921387.

Avery OT, Macleod CM, McCarty M. Studies on the chemical nature of the substance inducing transformation of pneumococcal types: induction of transformation by a desoxyribonucleic acid fraction isolated from pneumococcus type III. *J Exp Med*. 1944;79:137–158.

Echlin H, Rosch JW. Advancing genetic tools in *Streptococcus pneumoniae*. *Genes (Basel).* 2020 Aug 20;11(9):965. doi: 10.3390/genes11090965. PMID: 32825523; PMCID: PMC7563404.

Valente C, Cruz AR, Henriques AO, Sá-Leão R. Intra-species interactions in *Streptococcus pneumoniae* biofilms. *Front Cell Infect Microbiol*. 2022 Jan 5;11:803286. doi: 10.3389/fcimb.2021.803286. PMID: 35071049; PMCID: PMC8767070.

Kjos M, Miller E, Slager J, Lake FB, Gericke O, Roberts IS, Rozen DE, Veening JW. Expression of *Streptococcus pneumoniae* bacteriocins is induced by antibiotics via regulatory interplay with the competence system. *PLoS Pathog*. 2016 Feb 3;12(2):e1005422. doi: 10.1371/journal.ppat.1005422. PMID: 26840404; PMCID: PMC4739728.